Fine-Scale Foraging Behavior of Humpback Whales *Megaptera novaeangliae* in the Near-Shore Waters of the Western Antarctic Peninsula

by

Reny Blue Tyson

Marine Science and Conservation
Duke University

Date:_____

Approved:

_____
Douglas Nowacek, Supervisor

_____
Ari Friedlaender

_____
James Hench

_____
Daniel Rubenstein

Dissertation submitted in partial fulfillment of
the requirements for the degree of Doctor
of Philosophy in Marine Science and Conservation in the Graduate School
of Duke University

2014

ABSTRACT

Fine-Scale Foraging Behavior of Humpback Whales *Megaptera novaeangliae* in the Near-Shore Waters of the Western Antarctic Peninsula

by

Reny Blue Tyson

Marine Science and Conservation
Duke University

Date:_____
Approved:

_____
Douglas Nowacek, Supervisor

_____
Ari Friedlaender

_____
James Hench

_____
Daniel Rubenstein

An abstract of a dissertation submitted in partial
fulfillment of the requirements for the degree
of Doctor of Philosophy in Marine Science and Conservation in the Graduate School of
Duke University

2014

Abstract

High-resolution bio-logging tools were used to examine the fine-scale foraging behaviors of humpback whales (*Megaptera novaeangliae*) in the coastal waters of the Western Antarctic Peninsula during the austral autumn of 2009 and 2010. Discrete feeding events (i.e., lunges) were inferred from the biologging records of thirteen whales, including a mother and her calf. In general, humpback whales exhibited efficient foraging behaviors that allowed them to maximize energetic gains and minimize energetic costs as predicted by optimal foraging theory. They fed at a continuous and high rate in the upper portion of the water column (< 100 m) from approximately dusk to dawn when their prey (Antarctic krill, *Euphausia superba*) were most vulnerable and less costly to acquire (i.e., near the surface). When forced to dive to greater depths, they adjusted their behaviors (e.g., descent and ascent rates) so that they could maximize their foraging durations and increase their lunging rates. In addition, humpbacks appeared to accept short term (i.e., dive by dive) costs associated with depleted oxygen stores in favor of maximizing long term (i.e., daily) energetic gains. Such efficient behaviors are particularly beneficial for mother-calf pairs who have additional energetic costs associated with foraging, such as lactation (mother), growth (calf), and maintaining proximity. In addition, because the physiology of humpback whales is poorly understood yet critically important for predicting their behaviors in response to

fluctuations in their environmental conditions, foraging behaviors inferred from the bio-logging records were used to estimate their metabolic rates, oxygen storage capacities, and oxygen replenishment rates under the framework of optimal foraging theory. This research suggests that the current techniques used to estimate humpback whale oxygen stores is appropriate but that the estimation of metabolic rates of humpbacks while foraging and while traveling need to be addressed further. This work aims to increase the current understanding of humpback whale foraging behaviors along the Western Antarctic Peninsula so that appropriate measures can be taken to aid in their recovery and in the sustainability of the Antarctic marine ecosystem.

Dedication

I dedicate this dissertation to my mother, Dr. Gail Tyson, who got mad at me for jumping out of a plane...

....without her.

Co-Authorship Statement

The research presented in this dissertation is part of a collaborate study designed to elucidate the ecological relationships between humpback whale and Antarctic krill in the Western Antarctic Peninsula and aspects it have been previously published elsewhere (e.g., Nowacek et al. 2011, Ware et al. 2011, Espinasse et al. 2012, Johnston et al. 2012, Stimpert et al. 2012, Tyson et al. 2012, Friedlaender et al. 2013). Several colleagues contributed to my research and are (or will be) listed as co-authors on modified versions of each data chapter submitted for peer-review to scientific journals. Douglas Nowacek and Ari Friedlaender were co-principle investigators of the collaborative research project and supplied funding for much of the work. They are co-authors on all of my data chapters. Allison Stimpert and Colin Ware contributed significantly to the analysis of tag data presented in Chapters 2. Finally, James Clark helped me to design the simulated model to estimate humpback whale physiology in Chapter 4 and provided analytical support.

Contents

List of Tables

List of Figures

Acknowledgements

I am fortunate to have been surrounded by many supportive and inspirational people during my graduate tenure at Duke. Of all these people, my advisor, Doug Nowacek is the person I must first and foremost thank. I still question why he selected me, a naïve bright-eyed nineteen year old, to work in his lab eleven years ago at Florida State but I am forever grateful that he did. His decision that day completely changed my life for good and brought me into a field that I truly do love. His continuous optimism, trust, and encouragement have allowed me to grow as a scientist who is willing to take risks, to take stride when those risks don't pan out, and to share the wealth of those risks that result in high rewards with those around me. He has taught me that the science has no boundaries but that collaboration is necessary and fruitful for moving beyond what others thought was not possible (really, a blimp?). I am thankful to have had Doug as a boss, a teacher, a mentor, and a colleague, but most importantly, I am most thankful to have Doug as a friend.

My committee has been so supportive and insightful throughout this process and I thank each and every one of them for the discussions we shared and the time they spent helping me throughout this process. Discussions with Dan Rubenstein regarding behavioral ecology were inspiring and forced me to think outside the 'marine mammal' box in ways that greatly enhanced my study of animal behavior. Jim Hench truly

encouraged me to think creatively about my data analysis in ways that greatly influenced my appreciation for statistical methods and oceanography. Finally, I think it is fair to say that I would not have been able to do this research if it had not been for Ari Friedlaender. This research is in many ways his baby and he allowed me to come along for the ride and share in this adventure with him. I have had a blast doing this research alongside and learning from the 'famous' whale tagger and hope that this is just the beginning of our collaborative ventures.

I must next thank Dave Johnston and Andy Read. I have always considered these two to be my unofficial committee members and knew that if I asked them for help or assistance they would be there in a heartbeat (and they were!). Dave has inspired and encouraged me to become more involved with outreach activities and to think creatively about how to connect with the public (hooray for Ipads). Andy, my Antarctic buddy, welcomed me with open arms as an honorary Read Lab member on day one and has been truly broadened my perspective of ecology, conservation, and policy and how they intertwine. I hope to work with these two for years to come and will always cherish the nights we shared dancing at Palmer Station (yes, Andy danced).

My research collaborators are some of the most amazing people I have ever had the pleasure of working with. Colin Ware, Jim Clark, Alison Stimpert, Corrie Curtice, Amanda Katlenberg, Elliott Hazen, Joseph Warren, Pat Halpin, Ann Allen, Boris Espinassee. Meng Zhou, and Yiwu Zhou have contributed significantly to the success of

this research and I would not have been able to do this work without them. Also, the entire Antarctic field crew and all those who made this research happen are forever in my debt. Lindsey Peavey, Andrew Westgate, Elletta Revelli, Roland Arsenault, Megan O'Neill, Dan Powers, Chance Miller, and Julie Jackson specifically made this research experience unforgettable: rock band concerts and weed marathons just wouldn't have been the same without you.

The Duke Marine Lab is a special place and I truly want to thank every person who makes the lab what it is. Special thanks must go to Rachel Lo Piccolo, Danielle Waples, Kim Urian, Heather Foley, Zachary Swaim, Katie Wood, Patty Nolin, Janil Miller, Shirley Miller, Jen Beggs Dunn, Lisa Campbell, Cindy Van Dover, Hazel George, and Fred Tootle. These guys truly rock. My fellow PhD students, past and present, were amazing and truly made my time spent in Beaufort unforgettable. Matt Bowers, my brother from another mother, and Kenady Wilson were the best office mates a girl could ask for. I will miss our 'lady lounge' but am thankful to know that I will have them as life-long friends, colleagues, and collaborators. Kristina Cammen, Rebecca Gruby, Meagan Dunphy-Daly, Joy Stainstreet, Tara Essock-Burns, Lesley Thorne, Lynne Williams Hodge, Caroline Good, Shay Vieham, Julia Burrows, Goldie Phillips, Erin LaBrecque, Wendy Dow Piniak, Sara McDonald, and Christopher Ward especially made my graduate life an amazing one. Enjoying beers at backstreet or the Haus, hitting each

other with racquetballs (woops!), and enjoying wine and gossip while watching the latest Bachelorrete episode helped keep me sane during the tougher days.

Audrey, Scott, and Sadie Hernandez, Jennifer Sanctis, Meaghan Young, Amy Grover, Sarah Walker, and Wesley Wincek, my non-sciency friends, are truly my extended family. They have put up with me coming home smelly after cutting up dead whales, missing important moments in their life because I was away in the field, and disappearing for weeks on end to 'write'. I owe them my sincerest thanks for standing by me and my nerdyness during all these years. They have kept me grounded and are a constant reminder to me of what life is truly all about.

Steph, Jack, and Wyatt have been my extended family for years and I thank them sincerely for *everything* they have done for me. They truly have had my back through thick and thin during this experience and I am so thankful to have them in my life. Paul and Laura Moore have been so generous and supportive and I thank them you accepting me into their family and for loving me as if I was their own. My immediate family, may be a weird one, but is the best I could ever ask for. My sister Sherri and nephew Zane are 'da bomb' and my brother Ben has been and continues to be an inspiration to me every single day. My mom is the most selfless person I know and I can never thank her enough for all she has done for me. Whenever I thought about doing something new or unusual, she always responded with "why not, doesn't hurt to try." Its phrases like that,

which allowed me to believe I could travel to the moon and back again, then go out and actually do it.

Finally I must thank Jason Moore. I never imagined he would go on a second date with me five years ago after I told him I would be leaving in a few weeks to study whales in the Antarctic. But he did and every day since he has sat right next to me on this rollercoaster of life. Along the hills and troughs, he has been my strong and efficient rock. I will never be able to thank him enough for his love, patience, and support during this adventurous ride.

1. Introduction

Baleen whales (Mysteceti) include the largest animals ever to inhabit the planet (e.g., blue whale, *Balaenoptera musculus*) yet because of the inherent restrictions humans have in observing them in their natural environment (i.e., underwater), very little is understood about their foraging behavior at depth. This includes how they find, exploit, and respond to distributions of prey and how much food they need to consume to support their energetic needs. Because foraging is essential for an individual's survival and reproduction, this gap is limiting our understanding of the ecology and life history of these large, wide-ranging species.

Optimal foraging theory suggests that organisms are adapted to exploit resources as efficiently as possible; natural selection should favor foraging strategies that are efficient in minimizing costs (in time and energy) while simultaneously maximizing benefits (e.g., energy, nutrients) (Macarthur & Pianka 1966). When resources are distributed in a patchy manner, this optimal foraging strategy can be achieved by minimizing the time spent searching for or acquiring energy, or maximizing the total energy acquisition per unit time (Schoener 1987). Baleen whales deal with patchiness in prey resources by conducting annual migrations from low latitude breeding regions of limited food resources (winter) to high latitude regions with predictably abundant concentrations of prey (summer) (Mackintosh 1965). Unlike toothed whales (odontocetes), which pinpoint or hunt singular prey items such as fish or squid, baleen whales consume large amounts of patchily distributed prey efficiently from these

regions using bulk filtration (Williams 2006). They use keratinized plates of baleen to filter small zooplankton and/or small fish from ingested water by skim or continuous ram feeding (Balaendiae), suction feeding (Eschritiidae), or lunge feeding (Balaenopteridae).

1.1 Balaenopterid Foraging Ecology

Advancements in bio-logging technologies have greatly enhanced the current understanding of baleen whale foraging behavior. In particular, the use of these tools has resulted in large advances in detailing the kinematics and energetic costs of lunge feeding in Balaenopterids (e.g., blue whales; fin whales, *Balaenoptera physalus*; humpback whales, *Megaptera novaeangila;*, minke whales, *Balaenoptera bonaerensis*; hereafter referred to as rorquals) (Goldbogen et al. 2006, Goldbogen et al. 2007, Goldbogen et al. 2008, Friedlaender et al. 2009, Potvin et al. 2009, Goldbogen et al. 2010, Potvin et al. 2010, Doniol-Valcroze et al. 2011, Goldbogen et al. 2011, Ware et al. 2011, Wiley et al. 2011, Potvin et al. 2012, Simon et al. 2012, Tyson et al. 2012, Friedlaender et al. 2013, Goldbogen et al. 2013, Ware et al. 2013). Lunge feeding involves accelerating with a burst of energetic fluking towards and engulfing a mass of prey-laden water, filtering the prey from the ingested water through keratinized plates of baleen, and swallowing the captured prey. Rorquals have a series of longitudinal grooves of highly extensible, elastic blubber on the ventral side of their body (ventral groove blubber, VGB) that allow them to open their mouths wide to approximately 75 degrees (Brodie 1993) and engulf a

volume of water that may be greater than their body mass (Goldbogen et al. 2010). This process has been deemed the largest biomechanical event to take place on earth (Brodie 1993) and has been suggested to be energetically costly, limiting the maximum dive time of these large predators (Dolphin 1988, Croll et al. 2001, Acevedo-Gutierrez et al. 2002, Goldbogen et al. 2006, Goldbogen et al. 2007, Goldbogen et al. 2008). Recent work by Goldbogen et al. (2011) and Potvin et al. (2012), however, suggests that the foraging efficiency of rorquals can be significantly higher than other marine mammals by nearly an order of a magnitude when lunges target extremely dense patches of krill. This efficiency is attributed to the animals enhanced engulfment capacity, their rapid filter rate, and their low mass-specific metabolic rates associated with their large size (Goldbogen et al. 2011). Still, the rate at which rorquals acquire and use energy is largely unknown and needs to be more thoroughly examined and understood.

U-shaped foraging dives, in which whales directly descend to a foraging depth, perform a number of descending-ascending excursions linked to lunges during bottom time, and then directly ascend to the surface alternating between gliding and fluking behaviors are the most frequently described types of rorqual foraging behaviors performed at depth (Figure 1) and have been described in fin whales (Goldbogen et al. 2006), blue whales (Goldbogen et al. 2011), and humpback whales (Goldbogen et al. 2008, Ware et al. 2011, Simon et al. 2012). Bio-logging tools have allowed a further analysis into the three-dimensional structure of lunges at depth and an assortment of lunge techniques has been described. For example, rolling while lunging at depth has

been observed in blue, fin, and humpback whales (e.g., Hain et al. 1982, Corkeron et al. 1999, Goldbogen et al. 2006, Stimpert et al. 2007, Friedlaender et al. 2009, Canning et al. 2011, Goldbogen et al. 2013, Ware et al. 2013). Potvin et al. (2010) suggest that a lateral roll of 90° while lunging decreases the ability of potential prey to escape through the gaps in the mandibles that are present when the whale approaches from a flatter angle and thus may increase the amount of prey the whale can capture. Rolling can be extreme in the case of blue whales, which have been observed to perform 360° rolling maneuvers, allowing them to reorient their body and position their lower jaws so that they can engulf krill while inverted (Goldbogen et al. 2013). The authors suggest that these maneuvers may allow the whales to visually process the prey field and subsequently target the densest prey aggregations.

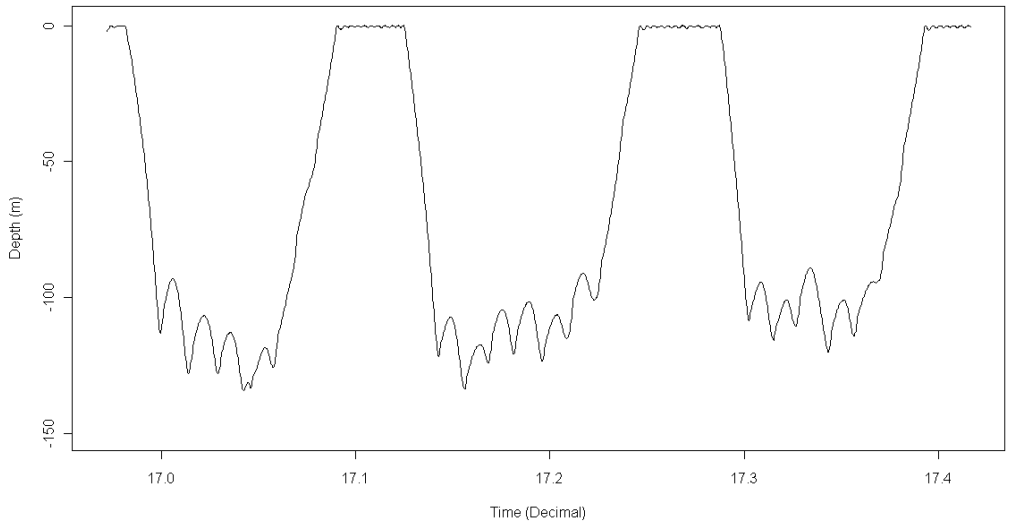

Figure 1: U-shaped foraging dives of a humpback whale. The descending and ascending excursions at depth have been linked to discrete feeding lunges.

Rorquals also execute various maneuvers at the seafloor and the ocean surface, which appear to further limit escape routes of their target prey. Bottom feeding, a technique in which the animal rolls on their side and 'brushes' the bottom, typically using the right side of their mouth (Hain et al. 1982), has been described in humpback whales in the Gulf of Maine (Hain et al. 1982, Canning et al. 2011, Friedlaender et al. 2013, Ware et al. 2013). This maneuver is correlated with American sand lance (*Ammodytes spp*.) seeking refuge in the substrate at night (Friedlaender et al. 2009). Crittercam video of humpback whales foraging at depth in this region revealed large numbers of sand lance located just above the seafloor where these lunges occur (Ware et al. 2013). Humpbacks also limit prey escape routes at the surface by corralling prey with

bubble nets or clouds (e.g., Juarasz & Juarasz 1979, Hain et al. 1982, Weinrich et al. 1992, Wiley et al. 2011), vertically lunging at such aggregations, and utilizing associated lobtail (Weinrich et al. 1992) and "free-form" feeding techniques (Hays et al. 1985, Wiley et al. 2011). In the Western Antarctic Peninsula (WAP), humpbacks have been observed to exhibit a repetitive looping behavior at the surface where they presumably exploit a single, small krill patch (Ware et al. 2011). This wide variety of maneuvers associated with lunging suggests that rorquals are plastic in their feeding behaviors and may be able to adapt to fluctuations in prey resources.

A few studies have attempted to quantify rorqual feeding behavior in relation to their prey (e.g., Dolphin 1987b, Croll et al. 2001, Goldbogen et al. 2008, Witteveen et al. 2008, Hazen et al. 2009, Goldbogen et al. 2011, Nowacek et al. 2011, Friedlaender et al. 2013) but none, to my knowledge, have quantified prey density at a fine-scale (i.e., the scale of a dive) in relation to feeding events. Opportunistic observations of whales in the Antarctic led Ainley et al. (2006) to suggest that rorquals may deplete prey enough at a fine scale that other krill predators, such as penguins, alter their foraging behavior and switch prey (Ainley et al. 2006). Again, hypotheses such as these cannot fully be addressed until a fine-scale examination of rorqual foraging ecology is undertaken.

1.2 Research Objectives

The objective of this research was to increase the understanding of fine-scale humpback whale foraging behaviors in the coastal waters of the WAP. This information

is critical in light of environmental changes observed and predicted in the region associated with rapid climate warming (Smith & Stammerjohn 2001, Vaughan et al. 2003, Parkinson 2004, Stammerjohn et al. 2008a, Stammerjohn et al. 2008b). In the following chapters, I describe several elements of humpback whale foraging behaviors that take place in this region, which were inferred from data collected using high-resolution bio-logging tools. In Chapter 2, I examine the foraging behaviors and synchrony of a mother and calf humpback whale pair and discuss the fitness implications of my findings. In Chapter 3, I combine theory with observations of whale behavior to examine how adult humpbacks allocate their time during foraging dives and assess if their foraging behaviors are energetically efficient. Finally in Chapter 4, I use observations of humpback whale foraging behavior to model aspects of their physiology, including metabolic rates and oxygen storage capacities. The findings of this research may be useful in future studies that attempt to predict the behavioral response of humpback whales and other rorquals to environmental and/or ecological change. Finally, I summarize my findings and their implications in Chapter 5. This work will provide baseline data regarding the foraging behaviors of humpback whales in the WAP and will make predictions regarding how these animals may respond to changes in this ecosystem.

1.3 General Materials and Methods

My work is part of a larger, inter-disciplinary collaborative study that was designed to elucidate the ecological and environmental relationships between humpback whales and krill along the WAP (e.g., Nowacek et al. 2011, Ware et al. 2011, Espinasse et al. 2012, Johnston et al. 2012, Stimpert et al. 2012, Tyson et al. 2012, Friedlaender et al. 2013). Humpback whales were chosen as the target study species for this research because they are the most abundant baleen whale in the near-shore waters of the WAP (Thiele et al. 2004, Friedlaender et al. 2006, Johnston et al. 2012), they forage almost exclusively on Antarctic krill (*Euphausia superba*; Mackintosh 1965, Ichii & Kato 1991, Kawamura 1994), and they are easily approachable from a small boat for tagging purposes (e.g., Friedlaender et al. 2009, Hazen et al. 2009, Nowacek et al. 2011, Friedlaender et al. 2013). Research was primarily conducted within several embayments of the WAP in the austral autumn of 2009 and 2010 from the ASRV *Laurence M. Gould* and the RVIB *Nathanial B. Palmer*, respectively. These vessels are operated and maintained by the United State Antarctic Program (USAP) and supported by the National Science Foundation (NSF). All research was permitted under the U.S. Marine Mammal Protection Act by the National Marine Fisheries Service Permit 808-1735, the Antarctic Conservation Act Permit 2009-014 and the Duke University Institutional Animal Care and Use Permit A041-09-02, which were awarded to DP Nowacek. All research was supported by NSF, USAP Grant ANT-07-39483. The following information

regarding materials and methods applies to all chapters of this dissertation. All other analyses will be chapter specific and will be described in detail when appropriate.

1.3.1 Study Area

Data for this research were collected in Wilhelmina Bay, Andvord Bay and Flandres Bay (Figure 2). The circulation patterns in the bays are heavily influenced by the Gerlache Current (Zhou et al. 2002), which starts from the southwest entrance of the Gerlache Strait at Flandres Bay and exits into the Bransfield Strait. The Gerlache Current is made up of Modified Circumpolar Deep Water (MCDW); a water mass made up of warm (up to 2° C), saline (> 34.6 ppt), and nutrient rich water that stimulates primary productivity on the WAP continental shelf and determines the ice condition in this region (Prezelin et al. 2000, Zhou et al. 2002). The MCDW is cooled as it intrudes upon the shelf due to the loss of heat to the atmosphere and mixing with local cold waters (Dinniman et al. 2011), and resultant temperature gradients (warm to cool) have been observed stretching from the current entrance to its exit into Bransfield Strait (Zhou et al. 2002). As the Gerlache Current flows throughout the Strait, mesoscale eddies and jets often form, specifically in the neighboring embayments (Nowacek et al. 2011, Espinasse et al. 2012), which provide an essential mechanism for the retention of biota and food supplies (i.e., mesoplankton for fish and krill; Nowacek et al. 2011, Espinasse et al. 2012). Krill aggregations have been observed being retained in such eddies that are near jets within these bays, which may allow them to stay in the eddies and feed on food

delivered by the jets while simultaneously avoiding being advected away (Nowacek et al. 2011, Espinasse et al. 2012).

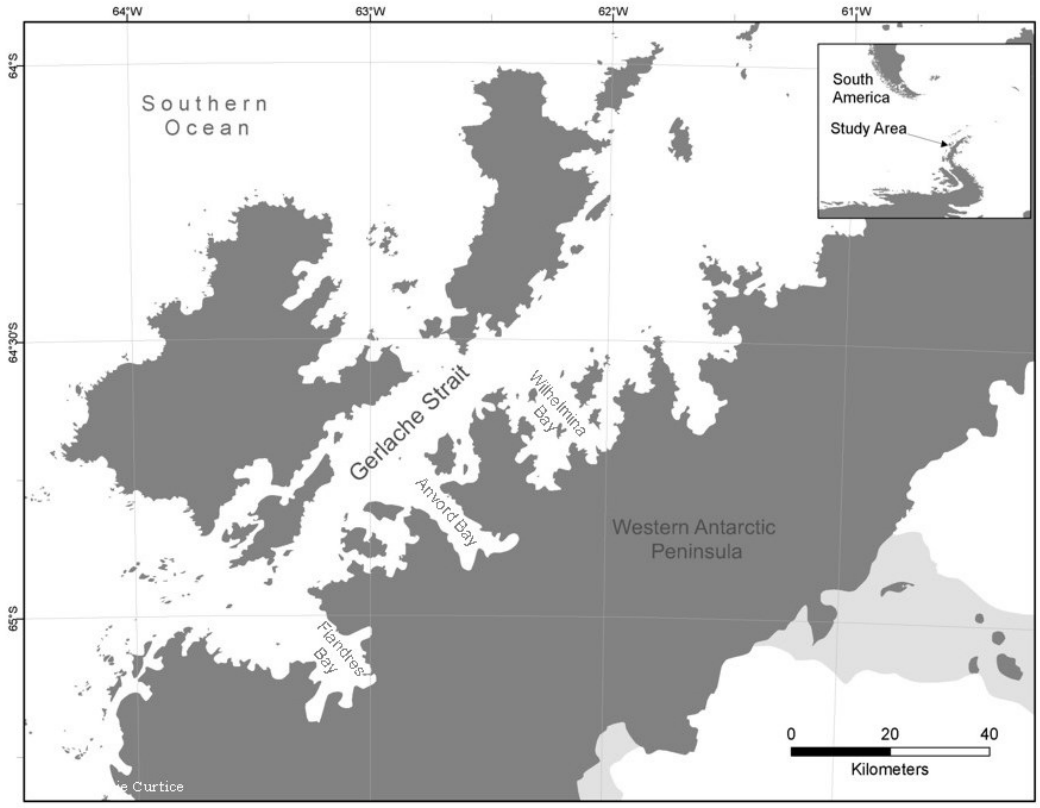

Figure 2: Study sites located along the Western Antarctic Peninsula: Wilhelmina Bay, Anvord Bay, and Flanders Bay.

In 2009, a persistent super-aggregation of Antarctic krill (the largest aggregation of krill reported in 20 years) was observed concurrent with the greatest density of humpback whales ever reported, ranging from 0.02 to 1.75 whales km^{-2} (5.1 whales per km^2, 12.1 % CV; Nowacek et al. 2011) in Wilhelmina Bay. The supper-aggregation of krill ranged from 10s of m to 10s of km in the horizontal plane and from 8 to 410 m in the

vertical plane and had an estimated overall mean krill density of 62 g m^{-3} and total biomass of 2.0 million tons (krill comprised 88.4% of the total measured acoustic backscatter). This aggregation was driven by local physical processes, primarily a small cyclonic eddy that occurred within the bay, which was driven by strong, episodic southerly katabatic winds (the bay had < 10 % occasional brash ice; Nowacek et al. 2011). These winds drove westward Ekman transport and induced a geostrophic northward coastal current (20 cm s^{-1}) off the western coast of the bay and the upwelling of deep nutrient rich MCDW from the Gerlache Strait in the southern and eastern portions of the bay (Nowacek et al. 2011). The eddy margins were nearly coincident with the spatial limits of the krill aggregations and the distribution of humpbacks tightly matched that of the krill aggregation. In 2010, a similarly dense krill aggregation was found in Wilhelmina Bay, however it was concentrated near the opening of the bay in open water; sea ice cover reached 100 % at the head of Wilhelmina Bay (Nowacek et al. 2011, Espinasse et al. 2012). A high density of humpbacks was also observed to be associated with this aggregation (Nowacek et al. 2011, Johnston et al. 2012), which was once again primarily retained by a mesoscale eddy that was located at the bay's mouth (Nowacek et al. 2011, Espinasse et al. 2012).

Anvord Bay is relatively narrow and its circulation appears to be opposite to the two-layer circulation patterns characteristic of an estuary (Nowacek et al. 2011). The surface cooling in the bay forms denser deep water producing the surface inward flow and deep outward flow. Flandres Bay (surveyed in 2010 only) is the warmest of these

three bays as it is located closest to the intrusion of the Gerlache Current. Smaller but still dense aggregations of krill and humpbacks were found in Anvord Bay in 2009 (Nowacek et al. 2011) and 2010 and in Flandres Bay in 2010 (unpublished data). Krill in these bays remained below 150 m instead of migrating to the surface; Espinasse et al. (2012) suggest that they may have been passively reducing their metabolism in preparation for the winter season.

1.3.2 Data Collection

Three-dimensional individual humpback whale diving behavior was inferred from data collected using digital acoustic recording tags (Dtags; Johnson & Tyack 2003) that were attached non-invasively to whales located within the study area (Table 1, Figure 3). The Dtag is a small, lightweight, pressure tolerant and waterproof bio-logging tool developed to continuously collect data on the fine-scale behavior of marine mammals. The Dtag has been successfully deployed on over 15 cetacean species (e.g., Nowacek et al. 2001, Johnson & Tyack 2003, Miller et al. 2004, Nowacek et al. 2004, Zimmer et al. 2005, Woodward et al. 2006, Friedlaender et al. 2009, Hazen et al. 2009, Ware et al. 2011, Wiley et al. 2011, Simon et al. 2012, Goldbogen et al. 2013) and its use has provided insights into several aspects of marine mammal ecology including diving, foraging, and social behavior as well as responses to anthropogenic sound.

Table 1: Whale ID, date, and location for each humpback whale tagged with a Dtag. Total time the tag was on each whale is also included. Whale IDs represent the julian day each individual was tagged and whether the individual was the first (a) or second (b) animal tagged that day.

Whale ID	Date	Location	Total tag time (hh:mm:ss)
122b	2009-May-02	Wilhelmina Bay	18:45:00
127a	2009-May-07	Wilhelmina Bay	25:00:00
136a	2009-May-16	Anvord Bay	23:00:00
140a	2009-May-20	Anvord Ba	22:33:00
148a	2009-May-28	Wilhelmina Bay	25:38:00
152a	2009-June-01	Wilhelmina Bay	22:30:00
132a	2010-May-12	Wilhelmina Bay	23:28:00
133a	2010-May-13	Wilhelmina Bay	22:36:20
139a	2010-May-19	Wilhelmina Bay	20:59:00
139b	2010-May-19	Wilhelmina Bay	23:42:00
146a	2010-May-26	Flandres Bay	20:01:00
151a	2010-May-31	Wilhelmina Bay	25:00:01
155a	2010-June-04	Flandres Bay	24:11:00
155b	2010-June-04	Flandres Bay	22:00:00

Dtags were placed on humpbacks using an 8 m carbon-fiber pole and were attached via four silicon suction cups to the dorsal surface of the animal, between the dorsal fin and the blowhole. Whale behavior was not visibly affected by the tagging (other than immediate startle responses by some), which is consistent with reports from other studies (e.g., Nowacek et al. 2004, Hazen et al. 2009). Preliminary examinations of the tag data suggested that the whales returned to their normal behavior within a few dive cycles.

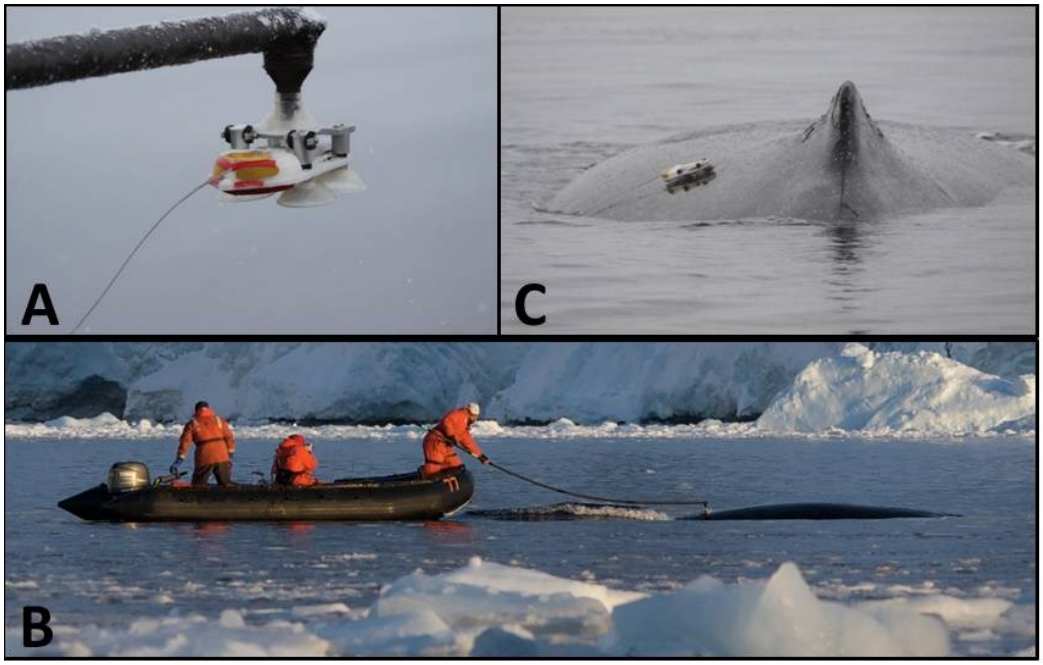

Figure 3: A) Dtag and suction cup attachment with VHF antenna visible at the bottom (Johnson & Tyack 2003); B) successful Dtag attachment; C) Dtag attached to a humpback whale.

The Dtag incorporates a hydrophone (96 kHz sampling rate), a pressure sensor, three-axis accelerometers, three-axis magnetometers, a thermistor (for water temperature), and an embedded VHF transmitter. Data from the pressure sensors, magnetometers, and accelerometers can be used to estimate depth, heading, pitch, and roll, respectively, at 50 Hz for approximately 24 hrs and are stored synchronously with audio data on flash memory within the tag. Prior to deployment, time on the tags was synchronized to GPS time to ensure the ability to synchronize data parameters (e.g., Friedlaender et al. 2009, Hazen et al. 2009) and the tags were de-gaussed to minimize nonlinearity in the magnetic sensor due to hard iron effects (i.e., magnetic fields held by metallic components within the tags; Johnson & Tyack 2003).

Tagged whales were tracked visually during daylight hours from a rigid inflatable boat that stayed within 500 m of the individual; surface behaviors were logged using standard behavioral methodology (Altmann 1974). The geographic position of the tagged whale was determined regularly (every few surfacings) by combining the known location of the inflatable boat, from GPS, and data from laser range finding binoculars used to pinpoint the whale's location in relation to the boat. Photographs of each tagged whale were periodically taken to record the position and orientation of the tag on the whale for calibration and photogrammetric purposes. At night, tagged whales were tracked with directional VHF antennas. An active release, which corrodes in sea water, was timed to release the tag once data storage was complete causing the tag to float to the surface. The VHF signal and a directional antenna were used to locate and retrieve the buoyant tag. Upon tag retrieval, post-tagging calibration was immediately conducted and the data were downloaded via infrared transmission. Post-tagging calibration accounts for hard iron and soft iron effects in the magnetometers (Johnson & Tyack 2003).

Dtags provide a continuous record of the animal's depth and orientation (pitch, roll and heading) during the tagging deployment. I used TrackPlot (Ware et al. 2006); a software program designed to interpret data from tags containing accelerometer, magnetometer, and pressure sensors; to generate a three-dimensional interpretation of each whale's movements while tagged (Figure 4). TrackPlot creates a 'pseudo-track' of the whales movements and behaviors by means of a form of dead reckoning based on

the time series of whale behaviors (Ware et al. 2011) and by assuming that the whale moves forward in the rostral direction. The rate of forward movement at any point on the track is either assumed to be constant (1 m s^{-1}; Goldbogen et al. 2008, Ware et al. 2011) or is based on the rate of depth change for an ascending of descending individual divided by the sine pitch of the angle (Ware et al. 2011). A 4 m wide by 1 m thick ribbon is generated using the whale reference frame time series (caudal, dorsal, and ventral axes) together with depth (Figure 4). A representation of fluke strokes are generated as estimates of the angular accelerations about the lateral axis in whale coordinates (Figure 4). The pseudo-track has been a valuable tool for understanding different kinematic behavioral patterns (e.g., Friedlaender et al. 2009, Hazen et al. 2009, Ware et al. 2011, Wiley et al. 2011, Goldbogen et al. 2013, Ware et al. 2013) and has been shown to accurately depict the individual's movement patterns (Schmidt et al. 2010). When sufficient surface fixes were available, tracks were geo-referenced (i.e., assimilation of known surface fixes to the dead-reckoned track) so that their underwater geographical position could be estimated (Dtags do not record horizontal position information).

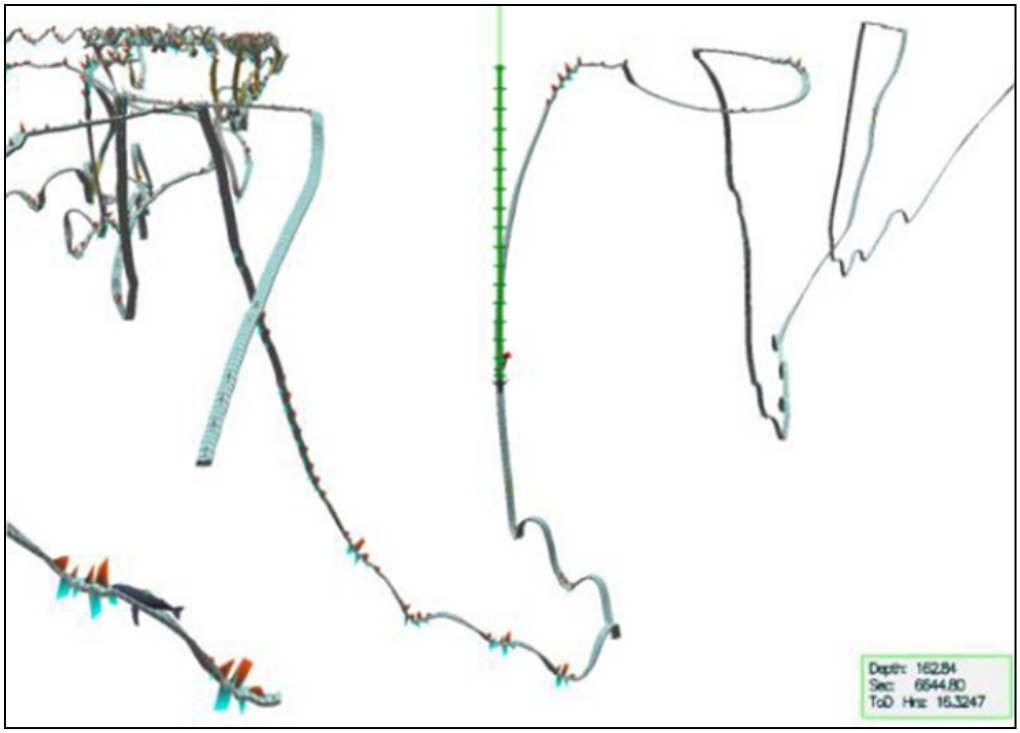

Figure 4: An example of a humpback whale pseduo-track created from data collected with Dtags within TrackPlot (Ware et al. 2006). The blue ribbon represents the whale's pseudo-track, the dashed vertical line represents depth (10 m bars), the horizontal arrow represents magnetic north, and the blue and red wedges along the track represent the magnitude of the frequency of fluke strokes. From Ware et al. (2011).

I identified feeding lunges from the Dtag records following methods detailed in Ware et al. (2011); a collaborative effort of this research. When lunging, a rorqual rapidly accelerates, opens its jaws once a sufficient speed (e.g., 3 m s^{-1}) has been obtained, and then rapidly decelerates due to the drag forces related to the opening of their buccal cavity (Goldbogen et al. 2006, Goldbogen et al. 2007, Potvin et al. 2009); flow noise recorded by the tag simultaneously increases as the animal accelerates and decreases as the animal is slowed. Goldbogen et al. (2006) pioneered a method using flow noise

recorded from hydrophones on tags to pinpoint discrete feeding lunges based on this notion. Ware et al. (2011) used an *in situ* method to estimate each tagged individual's speed to identify feeding luges. Speed was estimated from the rate of ascent or descent when pitched up or down at greater than 45° (speed = Δdepth/[sin(pitch)Δtime]). For sections of the pseudo-track that met this criterion, Ware et al. (2011) sampled 5 s intervals and used a Fourier transform of the tag's acoustic record to compute the average acoustic energy in different bands. Ware et al. (2011) applied a quadratic fit and calculated a regression of the acoustic energy against the estimated speed of the animal. Using the regression coefficients, the speed of the tagged animal at any interval where the animal was submerged could be plotted and feeding lunges could be identified. While this method provides only an estimate of speed, examinations of these speed estimates concurrent with both video footage and accelerometer data confirm that this method can be used to pinpoint lunge feeding events in rorquals (e.g., Goldbogen et al. 2006, Simon et al. 2012, Ware et al. 2013). Therefore, this same process was utilized in my research.

Ware et al. (2011) built an automatic lunge detecting filter within TrackPlot to pinpoint discrete feeding lunges executed by the tagged individuals based on the idea that the most reliable indicator of a lunge is a precipitous drop in the animal's speed. The lunge filter allows the user to examine the animal's estimated speed alongside a pseudo-track of its behavior aligned in time. I used this filter to identify putative lunges executed by each tagged humpback. I confirmed the presence of a lunge if all of the

following criteria (Goldbogen et al. 2006, Goldbogen et al. 2008, Ware et al. 2011, Simon et al. 2012) were met: 1) a bout of fluking associated with a distinct speed maximum; 2) continued swimming and fluking throughout the lunge, particularly during the deceleration; and 3) an isolated group of fluke strokes with a large well-defined excess acceleration followed by a period of gliding. Other aspects of whale behavior recorded by the Dtags such as dive times, maximum dive depths, and post-dive surface times were calculated using custom written code in either MATLAB® (MathWorks 2013b) or R (R Core Team 2013).

2. In Synch? Humpback Whale Mother and Calf Foraging Behavior: Insights from Multi-Sensor Suction Cup Tags*

2.1 Introduction

Synchronized behaviors, animals in proximity to one another, performing the same behavior at the same time, usually in parallel orientation (Fellner et al. 2006), are common in the early stages of cetacean (whale, dolphin, and porpoise) mother-calf relationships (e.g., Bel'Kovich 1991, Gubbins et al. 1999, Fellner et al. 2006). Synchrony serves several functions, such as receiving an aero- or hydrodynamic advantage by slipstreaming (Wiehs 2004, Noren et al. 2008, Noren & Edwards 2011), protection from predators (Norris & Schilt 1988), and social learning via imitation during developmental stages critical to survival (e.g., independent foraging behaviour; Whiten & Ham 1992, Whiten 2001, Fellner et al. 2006, Bender et al. 2009, Sargeant & Mann 2009). Synchronized behaviors observed in mother-calf southern right whale (*Eubalaena australis*) and humpback whale (*Megaptera novaeangliae*) pairs have provided evidence to suggest that mysticetes (baleen whales) and other cetaceans exhibit 'following' behavior (Taber & Thomas 1982, Thomas & Taber 1984, Szabo & Duffus 2008): a maternal strategy in which the offspring accompany their mother soon after parturition and are rarely more than several body lengths from her until they separate permanently (Lent 1974).

*A version of this chapter has been previously published as:
Tyson, R. B., Friedlaender, A. S., Stimpert, A. K., Ware, C., and Nowacek, D. P. (2012). Synchronous mother and calf foraging behaviour in humpback whales *Megaptera novaeangilae*: insights from multi-sensor suction cup tags. Marine Ecology Progress Series. 457: 209-220.

'Following' benefits the mother by not requiring her to return to her offspring and benefits the offspring by gaining maternal vigilance and defense as a means of predator avoidance and protection (Espmark 1971, Lent 1974, Estes 1976, Fisher et al. 2002). Therefore, synchronized behaviors associated with following in cetacean mother-calf pairs may be critical for the success of the pair's behavioral development.

Compared to terrestrial animals that exhibit a following maternal strategy, humpbacks and other baleen whales are constrained in that their young typically suffer from a reduced physiological capacity to dive relative to older conspecifics and therefore do not dive as frequently or as long as their mothers (Würsig et al. 1984, Szabo & Duffus 2008). If the mother-calf pair do not want to lose the benefits of their close proximity when the mother makes long-duration dives (e.g., foraging dives), one individual must actively modify its behavior in relation to the other individual. On a foraging ground in southeastern Alaska, mother humpback whales modified their behavior in the beginning of the foraging season by shortening the duration of their dives whenever their offspring remained at the surface, presumably to minimize the duration of their separation (Szabo & Duffus 2008). Later in the season, however, as the calves grew and gained independence, the mothers became significantly less responsive to their offspring and performed longer dives, thereby forcing their offspring to actively modify their behaviors and increasingly synchronize their dives with their mothers (Szabo & Duffus 2008). This shift has also been documented in southern right whales where calves are primarily responsible for maintaining contact with their mothers at the end of their foraging season (Taber & Thomas 1982). Thus, the mother's foraging efficiency (i.e.,

amount of energy consumed per unit of energy expended while acquiring food) may be low early in the foraging season because she is primarily responsible for maintaining the pair's proximity and may increase later in the season as the calf takes over this responsibility. In addition, once the calf can begin to forage independently, the energetic burden of lactation for the mother will decrease. Humpback calves may begin to feed independently as early as six months old, although they may nurse for up to a year (Van Lennep & Van Utretcht 1953, Chittleborough 1958, Clapham & Mayo 1987).

Humpback whales belong to a group of baleen whales known as rorquals (Balaenopteridae), which in Antarctica forage primarily on small euphausiid crustaceans (e.g., Antarctic krill, *Euphausiia superba*) and other small prey by lunge feeding. Lunge feeding involves accelerating with a burst of energetic fluking towards and engulfing a mass of prey-laden water that may equal be greater than their body mass (Goldbogen et al. 2010). The whales then filter the prey from the ingested water through keratinized plates of baleen and swallow the captured prey. Advancements in bio-logging technologies have enabled a better understanding of the kinematics and energetic costs of lunge feeding in fin (*Balaenoptera physalus*), blue (*Balaenoptera musculus*), and humpback whales (*Megaptera novaeangliae*) (hereafter referred to as rorqauls; Goldbogen et al. 2006, Goldbogen et al. 2007, Goldbogen et al. 2008, Friedlaender et al. 2009, Potvin et al. 2009, Goldbogen et al. 2010, Potvin et al. 2010, Doniol-Valcroze et al. 2011, Goldbogen et al. 2011, Ware et al. 2011, Wiley et al. 2011, Potvin et al. 2012, Simon et al. 2012, Tyson et al. 2012, Friedlaender et al. 2013, Goldbogen et al. 2013, Ware et al. 2013); however, to my knowledge, feeding lunges have not been documented in a mother-calf

rorqual pair. Mother-calf pairs have additional energetic and behavioral costs associated with foraging compared to other non-lactating females and/or adult males, such as the cost of lactation (mother; Lockyer 2007) and the cost of growth (calf). Understanding the foraging behavior of mother-calf pairs is critical to understanding their energetic demands during the calf's first year.

In the Southern Ocean, humpback calves are born in the winter and early spring in calving grounds found off of Australia, Africa, Oceania, and South America (Chittleborough 1965, Mackintosh 1965, Florez-Gonzalez 1991); early August is the peak birth month (Chittleborough 1958, 1965). Several months later, calves migrate with their mothers to their foraging grounds (e.g., Western Antarctic Peninsula (WAP); Mackintosh 1965, Clapham 1996) where they typically remain and forage on euphausiids from late spring through late autumn (Baker et al. 1986, Clapham & Mayo 1987, Baraff & Weinrich 1993). The majority of mother-calf pairs will separate during, or shortly before, their second winter, although a few pairs remain associated for two years (Clapham & Mayo 1987, Baraff & Weinrich 1993).

To my knowledge, all inferences regarding fine-scale baleen whale mother-calf relationships have come from boat- or land-based surface observations, aerial surveys, or from underwater video recordings (e.g. Taber & Thomas 1982, Baker et al. 1986, Baraff & Weinrich 1993, Szabo & Duffus 2008, Zoidis et al. 2008, Cartwright & Sullivan 2009). In this chapter, I used data collected from high-resolution digital acoustic recording tags (Dtags; Johnson & Tyack 2003) to describe the first record of a long-term (~20 hr) continuous underwater relationship and concurrent foraging behavior of a

baleen whale mother-calf pair. I identified feeding lunges executed by both whales and compare the frequency of lunges and related dive parameters, including the number of lunges per dive, maximum dive depth, dive duration, post-dive surface duration, and within-dive inter-lunge interval associated with feeding to assess how these parameters may relate to the energetic demands of each animal. I also examined the synchrony of the pair in terms of their feeding events and their underwater behavior to assess the structure of the pair's relationship. Based on observations made by Szabo and Duffus (2008), I predicted that the pair's association was waning as the calf was likely eight to twelve months old at the time of tagging (i.e., the austral autumn).

2.2 Methods

On May 19, 2010, Dtags (Johnson & Tyack 2003) were attached to an adult female humpback whale and her calf in Wilhelmina Bay to continuously collect data on their fine-scale behavior (WAP; Figure 5). The pair was approached using a rigid-hulled inflatable boat with a four-stroke outboard engine and Dtags were placed non-invasively via suction cups on the dorsal surface of the whales, between the dorsal fin and the blowhole, using an 8 m carbon-fiber pole. The Dtag incorporates a hydrophone (sampling rate up to 96 kHz), a pressure sensor to measure depth, three-axis accelerometers, three-axis magnetometers, and an embedded VHF transmitter. The pressure sensors, magnetometers, and accelerometers measured depth, heading, pitch, and roll, respectively, at 50 Hz, which was stored synchronously with audio data on flash memory (16 GB) within the tag. Prior to deployment, the time on the tags was

synchronized to the GPS time to ensure the ability to synchronize data parameters (e.g., Friedlaender et al. 2009, Hazen et al. 2009).

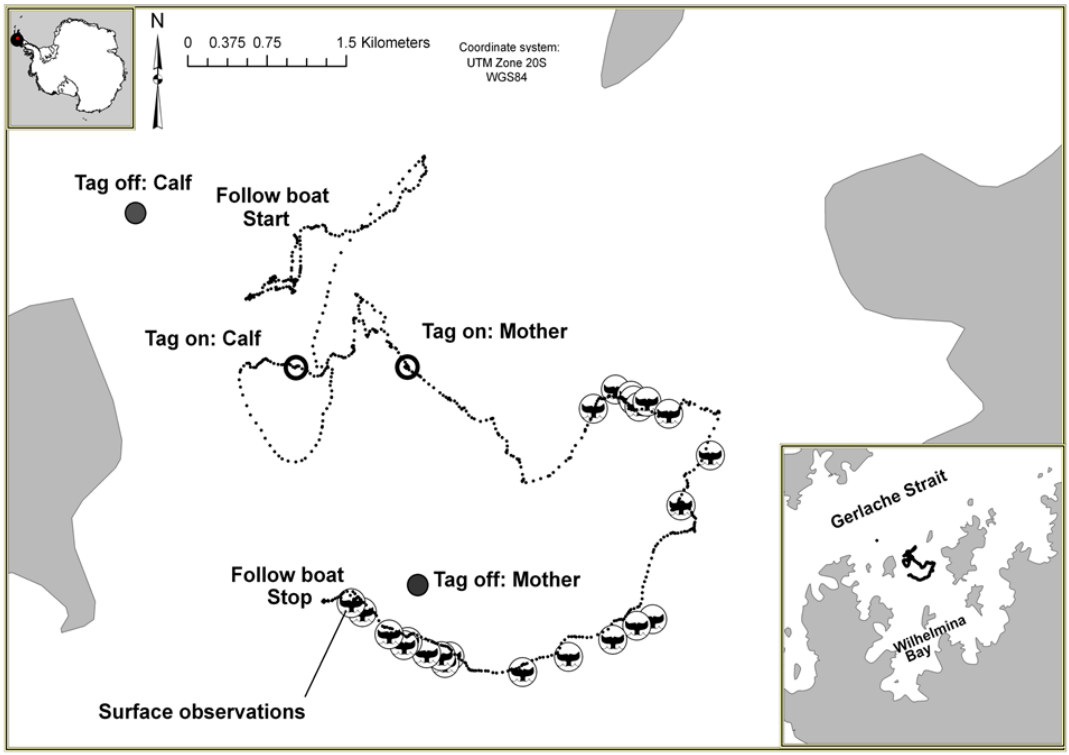

Figure 5: Locations where the mother and calf were tagged (open circles), tracked (dotted line), observed at the surface (fluke symbols), and where their tags released (closed circles); May 19-20, 2010, Wilhelmina Bay, Antarctica. Note that the mother's tag released 4 h 6 min before the calf's tag released; therefore, the separation in tag off locations is not necessarily representative of the pair being separated in space.

The mother was tagged at 11:02:33 (tag start time: 11:02:58 local time, GMT - 5 hr) while the calf was tagged 49 minutes later at 11:51:56 (tag start time: 11:52:17) (Figure 5). Whale behavior was not visibly affected by the tagging (other than immediate startle responses), which is consistent with reports from other studies (e.g., Nowacek et al.

2004, Hazen et al. 2009). The tagged whales were tracked visually during daylight hours (9:11:00 – 14:59:00) from a rigid-hulled inflatable that stayed within 500 m of the pair and they were tracked with directional VHF antennas at night. An active release, which corrodes in seawater, was timed to release the tags once data storage was complete (approximately 24 hours), causing the tag to float to the surface. Tags released from the animals at 7:46:00 (mother) and 11:52:07 (calf) on May 20, 2010. Upon tag retrieval, post-tagging calibration was immediately conducted and the data were downloaded via infrared transmission.

I used TrackPlot (Ware et al. 2006) to visualize and analyze the pair's simultaneous three-dimensional orientations (depth, pitch, roll, and heading). TrackPlot creates a 'pseudo-track' of each whale's movements and behaviors using dead-reckoning based on the time series of whale orientations and by assuming that the whale moves forward in the rostral direction (Ware et al. 2011). The rate of forward movement at any point on the track is either assumed to be constant (1 m sec^{-1}) or is based on the rate of depth change for an ascending or descending individual divided by the sine pitch of the angle (Ware et al. 2011). Dtags do not provide position information (e.g., GPS points) so known fixes need to be integrated to the dead-reckoning process wherever possible to establish horizontal positions. These known fixes were derived from visual observations made by observers in the rigid-hulled inflatable when the animal surfaced during the Dtag deployment. Most of the tag attachment period of this pair, however, was at night and only 30 and 27 geo-referenced locations were made for the mother and calf, respectively, during daylight. Therefore, the lack of fixes for the majority of the

concurrent records (e.g., night-time) hinders me from confidently interpreting the pair's absolute geographic position. Instead, I could only assess the pair's vertical proximity to each other in the water column (i.e., calculated as the difference in depth of the pair at each specific time). I also used TrackPlot to extract summary data for each dive (defined here as an excursion > 10 m; Goldbogen et al. 2006), including dive duration (sec), post-dive surface duration (sec), and the maximum depth (m) of each dive. I synchronized extracted track and dive data in Microsoft® Excel based on the time parameter.

I identified feeding lunges executed by each whale from flow noise recorded on the Dtag hydrophone (Goldbogen et al. 2006, Goldbogen et al. 2008, Ware et al. 2011, Simon et al. 2012). When lunging, a rorqual rapidly accelerates, opens its jaws once a sufficient speed (e.g., 3 m s^{-1}) has been obtained, and then rapidly decelerates due to the drag forces related to the opening of its buccal cavity (Goldbogen et al. 2006, Potvin et al. 2009); flow noise will simultaneously increase as the animal accelerates and decrease as the animal is slowed. Ware et al. (2011) used flow noise as an estimate of speed to successfully detect lunges from humpback whales and developed an automatic lunge-detecting filter within TrackPlot. The lunge filter (which detects precipitous drops in the animal's speed) allows the user to examine the putative lunges and the animal's estimated speed alongside a pseudo-track of its behavior aligned in time. I used this filter to detect feeding lunges executed by the mother and the calf. I also scanned the entire Dtag records in TrackPlot for missed lunges. I excluded lunges detected at a depth shallower than 10 m from analyses due to possible interference from surface interactions (i.e., abrupt changes in flow noise due to surfacing).

I used the following criteria to confirm the presence of a lunge: 1) an isolated bout of fluking (identified from angular accelerations about a lateral axis) associated with a distinct speed maximum, followed by a rapid reduction in speed, followed in turn by a period of gliding; and 2) continued swimming and fluking throughout the lunge, particularly during the deceleration (Goldbogen et al. 2006, Goldbogen et al. 2008, Ware et al. 2011, Simon et al. 2012). I logged the times of the confirmed lunges in Excel and plotted them with the animal's dive profiles. I defined a feeding dive to be any dive for which at least one lunge was detected. I recorded the number of lunges per dive, the dive duration, the post-dive surface duration, and the maximum depth of each feeding dive to examine and compare feeding effort and behavior within and between whales. I performed least-squares linear regressions to determine the relationships between these parameters. Two-sample Students t-tests were computed to assess the probability that these relationships (e.g., dive duration by number of lunges per dive) were significantly different for the mother and for the calf. I also used two-sample Students t-tests to examine the probability that the pair's mean within-dive inter-lunge intervals were significantly different. I used a significance level of 0.05 for all statistical tests. I examined synchrony in terms of feeding events by comparing the time and depth of the pair's lunges.

I evaluated the synchrony of underwater behaviors throughout the concurrent dive records was evaluated using a cross-correlation analysis (Pearson product-moment correlation coefficient for angular and non-angular variables) in the software program R (R Core Team 2013) (R Core Team, 2013). First, to compare the pair's overall similarity in

depth, pitch, roll, and heading, I computed correlation coefficients for both the entire concurrent tag records and at lagged time intervals; correlation coefficients (r) vary from 1.0 (highly positively correlated) to -1.0 (highly negatively correlated), with zero corresponding to no correlation. For the purpose of this chapter, r-values greater than 0.5 indicated that the animals were generally behaving synchronously (i.e., their behaviors were positively correlated) and r-values greater than 0.9 indicated that the animals were behaving very synchronously (Cohen 1988). When lagging the tracks for the cross-correlation analyses, I assumed that if the animals exhibited synchronized behaviors, the cross correlation function would have the greatest correlation at a lag time close to zero. Second, to examine how synchrony changed over the duration of the concurrent tag records and during different behavioral states (e.g., feeding dives versus non-feeding dives), I computed r-values for each dive by comparing the depth, pitch, roll, and heading of each of the mother's dives to the calf's respective depth, pitch, roll, and heading at the same times. I examined the percentage of r-values > 0.5 and > 0.9 to compare differences in synchronized behaviors between behavioral states (e.g., neither animal feeding during the dive, both animals feeding during the dive, only the mother feeding during the dive, only the calf feeding during the dive). Synchrony of diving and surfacing behaviors was examined by pairing synchronized dives in time and then examining their temporal separation in their descent (when they were submerged < 1 m depth) and in their surfacing (when they were > 1 m depth). Synchrony in feeding lunges was also examined by comparing the time and depth of the mother's lunges to the time and depth of the calf's lunges.

2.3 Results

The tags logged 19 hr 54 min of concurrent recordings; data reported hereafter refer only to the time when the two animals were simultaneously tagged (11:51:17 May 19, 2010 – 7:46:00, May 20, 2010). I recorded 285 dives from the mother's tag (maximum depth = 164.04 m, mean ± SD = 59.24 ± 38.19 m) and 281 dives from the calf's tag (maximum depth = 249.80 m, mean ± SD = 46.20 ± 39.32 m). The pair's vertical proximity was within 20 m (approximately two body lengths) for 71.22 % of the records.

2.3.1 Foraging Behaviors

Feeding lunges were identified for both animals (Figure 6). The mother executed 792 lunges over 246 foraging dives while the calf executed 118 lunges over 30 foraging dives (note: lunges were not included if they were executed shallower than 10 m). Prior to feeding, the pair generally rested near the surface (as seen from surface observations during daylight hours) and executed a few exploratory dives (defined here as dives > 50 m where no lunges were executed). The mother then initiated feeding at 16:22:00 and fed continuously and regularly until her tag came off (Figure 6). The calf, however, initiated feeding at 17:00:08 and executed 95.80 % of its lunges by 19:28:21. The mother and calf both lunged between one and multiple times per feeding dive (mean ± SD: 3.22 ± 1.88 and 3.93 ± 2.36 lunges per dive, respectively), with the maximum number of lunges executed per dive equaling eight and nine, respectively (Table 2). The mother's within-dive inter-lunge interval (ILI) was higher and had a smaller variance than the calf's (mean ± SD = 46.33 ± 8.10 and 33.71 ± 10.32 sec, respectively; $t = 13.07$, $df = 634$, $p < 0.01$);

variances between the animals were significantly different ($F = 0.62$, $df = 546$; $p < 0.01$). Additionally, the mother's ILI was consistent throughout the tag record ($y = 0.02\ x + 45.92$, $p < 0.01$) and the change in ILI was not significantly different than zero ($p = 0.82$).

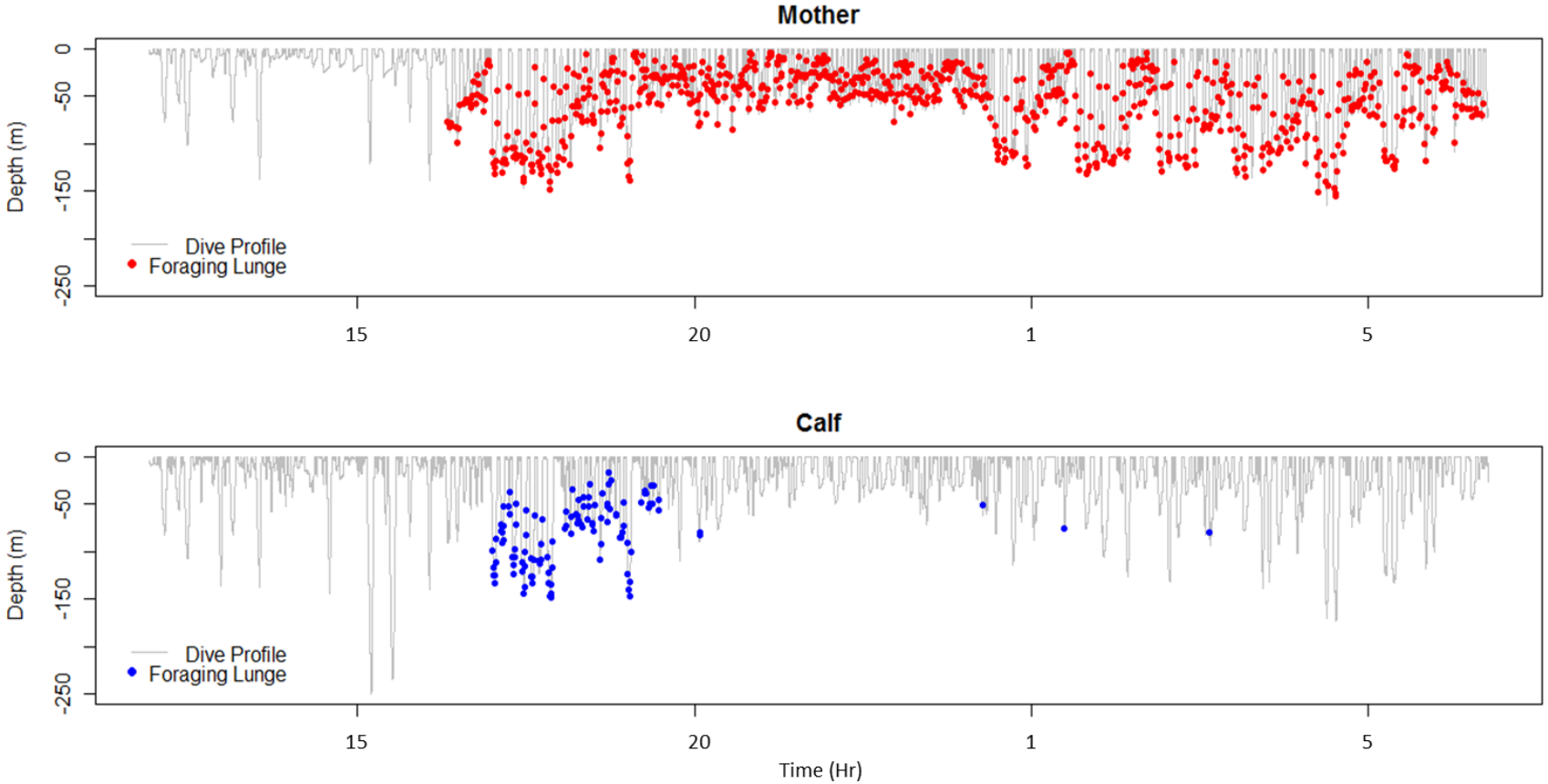

Figure 6: Dive profiles (depth versus time) and foraging lunges executed by the mother (A) and her calf (B) during the duration of the concurrent tag records. Note: simultaneous recordings began at 11:51:17 on May 19, 2011, occurred overnight, and ceased when the mother's tag came off at 7:42:00 on the morning of May 20, 2010.

An increased number of lunges executed on a foraging dive was associated with longer mean dive durations for both animals (mother: $F = 5592$ on 1 and 252 df, $R^2 = 0.96$, $p < 0.01$; calf: F = 33.81 on 1 and 28 df, $R^2 = 0.55$, $p < 0.01$), longer mean post-dive surface durations (mother: $F = 180.90$ on 1 and 252 df, $R^2 = 0.42$, $p < 0.01$; calf: $F = 32.43$ on 1 and 28 df, $R^2 = 0.54$, $p < 0.01$), and deeper mean maximum dive depths (mother: $F = 735.50$ on 1 and 252 df, $R^2 = 0.75$, $p < 0.01$; calf: $F = 55.98$ on 1 and 28 df, $R^2 = 0.67$, $p < 0.01$); these relationships were more consistent for the mother (always increasing) than for the calf (Table 2, Figure 7). Additionally, the calf dove shorter and shallower than its mother when comparable numbers of lunges were executed during a given dive (mother versus calf dive duration by number of lunges: $t = -6.79$, $df = 282$, $p < 0.01$; maximum dive depth by number of lunges $t = 5.45$, $df = 282$, $p < 0.01$, respectively). However, there was no significant difference in the post-dive surface duration between the mother and calf when compared with the number of lunges executed per foraging dive, dive duration, and maximum dive depths (mother versus calf post-dive surface duration by number of lunges: $t = -1.71$, $df = 282$, $p = 0.09$; post-dive surface duration by dive duration: $t = 0.63$, $df = 282$, $p = 0.53$; and post-dive surface duration by maximum dive depth: $t = -0.34$, $df = 282$, $p = 0.71$, respectively).

Table 2: Mean (± SD) values of dive duration (sec), post-dive surface duration (sec), and maximum dive depth (m) per number of lunges executed on a dive.

Number of lunges per dive		1	2	3	4	5	6	7	8	9
Number of dives	Mother	69	23	48	47	27	16	13	3	0
	Calf	5	6	4	3	4	2	4	1	1
Dive duration	Mother	36.20 ± 9.53	94.68 ± 15.40	151.78 ± 20.52	209.61 ± 27.28	260.03 ± 36.39	309.39 ± 23.93	354.07 ± 21.01	387.60 ± 32.02	—
	Calf	172.64 ± 74.91	156.93 ± 86.95	149.80 ± 21.54	186.93 ± 31.19	220.40 ± 47.90	310.40 ± 2.26	294.60 ± 25.21	346.40	382.40
Post-dive surface duration	Mother	21.22 ± 18.83	25.60 ± 18.58	34.67 ± 27.27	62.55 ± 33.69	67.97 ± 42.07	97.92 ± 54.19	89.27 ± 41.90	140.4 ± 16.74	—
	Calf	30.72 ± 30.29	54.13 ± 43.04	45.20 ± 28.43	45.87 ± 32.62	81.40 ± 52.19	97.20 ± 14.14	147.80 ± 45.73	129.60	172.00
Maximum dive depth	Mother	22.21 ± 6.11	45.38 ± 14.18	66.06 ± 16.35	75.80 ± 25.52	87.24 ± 26.40	113.53 ± 25.07	125.99 ± 21.00	138.19 ± 11.25	—
	Calf	64.33 ± 21.21	60.87 ± 16.05	71.67 ± 11.20	84.24 ± 20.72	78.20 ± 8.13	140.02 ± 10.25	118.36 ± 19.08	146.79	150.36

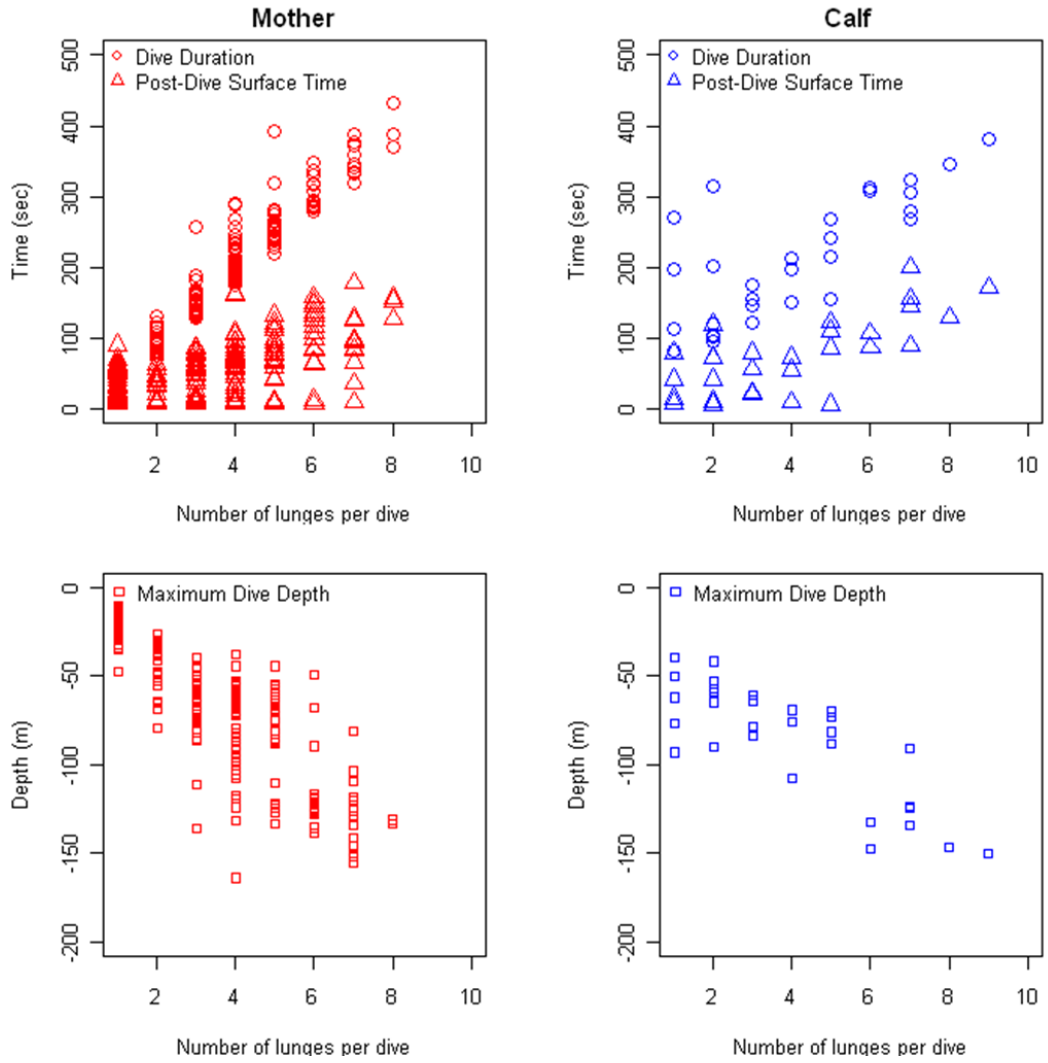

Figure 7: Mean dive durations (sec), post-dive surface durations (sec), and maximum depth (m) values for foraging dives executed by the mother and its calf.

2.3.2 Synchronous Behaviors

Cross-correlation analyses of the mother and calf's depth, pitch, roll, and heading for the entire concurrent tracks were derived to determine the correlation of the pairs' behaviors. Depth was positively correlated ($r = 0.62$, $p < 0.01$) and was greatest when the calf's track lagged behind the mother's track by 4.5 sec ($r = 0.62$, $p < 0.01$). Pitch and heading were also positively correlated (pitch: $r = 0.35$, $p < 0.01$; heading: $r = 0.36$, $p <$

0.01); however, this correlation was weaker than the correlation for depth. Pitch and heading were most correlated when the calf's track lagged behind the mother's track by 5 and 11 sec, respectively. Rolling was not significantly correlated ($r = 0.02$, $p < 0.01$) and was therefore not considered in further analyses. Correlation coefficients calculated for depth, pitch, and heading for each dive varied during the concurrent tag record and will be discussed in more detail below. In terms of their diving and surfacing behaviors, the pair dove and surfaced within ± 20 sec of each other for 57.81 % and 44.40 % of their dives, respectively. Within these ± 20 sec dives, the mother dove and surfaced before the calf 45.27 % and 54.78 % of the time while the calf dove and surfaced before the mother 20.95 % and 33.91 % of the time; the pair dove and surfaced at approximately the same time (within ± 1 sec) 33.78 % and 11.30 % of this time, respectively.

Correlation coefficients calculated for the pair's depth, pitch, and heading varied throughout the concurrent tag records and between behavioral states (Figures 8 and 9). Depth and pitch were highly positively correlated at the beginning of the concurrent record when the animals were resting and gradually weakened when the pair became more active and started making exploratory dives (~15:30:00) (Figure 8 A, B); heading showed a similar pattern but with lower *r*-values overall (Figure 8 C). Correlation coefficients were highly positively correlated again when the mother initiated feeding (16:22:00) and strengthened further when the calf joined its mother in feeding (17:00:08). After the calf stopped feeding (19:28:21), and for the remaining duration of the concurrent records, the correlation coefficients were variable, with lower *r*-values occurring when the mother was feeding at shallow depths in the middle of the night

(presumably following the diel vertical migration of krill; Espinasse et al. 2012, Friedlaender et al. 2013) and higher *r*-values when the mother was performing deeper foraging dives later in the morning. The percentage of *r*-values for depth, pitch, and heading that were > 0.5 and > 0.9 for the varying behavioral states (Figure 9) are shown in Table 3 (note: there were no dives during which only the calf was foraging).

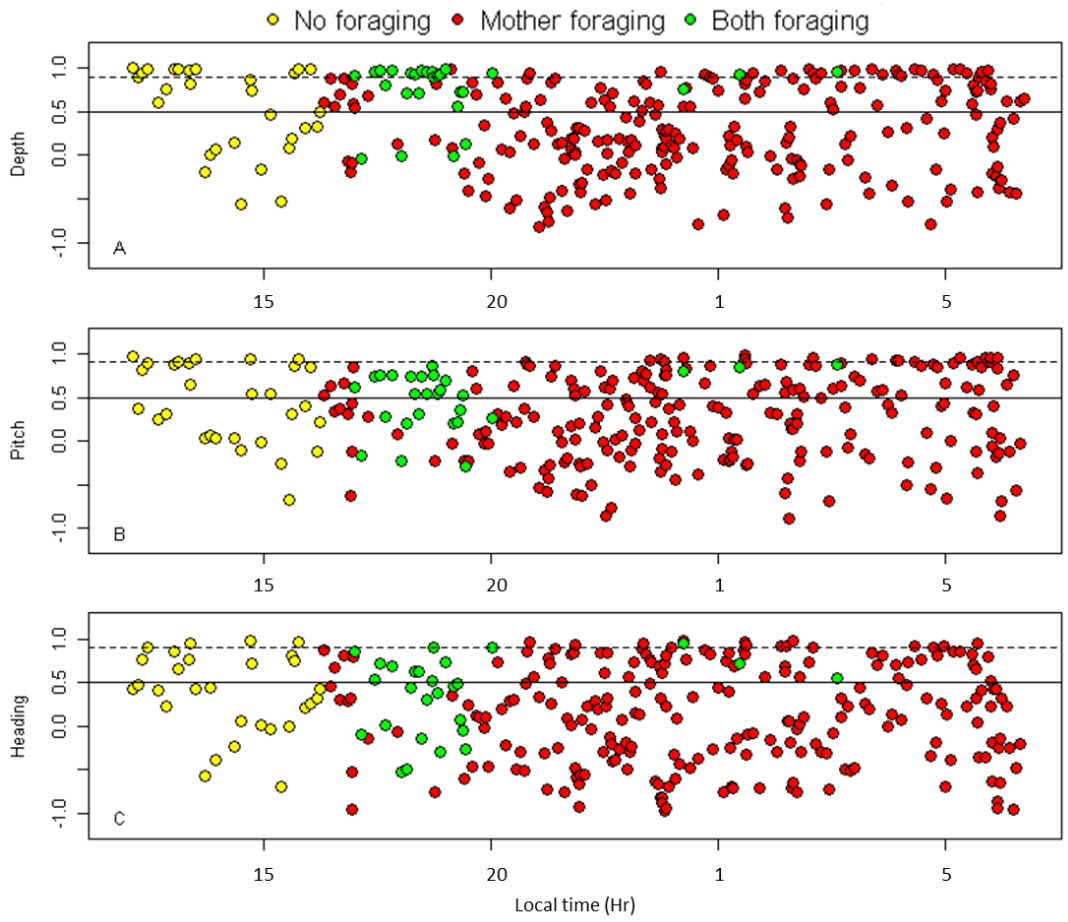

Figure 8: Pearson's product-moment correlations coefficients calculated for each dive for the duration of the concurrent tag records: A) correlation of depth behavior; B) correlation of pitch behavior; and C) correlation of heading behavior. The solid horizon line represents *r* = 0.5 (i.e., synchronized behavior), while the dashed horizontal line represents *r* = 0.9 (i.e., highly synchronized behavior).

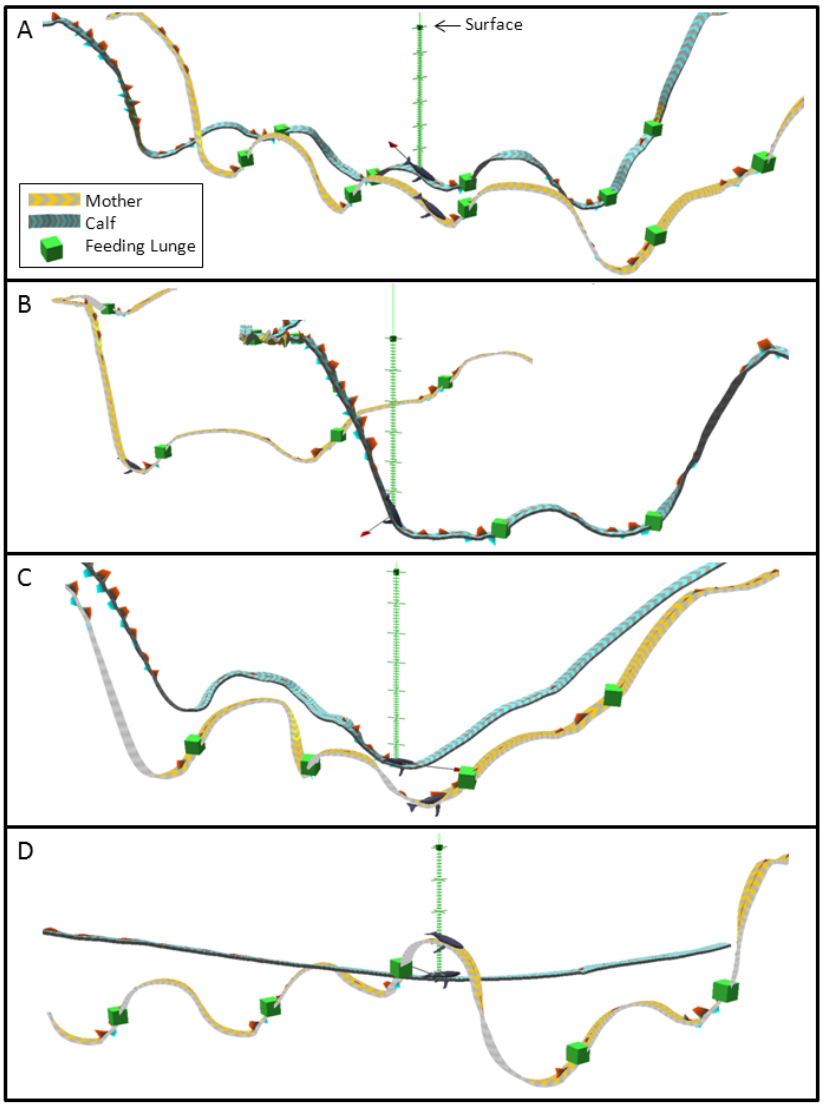

Figure 9: Three-dimensional visualizations of the mother and calf's dive behavior during varying behavioral states (TrackPlot, Ware et al. 2006). The mother's track is yellow while the calf's track is blue; feeding lunges are represented as green boxes on the pseudo-track. The dashed vertical line represents depth (10 m increments from the surface), the horizontal arrow represents magnetic north, and the wedges along the track represent the magnitude and frequency of fluke strokes (identified from angular accelerations about a lateral axis). Note: horizontal proximity is approximated based on surface fixes (N = 30, 27 for the mother and calf, respectively) and dead-reckoning techniques and may not represent the true horizontal proximity. A) A synchronized dive during which both animals are foraging; B) an unsynchronized dive during which both animals are foraging; C) a synchronized dive during which the mother is foraging and the calf is not foraging but swimming nearby; and D) an unsynchronized dive during which the mother is foraging and the calf is not foraging and not swimming synchronously.

Table 3: Percent of correlation coefficients that were greater than 0.5 (synchronous behaviour) and greater than 0.9 (highly synchronous behaviour) for the pair's depth, pitch, and heading.

	Depth	Pitch	Heading
Neither foraging	62.07, 34.48	48.28,17.24	37.93, 10.34
Both foraging	85.19, 59.26	62.96, 0.00	48.15, 11.11
Only mother foraging	36.36, 10.45	38.18, 9.09	31.36, 6.36

Values are percentages of r values > 0.5, > 0.9

Lunges performed by the calf appeared to be synchronized with lunges performed by its mother in terms of time and depth. Indeed, 84.26 % and 79.63 % of the calf's lunges were performed within ± 20 sec and within ± 20 m, respectively, of its mother's lunges while 35.19 % and 53.70 % were performed within ± 5 sec and within ± 5 m, respectively. Of these, the mother lunged before the calf 60.19 % of the time and shallower than the calf 52.78 % of the time. In addition, 97.46 % of the calf's lunges were executed during a dive in which its mother was also foraging. The mother, however, did not appear to forage based on whether or not her calf was simultaneously foraging or exhibiting synchronized behaviors (based on the continuity and regularity of her within-dive ILIs).

2.4 Discussion

This analysis represents the first record of a long-term (~20 hr) continuous underwater relationship and concurrent foraging behavior of a baleen whale mother-calf pair. Because the calf that was tagged was likely between eight and 12 months old (assuming it was born in the previous winter or early spring), my findings represent a

snapshot of the period of time when the calf was gaining independence and was becoming more responsible for maintaining proximity to its mother. This is supported by the mother's foraging behavior, which did not appear to change according to changes in the calf's behavior (e.g., her ILI was consistent and stable for the duration of the time she spent foraging, despite changes in the calf's behavior), and was instead likely a function of the vertical position of the prey (Croll et al. 2005, Friedlaender et al. 2009, Hazen et al. 2009, Goldbogen et al. 2011). In accordance, the calf appeared to be primarily responsible for altering and synchronizing its behaviors to its mother throughout the concurrent tag records. This is similar to other humpback whale calves (Szabo & Duffus 2008, Cartwright & Sullivan 2009), southern right whale calves (Taber & Thomas 1982, Thomas & Taber 1984), and other mammals, such as infant rhesus monkeys (*Macaca mulatta*) (Berman 1980), during the later stages of the mother-offspring relationship.

While both animals exhibited feeding lunges, there were some striking differences in the frequency and duration of their foraging behaviors that likely correspond to the changes associated with the calf gaining nutritional independence and weaning. For instance, as previously stated, once the mother began feeding, she continued to consistently and regularly feed without resting for any significant period of time. In addition, she executed more lunges ($N = 792$) than have been previously been described for other adult humpback whales (unknown age/sex) tagged for similar durations in the WAP (Ware et al. 2011). These findings may be explained by her spending less energy on her calf due to the calf's decreasing vulnerability to being left

alone more frequently and for longer periods of time, and spending more energy attending to the increased demands on her personal fitness (e.g., replenishing energy reserves diminished from lactation and the recent migration, and increasing energy reserves for successful future migrations and successful rearing of additional offspring).

While the calf may have still been nursing (although we saw no apparent evidence of its occurrence), the calf executed 118 feeding lunges over 30 dives. Interestingly, the calf primarily foraged between 17:00:08 and 19:28.21. There are several potential reasons for why its foraging behavior was so discrete in frequency and in duration. First, if the calf was still nursing then its feeding lunges were likely to obtain supplemental energy in addition to nursing. Second, the calf may require proportionally less food than larger animals to support its resting metabolism. Third, when young animals are less active their metabolic rates decline (Arnould et al. 2003) and energy is preferentially allocated to growth (Sibley & Calow 1986). Thus, it may be beneficial for the calf to spend only a small portion of its time feeding and a larger portion of its time either resting near the surface or swimming in synchrony with its mother gaining the associated hydrodynamic advantage (Noren et al. 2008, Noren & Edwards 2011). This would allow the calf to dedicate more of its energy to growth, which is important for its survival; a large body size reduces the costs associated with travel during migrations (Williams 1999), increases the individual's breath holding and oxygen storage capacity (Schreer & Kovacs 1997), reduces the risk of predation (Chittleborough 1958), and enhances future reproductive success (Spitz et al. 2002).

While adult rorqual dives have been characterized by a gliding descent with a low rate of fluking, a series of lunges at depth, and an ascent to the surface powered by steady fluking (Goldbogen et al. 2006, Goldbogen et al. 2008), preliminary examinations of the calf's dive plot reveal that the calf beat its flukes frequently on the descent, performs a series of lunges at depth, and then ascends to the surface with few, if any, fluke strokes. Positively buoyant whales, such as right whales (*Eubalaena glacialis*; Nowacek et al. 2001) and sperm whales (*Physeter macrocephalus;* Miller et al. 2004) are known to actively stroke to depth and glide during ascent. Aoki et al. (2011) found that an increase in fat content in a Northern elephant seal (*Mirounga angustirostris*) resulted in an increased descent stroke rate and decreased ascent stroke rate. This suggests that the calf is more buoyant than its mother and must expend more energy to stay submerged. Further work to characterize buoyancy and fluking effort differences between mother and calf pairs should be conducted to examine this hypothesis more closely.

The frequency of lunges executed per dive has been associated with deeper maximum dive depths, longer dive durations, and longer post-dive surface durations in humpback whales (Dolphin 1987a, c, Goldbogen et al. 2008, Ware et al. 2011), fin whales (Croll et al. 2001, Acevedo-Gutierrez et al. 2002, Goldbogen et al. 2006, Goldbogen et al. 2007), and blue whales (Croll et al. 2001, Acevedo-Gutierrez et al. 2002, Goldbogen et al. 2011). Our results (Figure 7, Table 2) are consistent with these findings and thus provide further support for the hypothesis that lunge feeding is energetically costly. Interestingly, the mother and calf had proportionally equivalent post-dive surface durations (i.e., recovery times) when considering the number of lunges executed per

dive, dive durations, and maximum dive depths. This suggests that foraging dives executed by the mother and calf of comparable foraging effort were equivalently energetically costly. Despite this, the calf dove shallower and had shorter dive durations than its mother for comparable number of lunges executed per dive. These findings are likely related to the calf's limited oxygen capacity and possibly greater buoyancy. The duration for which a diving animal can remain underwater is related to its oxygen storage capacity, the rate at which it uses stored oxygen, and its anaerobic capacity (Schreer & Kovacs 1997); as such, larger animals are better equipped to dive. Thus, a humpback calf should exhibit shorter dives for similar dive depths and durations than its larger mother.

My results also further support the hypothesis that humpback whales exhibit a following maternal strategy (Lent 1974, Szabo & Duffus 2008). While the pair was not always traveling together, they were within a vertical distance of ± 20 m for 71.40 % of the concurrent records and exhibited a high percentage of synchronized dives in terms of their depth, pitch, and heading (Figure 9, Table 3). In addition, the pair's depth was most highly correlated when the calf's track was lagged 4.5 sec behind its mother. Also, when the calf was feeding, it lunged after its mother 60.2 % of the time. These findings suggest that the pair were generally traveling and feeding in synchrony with each other with the calf traveling and feeding closely behind.

Interestingly, a higher percentage of positively correlated dives were found when both animals were feeding than when neither animal was feeding or when just the mother was feeding. There are several beneficial reasons for the calf to synchronize its

feeding behavior with its mother, including learning how to forage and/or benefiting from the food its mother has found. In addition, synchrony during foraging may ease the energetic costs associated with foraging for the calf by gaining the hydrodynamic advantages associated with synchronized swimming (Noren et al. 2008, Noren & Edwards 2011). This may contribute to the equivalent recovery times we found for the mother and the calf for comparable foraging dive efforts. When the calf was not feeding, it would go in and out of synchrony with its mother (shown by the fluctuation in r values; Figure 9), generally behaving independently of its mother when its mother was feeding near the surface and re-synchronizing its behaviors when the mother made deeper feeding dives. This suggests that while the mother was feeding near the surface, the calf could behave independently of its mother while maintaining a close proximity but when the mother executed deeper dives, the calf had to join and synchronize its behavior in order to maintain similar levels of proximity.

While my findings only represent ~20 hrs of a single humpback whale mother-calf pair, they demonstrate how bio-logging tools can enhance our understanding of marine animals during periods that are critical for their behavioral development. It is important to note that the behavior of mother-calf pairs can vary widely across pairs and over time (Taber & Thomas 1982, Cartwright & Sullivan 2009) and therefore more tags need to be deployed on additional mother-calf pairs at varying times during the first year of their relationship. Such attempts should take the appropriate measures to minimize disturbance during tagging, however, as mother-calf pairs may be more

sensitive to boat approaches than groups of adults (Stimpert et al. 2012). These efforts will enable us to gain a better understanding of early baleen whale behavioral ontogeny.

3. How Should a Clever Whale Allocate Foraging Time and Effort

3.1 Introduction

Optimal foraging theory (OFT) suggests that organisms should favor foraging strategies that are efficient in minimizing costs (e.g., time, energy) while simultaneously maximizing benefits (e.g., energy, nutrients) (Macarthur & Pianka 1966). Models based on this premise have been developed to examine the efficiency of foraging behaviors in air-breathing diving animals, such as birds and marine mammals, under the framework of central-place foraging (Orians et al. 1979), where the surface acts as the central place (Houston & Mcnamara 1985) (e.g., Croll et al. 2001, Thompson & Fedak 2001, Acevedo-Gutierrez et al. 2002, Doniol-Valcroze et al. 2011, Heaslip et al. 2014). One of the most widely used models for this purpose is a time-allocation model developed by Kramer (1988) and later modified by Houston and Carbone (1992), which predicts the optimal foraging, dive, and surfacing durations of divers in response to changes in foraging depth. The model is based on the assumption that the amount of time traveling to and from a prey patch will increase with increasing prey patch depth. Consequently, the amount of time spent recovering on the surface after a dive will increase (Kooyman & Ponganis 1998) and the proportion of time available for foraging will decrease (Kramer 1988, Houston & Carbone 1992). Under these assumptions, air-breathing diving animals should spend the amount of time at the surface obtaining oxygen that will maximize the proportion of time spent in the foraging area (Kramer 1988, Houston & Carbone 1992).

Given the cost in energy and time of deep dives, animals should prefer to feed at shallow depths if prey can be obtained equivalently (Charnov 1976). When prey patch structure varies by depth, however, divers should forage within shallower patches until the search, capture, and handling of prey times outweigh the net energetic gain from consumption (Macarthur & Pianka 1966). When forced to dive to greater depths to find sufficient prey patches, divers should adjust time allocation within their dives by, for example, increasing their ascent and/or descent rates to maximize bottom time (Mori 1998, Doniol-Valcroze et al. 2011). This change in behavior may allow them to compensate for travel costs by increasing their rate of prey encounters and ultimately prey captures (Thompson & Fedak 2001).

It has been assumed that rorquals (i.e., Balaenopterids) forage according to OFT (Dolphin 1987b, 1988, Hazen et al. 2009, Doniol-Valcroze et al. 2011); however, this has been hard to test quantitatively due to the difficulty in describing their foraging behavior at depth, specifically in direct relation to prey access and availability. Acevedo-Gutierrez et al. (2002) were the first to use an OFT model to examine foraging behaviors in rorquals. They found that the foraging dives of blue (*Balaenoptera musculus*) and fin whales (*Balaenoptera physalus*) measured with time-depth recorders were shorter than predicted by OFT (Houston & Carbone 1992) and suggested that this was due to a high cost of lunge feeding. Lunge feeding has been deemed as the largest biomechanical event to take place on earth (Brodie 1993) because it involves accelerating with a burst of energetic fluking towards a prey patch then rapidly decelerating as the whale opens its buccal cavity to approximately 75 degrees (Brodie 1993) to consume a mass of prey-

laden water that may be greater than the whale's total body mass (Goldbogen et al. 2010). Doniol-Valcroze et al. (2011) similarly predicted dive durations of blue whales but also took into consideration their lunging rates (inferred from estimates of the whale's swim speeds *sensu* Goldbogen et al. 2008) and updated estimates of their metabolic rates (Potvin et al. 2009, Goldbogen et al. 2010). They found that an optimal framework did predict blue whale foraging patterns: blue whales increased their foraging times within dives to compensate for longer travel durations and to optimize resource acquisition, and shallow dives were short and yielded the highest feeding rates (Doniol-Valcroze et al. 2011).

In this chapter, I predicted the optimal foraging durations, dive durations, and post-dive surface durations of humpback whales (*Megaptera novaeangliae*) following Houston and Carbone (1992). I compared the predicted durations to observed durations recorded with high-resolution, multi-sensor digital acoustic recording tags (Dtags; Johnson & Tyack 2003) that were attached to humpback whales foraging in the Western Antarctic Peninsula (WAP) (Nowacek et al. 2011, Stimpert et al. 2012, Tyson et al. 2012, Friedlaender et al. 2013) and assessed model agreement. Based on previous observations of rorqual foraging behavior (e.g., Dolphin 1987b, 1988, Acevedo-Gutierrez et al. 2002, Hazen et al. 2009, Doniol-Valcroze et al. 2011, Friedlaender et al. 2013), I predicted that humpback whales in the WAP would allocate their time according to OFT: during a dive, humpbacks would maximize the proportion of time available for foraging and minimize the proportion of time required for traveling and recovering at the surface regardless of dive depth.

3.2 Methods

3.2.1 Observed Whale Behavior

Three-dimensional individual humpback whale diving and foraging behaviors were inferred from digital acoustic recording tags (Dtags) attached non-invasively to whales in Wilhelmina Bay, Anvord Bay, and Flanders Bay (WAP) between May and June 2009 and between June and July 2010. Dtags incorporate a pressure sensor, three-axis accelerometers, and three-axis magnetometers to measure depth, heading, pitch, and roll, respectively, at 50 Hz during the tag deployments as well as a hydrophone (sampling rate of 96 KHz) and a an embedded VHF transmitter (Johnson & Tyack 2003). Recorded measurements were stored synchronously with audio data on flash memory within the tag. Dtags were placed on humpbacks using an 8 m carbon-fiber pole and were attached via four silicon suction cups to the dorsal surface of the animal, between the dorsal fin and the blowhole. Whale behavior was not visibly affected by the tagging (other than immediate startle responses by some), consistent with other studies (e.g., Hazen et al. 2009, Nowacek et al. 2011).

Tagged whales were tracked visually during daylight hours from a rigid inflatable boat that stayed within 500 m of the individual; surface behaviors were logged using standard behavioral methodology (Altmann 1974) to calibrate measurements recorded by the tag. Photographs of each tagged whale were periodically taken to record the position and orientation of the tag on the whale for calibration and photogrammetric purposes. At night, tagged whales were tracked with directional VHF antennas. An active release, which corrodes in sea water, was timed to release the tag once data

storage was complete (approximately 24 hrs) causing the tag to float to the surface. The VHF signal and directional antenna were used to locate and retrieve the buoyant tag. Upon tag retrieval, post-tagging calibration was immediately conducted and the data were downloaded via infrared transmission. Post-tagging calibration accounts for hard iron and soft iron effects in the magnetometers (Johnson & Tyack 2003).

I used TrackPlot (Ware et al. 2006) to generate a three-dimensional time series (i.e., a pseudo-track) of each whale's estimated movements (see Ware et al. 2006, Ware et al. 2011; Figure 10) and it's embedded automatic lunge detector to identify feeding lunges. This detector pinpoints putative lunges using an algorithm that finds distinct fluctuations in the flow noise recorded by the hydrophone within the Dtag, which are indicative of the whale's speed (Ware et al. 2011) and hence the rapid accelerations and decelerations characteristic of lunging (Goldbogen et al. 2006, Ware et al. 2011). I only confirmed the presence of a lunge if all of the following were observed: (1) an isolated bout of fluking associated with a distinct speed maximum, followed by a rapid reduction in speed, followed in turn by a period of gliding; (2) continued swimming and fluking throughout the lunge, particularly during the deceleration phase (Goldbogen et al. 2006, Goldbogen et al. 2008, Ware et al. 2011, Simon et al. 2012, Tyson et al. 2012); and (3) the whale was deeper than 3 m (lunges executed shallower than 3 m were excluded from analyses due to detection capabilities being diminished because of surface interactions; i.e., abrupt changes in flow noise when the whale surfaced). I also scanned all pseudo-tracks for missed lunges and manually added that adhered to these criteria to the database.

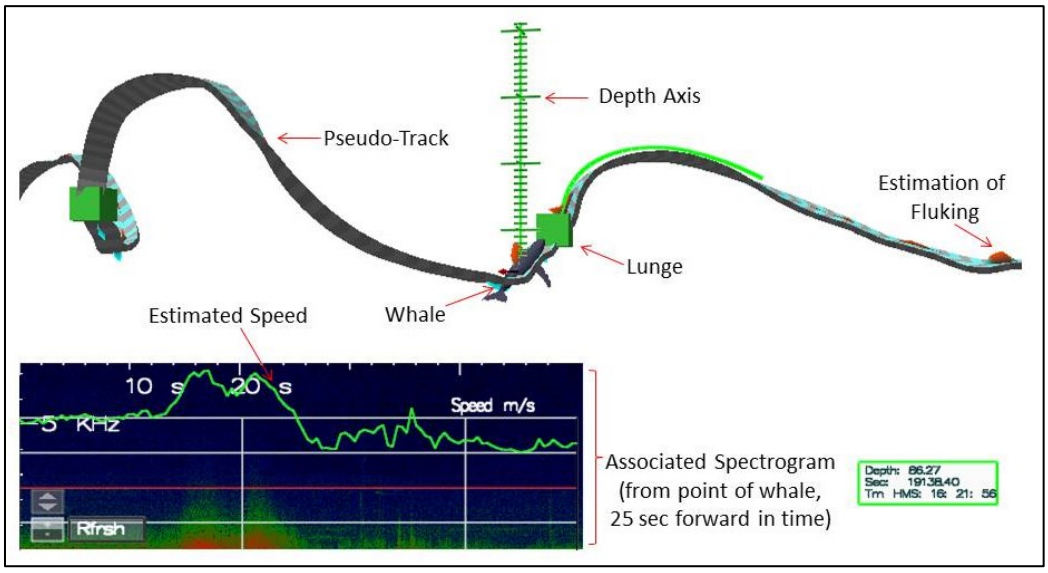

Figure 10: A whale's pseudo-track with associated acoustic spectrogram and estimated speed (green line overlaid onto spectrogram) shown in TrackPlot (Ware et al. 2006). The drop in speed shown on the spectrogram is indicative of a lunge performed by the whale, which is represented as a green box on the pseudo-track.

I used custom code built for Dtag analyses to determine the dive durations, post-dive surface durations, and maximum dive depths of each dive (defined as any submergence greater than 3 m) for each tagged whale in the software program MATLAB® (Johnson & Tyack 2003, MathWorks 2013b). I defined feeding dives as any dive for which a feeding lunge was detected (Friedlaender et al. 2013) and used the software program R (R Core Team 2013) to assign the appropriate lunge counts to each feeding dive.

3.2.2 Optimal Model Based On Time Allocation

I used a time allocation OFT model (Houston & Carbone 1992) to compare the foraging behaviors of humpback whales inferred from the Dtags to those predicted by OFT. I divided observed feeding dives into three parts for use in the model: i) travel duration, τ; ii) foraging duration, t; and iii) post-dive surface duration, s (Kramer 1988, Houston & Carbone 1992). I calculated t as the duration of time starting from the moment the first lunge was executed (i.e., mouth opening) on a dive to the moment the last lunge on that dive was completed (this included an estimated filter duration for an average sized humpback whale (13.00 sec; Goldbogen et al. 2012). I considered τ to be total dive duration, u ($u = \tau + t$), minus t.

Following Houston and Carbone (1992), I assumed that a whale that spends time s on the surface following a dive gained oxygen as:

$$x(s) = K(1 - e^{-as}), \quad (1)$$

where K is the total oxygen storage capacity and α is the initial proportional exchange rate of oxygen at the surface. While diving, I assumed that a whale would use oxygen at a rate of m_τ when traveling and m_t when foraging (Kramer 1988, Houston & Carbone 1992, Carbone & Houston 1996) and that all feeding dives were balanced (Houston & Carbone 1992): all of the oxygen stored prior to each dive would be used during the present dive (in contrast to all of the oxygen that can be stored; Houston 2011):

$$x(s) - m_\tau \tau + m_t t = 0. \quad (2)$$

(i.e., the dives are aerobic). In addition, I assumed that a whale would maximize the proportion of time during a dive cycle (π) foraging:

$$\pi = \frac{t}{t + \tau + s}, \tag{3}$$

which is equivalent to maximizing $t/(\tau + s)$ (see Houston & Carbone 1992). I eliminated t from this proportion with its equivalent from equation 2 to get:

$$\pi(s) = \frac{x(s) - m_\tau \tau}{m_t(s + \tau)}. \tag{4}$$

The value of s^* that maximizes equation 4 also maximizes t (Houston & Carbone 1992). Because the optimality condition states that $\pi' = 0$ and because $x'(s) = m_\tau$, I simplified equation 4 to get:

$$x(s) - m_\tau t = x'(s)(s + \tau) \tag{5}$$

I then determined the optimal surface duration, s^*, for a given dive as a function of τ, m_τ, K, and α by solving

$$K\left(1 - e^{-as^*}\right) - m_\tau \tau - \alpha K e^{-as^*}(s^* + \tau) = 0 \tag{6}$$

numerically for s^* (Houston & Carbone 1992, Stephens et al. 2008) (Table 4).

Table 4: Descriptions, equations, and values of parameters used in the optimal model. *m_τ was converted from W to L O_2 s^{-1} for use in the optimal model. The calculation of m_τ factors in an estimated energetic savings attributed to gliding behaviors (Williams 2001).

Parameter	Description (units)	Equation	Value	Reference
L	Length (m)		13.45	Clapham and Mead (1999)
M	Body Mass (kg)	16.473 x $L^{2.95}$	35196.82	Lockyer (1976)
K	Total oxygen storage capacity (L)	0.03 x $M^{1.05}$	1782.17	Stephens et al. (2008)
α	Initial rate of oxygen replenishment (s^{-1})	0.09 x $M^{-0.33}$	0.02	Stephens et al. (2008)
m_τ	Metabolic rate while traveling (W)	6 x 4 x $M^{0.75}$	2.95	Potvin et al. (2012)
m_τ	*Metabolic rate while traveling (L O_2 s^{-1})	m_τ – (m_τ x 0.28)	2.12	Williams (2001)
m_t	Metabolic rate while foraging (L O_2 s^{-1})	1.78 x m_τ	3.78	Potvin et al. (2009), Goldbogen et al. (2010), Donio-Valcroze et al. (2011)
V	Vertical speed (m s^{-1})		1.00	Goldbogen et al. (2008), Ware et al. (2011)

I determined the values of s^* for an average sized humpback whale (13.45; Clapham & Mead 1999) diving to depths ranging from 0 – 400 m (depths are representative of the study region's bathymetry). I assumed a constant vertical speed (V) of 1 m s^{-1} to express t as a function of target depth in the model as suggested by Doniol-Valcroze et al. (2011) (i.e., target depth = 2 x V x predicted depth). This speed is supported by data recorded from Dtags attached to humpback whales (Goldbogen et al. 2008, Ware et al. 2011). Given an estimate of m_t (metabolic rate while foraging; Table 4), I substituted values of s^* into equation 2 to yield estimates of optimal foraging durations, t^*, and calculated optimal dive durations, u^*, as $t^* + \tau$ (Houston & Carbone 1992). I derived all model predictions and examined all comparisons to observed data with custom written code in R (R Core Team 2013).

I predicted the number of lunges executed per dive (l^*) as t^* divided by the mean lunge duration of an average sized whale (14 m, 41 sec; Potvin et al. 2012) and compared them to the observed number of lunges executed per dive (l) as an additional assessment of the whale's foraging behaviors and how they compared to the OFT model. Finally, I predicted the diving lactate threshold (DLT), the dive duration at which post-dive lactate concentration increases (Kooyman 1985, Butler & Jones 1997, Butler 2006), for an average sized humpback whale (Table 4) for depths (p) ranging from 0 – 400 m as:

$$\mathrm{DLT(p)} = \left(\frac{\mathrm{p}}{V} \times 2\right) + \left(\frac{K - m_\tau \times \frac{\mathrm{p}}{V} \times 2}{m_t}\right) \quad (7)$$

(Doniol-Valcroze et al. 2011).

In the execution of the OFT model, each dive is treated as an independent sample. Therefore, two major assumptions of the model are that each whale has *K* oxygen stores available at the beginning of every foraging dive and that all of *K* is used during that foraging dive. To assess if these assumptions were upheld, I calculated the amount of oxygen used during each foraging dive following $m_\tau \tau + m_t t$ and gained after each foraging dive following $K(1\text{-}e^{-as})$ and determined if they were equivalent. To further examine how humpbacks used oxygen while foraging and to assess how their behaviors may have affected the model comparisons, I calculated the rate of change in oxygen stores throughout the tagging records, $X(s)$:

$$X(s_{i+1}) = X(s_i) - m_\tau \tau_i + m_t t_i + K(1 - e^{-as_i}), \quad (8)$$

where $X(s_1)$ of each individual was equal to *K* (Table 4). Non-foraging dives were included in this iteration (e.g., resting dives; Friedlaender et al. 2013) and used $m_t t_i$ set to zero (i.e., no foraging costs). This calculation allowed for an examination of oxygen balance over time scales ranging from a single foraging dive to entire foraging periods (c.a. 16 hrs).

3.2.3 Statistical Analyses

Model validity needed to be assessed (Mayer & Butler 1993), therefore I tested the fit of my data (i.e., *u*, *s*, *t, and l*) to the model predictions (i.e., *u**, DLT, *s**, *t**, and *l**) in several ways. I calculated the residuals of observed versus predicted values ($y_i - \hat{y}_i$), the standard deviation of the model prediction error (i.e. root mean squared error; RMSE),

the Pearson's product moment correlation of y_i and $\hat{y}_i$(Guisan & Zimmerman 2000), and the modelling efficiency (*ME*; Loague & Green 1991, Mayer & Butler 1993):

$$ME = 1 - \frac{\sum(y_i - \hat{y}_i)^2}{\sum(y_i - \overline{y_i})^2}. \quad (9)$$

ME values equal to 1 indicated a perfect match of y_i and $\hat{y}_i$; *ME* values equal to 0 indicated that the fit of y_i and $\hat{y}_i$ is equal to the fit of y_i and $\overline{y_i}$; and *ME* values less than 0 indicated the $\overline{y_i}$; is a better predictor of the data than $\hat{y}_i$. I also computed linear regressions of y_i and $\hat{y}_i$ and tested if they deviated significantly from 1 and 0, respectively (Smith & Rose 1995). All samples in this chapter were tested for normality, linearity, homoscedasticity, and outliers and statistical tests were determined based on the outcome of the sample's adherence to these assumptions. I assessed individual variability by examining dive variables for each tagged whale separately and conducted a principal component analysis to determine the influence that such variations may have had on the data. I conducted all statistical analyses in R (R Core Team 2013) and used a significance level of 0.05.

3.3 Results

I examined Dtag data collected from 13 adult humpback whales for this chapter (Table 5). I detected feeding lunges from each tagged whale's tag record but the number of lunges executed by individual varied from 40 (whale identification (ID): 140a) to 943 (whale ID: 146a). The number of lunges executed per foraging dive (*l*) ranged from 1 to 13 with a median of 2 and a mean (± SD) of 2.90 (± 2.36). The number of foraging dives

(*N*) detected ranged from 7 (whale ID: 140a) to 462 (whale ID: 152a) by individual, for a total sample of 2365 foraging dives. Tagged whales generally exhibited an extreme diel feeding pattern (Friedlaender et al. 2013): they started feeding near dusk (14:00:00, GMT − 5 hr), fed constantly through nighttime, stopped feeding by 07:00 the next morning, and rested or traveled for the rest of the day before starting the cycle over again (Figure 11; see Friedlaender et al. 2013 for more details). While maximum dive depths varied by individual (Figure 11 A; AOV: $df = 12, 2352$, $F = 374.18$, $p < 0.001$), 81.27 % of all foraging dives ($N = 1922$) were to maximum dive depths shallower than 100 m (Figure 11 B) and were distributed primarily between 5 and 40 m ($N = 1098$, 46.23 %) and between 60 and 90 m ($N = 529$, 22.37 %).

Table 5: Dtag deployment information. Whale ID, tag on date, tag start time, and tagging location are shown as well as the number of lunges and foraging dives detected for each whale.

Whale ID	Tag on date	Tag start time (GMT − 5 h)	Tagging location	Total tag on time (hrs)	Number of lunges (*l*)	Number of feeding dives (*N*)
122b	2009-May-02	14:28:44	Wilhelmina Bay	18.4	620	419
127a	2009-May-07	08:42:03	Wilhelmina Bay	24.6	383	89
136a	2009-May-16	09:09:54	Anvord Bay	23.0	456	82
140a	2009-May-20	10:58:03	Anvord Bay	22.5	40	7
148a	2009-May-28	09:48:17	Wilhelmina Bay	25.2	578	225
152a	2009-June-01	10:39:24	Wilhelmina Bay	22.3	826	462
132a	2010-May-12	09:58:38	Wilhelmina Bay	23.1	317	97
133a	2010-May-13	12:03:50	Wilhelmina Bay	22.2	392	102
139a	2010-May-19	11:02:58	Wilhelmina Bay	20.6	847	292
144a	2010-May-24	14:05:18	Wilhelmina Bay	21.1	943	307
146a	2010-May-26	15:17:42	Flandres Bay	20.0	498	64
151a	2010-May-31	10:23:51	Wilhelmina Bay	24.6	573	160
155a	2010-June-04	09:42:03	Flandres Bay	22.2	390	59
				Totals	6863	2365

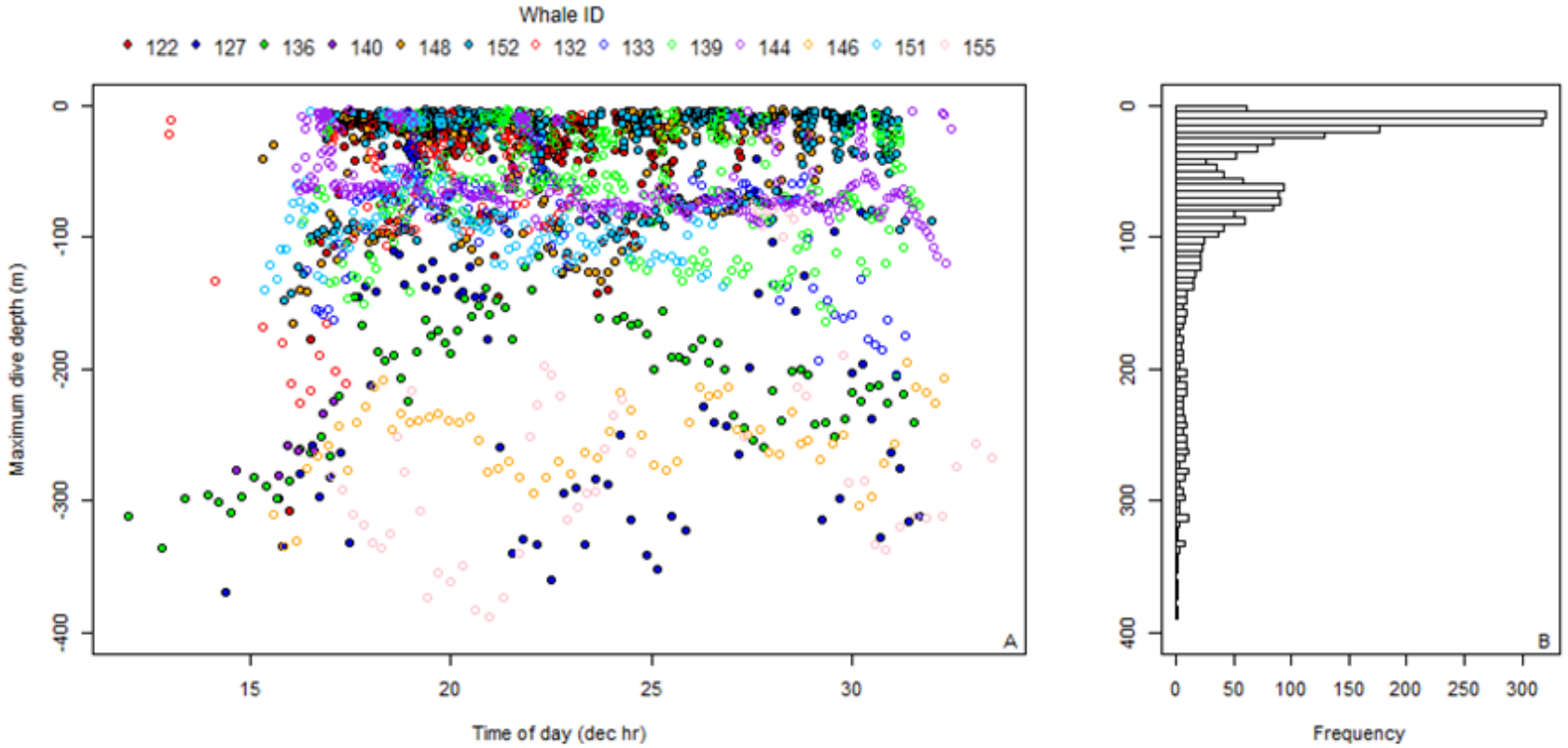

Figure 11: Temporal distribution (A) and frequency (B) of the maximum dive depths of foraging dives. Note: values are color coded by whale ID (A) for comparison.

3.3.1 Model Agreement

3.3.1.1 Observed Versus Predicted Foraging Behaviors

I predicted the foraging durations (t^*) as well as the number of lunges executed per dive (l^*) for an average sized humpback whale and compared them to their respective values (t and l) recorded by the Dtags (Figure 12 A, C, and E). Predicted foraging durations were not consistent with t (Figure 12 A). Three hundred fifty-three dives had longer t than t^* (14.93 %), while 2012 dives has shorter t than t^* (85.07 %). Of these two groups, 84.70% (N = 299) and 89.76% (N = 1868) of dives with longer and shorter t than t^* were deeper and shallower than 100 m, respectively (note: 100 % of dives shallower than 49.56 m had t shorter than t^*). The Pearson's product moment correlation coefficient for t^* and t was low (r = 0.25, p < 0.001; i.e., they were not correlated) and the ME value was negative (ME = -0.54) suggesting that the model cannot be recommended for the observed data. Shallow dives generally had shorter t than t^*, while deeper dives generally had longer t than t^* (the 25 and 75 % quartile of dives with shorter and longer t than t^* was 11.65 m and 67.32 m and 126.72 m and 267.45 m, respectively). Foraging durations of dives to intermediate depths (approximately 50 to 180 m) were most similar to t^* (they had the lowest RMSE values; Figure 12E). In addition, the mean depths of foraging dives with t values that were shorter than or longer than t^* were significantly different (mean ± SD = 42.02 ± 39.30 m and 203.05 ± 83.04 m, respectively; Wilcoxon Rank Sum Test: W = 687973, p < 0.001).

Lunge counts per dive were also not predicted by the OFT model (Figure 12 B, D, and E). Four hundred one dives had more l than l^* (16.96 %), while 1964 dives had fewer

l than *l** (83.04 %). The Pearson's product moment correlation coefficient for *l* and *l** was low ($r = 0.33$, $p < 0.001$; i.e., they were not correlated) and the *ME* value was negative (*ME* = -0.31). Similar to the agreement of *t* and *t**, *l* of dives to intermediate depths (approximately 60 to 170 m) were most similar to *l** (Figure 12 F). Lastly, observed *t* and *l* were significantly positively correlated with each other ($r = 0.95$, $p < 0.01$) and with *u* ($r = 0.92$, $p < 0.001$; $r = 0.86$, $p < 0.001$; respectively), but not with *s* ($r = 0.46$, $p < 0.001$; $r = 0.40$, $p < 0.001$; respectively) or τ ($r = 0.54$, $p < 0.001$; $r = 0.49$, $p < 0.001$; respectively).

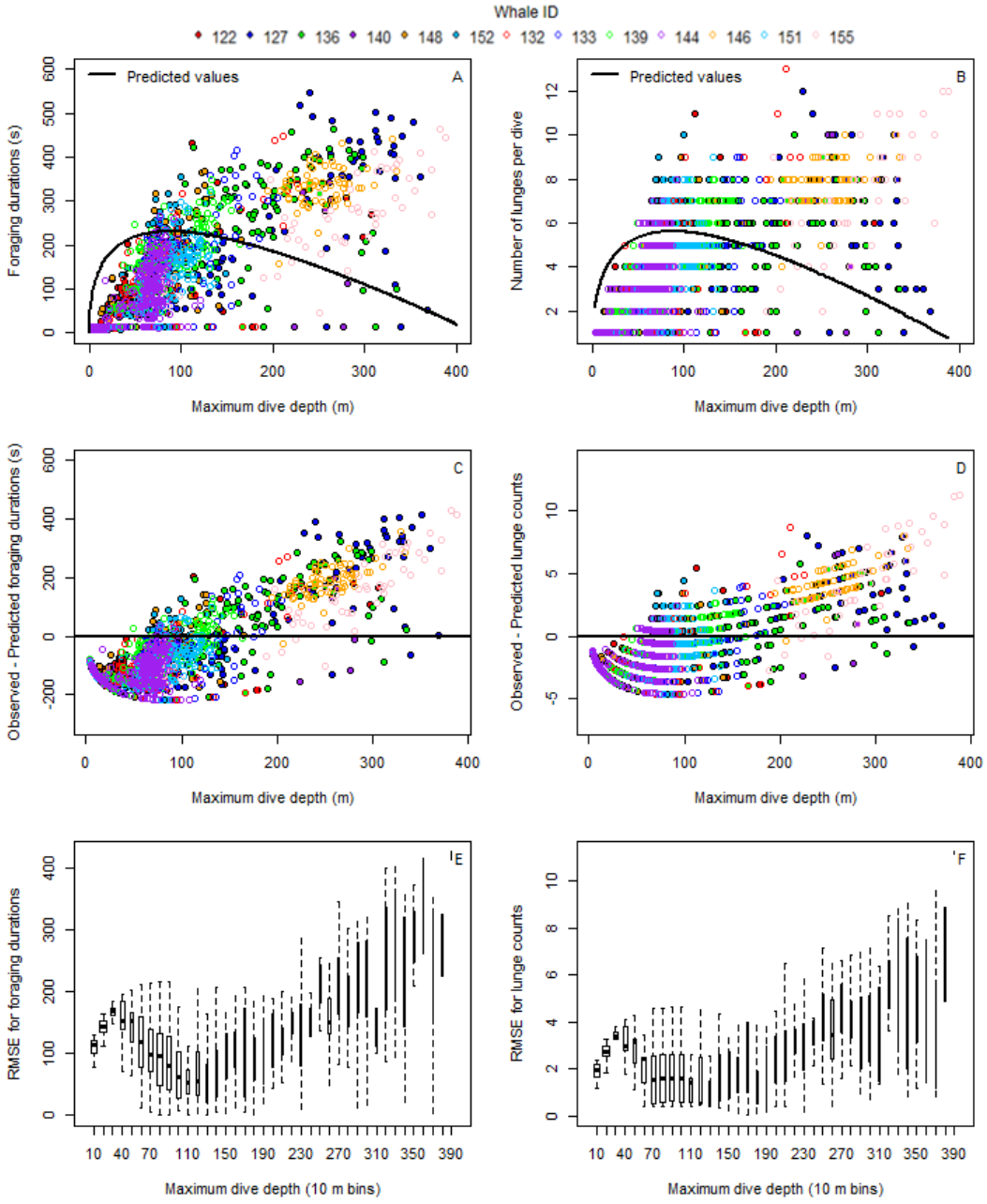

Figure 12: Observed and predicted values (A and B), raw residuals (yi – ŷi) (B and C), and root mean squared errors (E and F) of foraging durations and the number of lunges exectued per dive, respectively, as a function of maximum dive depth. Note: values are color coded by whale ID (A - D) for comparison. The boxes in E and F are drawn with widths proportional to the square-roots of the number of observations in each group and outlying data points are excluded (R Core Team 2013).

The relationships between t and l with u and s are shown in Figure 13 along with their respective predicted values. The observed values of t and l in relation to u were positively correlated to their predicted relationships (Figure 13 A and B: $r = 0.79$, $p < 0.001$ and $r = 0.92$, $p < 0.001$; respectively). In addition, the predicted relationships between l^* and u^* agreed with the observed relationships between l and u ($ME = 0.39$); the ME for t and u against t^* and u^* was low ($ME = -0.04$). Model fit varied with l (AOV of RMSE values: $df = 12, 2352$, $F = 64.05$, $p < 0.001$), with dives having 8 or more lunges being most similar to the model predictions (and statistically similar to one another; Tukey multiple comparison of means: $p < 0.001$). The observed values of l in relation to s were also positively correlated to their predicted relationship (Figure 13 D: $r = 0.64$, $p < 0.001$), but the observed values of t in relation to s were not (Figure 13 C: $r = 0.38$, $p < 0.001$). ME values for both comparisons were negative suggesting poor model fit (ME= -6.68 and $ME = -4.65$, respectively). Again, model fit varied with l (AOV of RMSE values: $df = 12, 2352$, $F = 326.7$, $p < 0.001$), with fit decreasing with increasing lunge counts per dive (Figure 13 D).

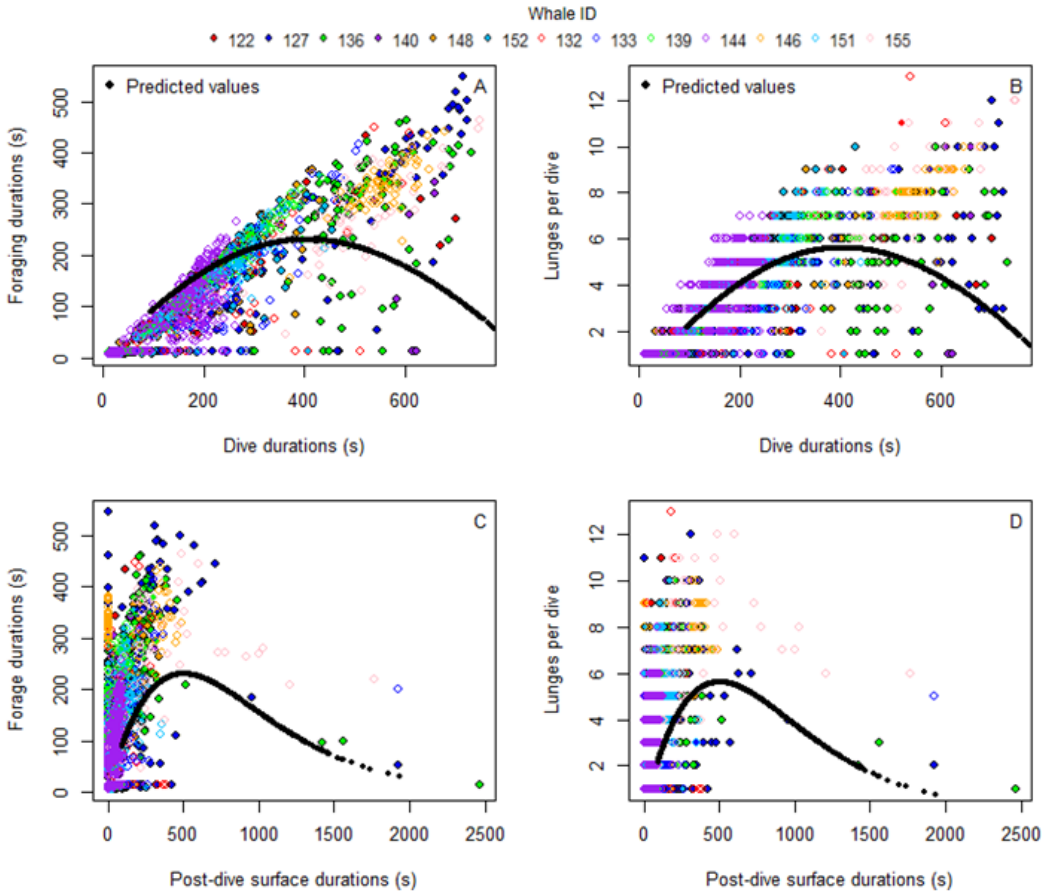

Figure 13: Observed and predicted foraging durations and lunge counts as a function of dive durations and post-dive surface times, respectively. Note: values are color coded by whale ID for comparison.

3.3.1.2 Observed Versus Predicted Dive Durations

I compared predicted dive durations (u^*) of to their respective durations (u) recorded by the Dtags (Figure 14). The OFT model predicted that u^* would increase rapidly at shallow depths then increase at a decreasing rate with increasing depth. The Pearson's product moment correlation coefficient for u^* and u were significantly positively correlated ($r = 0.95$, $p < 0.001$) and the ME was greater than zero ($ME = 0.10$) suggesting fair model fit. The slope of the linear regression between u and u^* was close

to 1, suggesting that the prediction accuracy did not vary with depth ($y = 163.93 + 0.91x$, $R^2 = 0.91$, $p < 0.001$). However, a closer examination of the residuals between u and u^* (Figure 14 B) and the RMSE values (Figure 14 D), suggests that dives to maximum depths between approximately 30 and 160 m and greater than 340 m had durations that were less similar to u^* than dives with maximum depths shallower than 30 m or between 170 m and 340 m. While 98.99 % of foraging dives ($N = 2341$) had shorter durations than u^*, the mean maximum dive depths of foraging dives with shorter or longer u than u^* ($N = 2341$, 98.99 % and $N = 24$, 1.01%, respectively) were significantly different (mean ± SD = 65.09 ± 74.24 m and 160.02 ± 95.24 m, respectively; Wilcoxon Rank Sum Test: $W = 45729$, $p < 0.001$). Regardless of model agreement, dive durations increased with maximum dive depths ($y = 2459 + 2.11x$, $R^2 = 0.91$, $p < 0.001$) and were strongly positively correlated with this parameter ($r = 0.95$, $p < 0.001$).

The DLT was predicted to increase with increasing maximum dive depth (Figure 14 A). The Pearson's product moment correlation coefficient for u and the predicted DLTs was similar ($r = 0.95$, $p < 0.001$) to that of u^*, but the ME value was negative ($ME = -4.27$) suggesting the model does not describe the data. The slope of the regression of u and DLT ($y = -1109 + 2.40x$, $R^2 = 0.91$, $p < 0.001$), and an examination of the residuals (Figure 14 C) and of the RMSE (Figure 14 E) suggests that the prediction accuracy of DLT varied with depth. Increasing maximum dive depths had u that were increasingly similar to DLT (i.e., residuals were increasingly larger and RMSE values were increasingly smaller) up to approximately 210 m (Figure 14 A, C, and E). Dive durations for dives to maximum depths greater than 210 were equally similar to DLT (Tukey

multiple comparisons of RMSEs for all n by n comparisons, $p > 0.05$). The mean maximum dive depths of foraging dives that were shorter or longer than the DLT predictions were significantly different (mean ± SD = 65.84 ± 74.86 m and 237.69 ± 7.77 m, respectively; Wilcoxon Rank Sum Test: $W = 6659$, $p < 0.08$). Note, however, that only three dives had dive durations longer than their predicted DLT and these dives were all executed by whale w127a (Figure 14 A and C). In addition, these dives also had longer t and s than t^* and s^*, respectively, and had a higher l than l^* (12, 11, 7 versus 4, 4, 4; respectively).

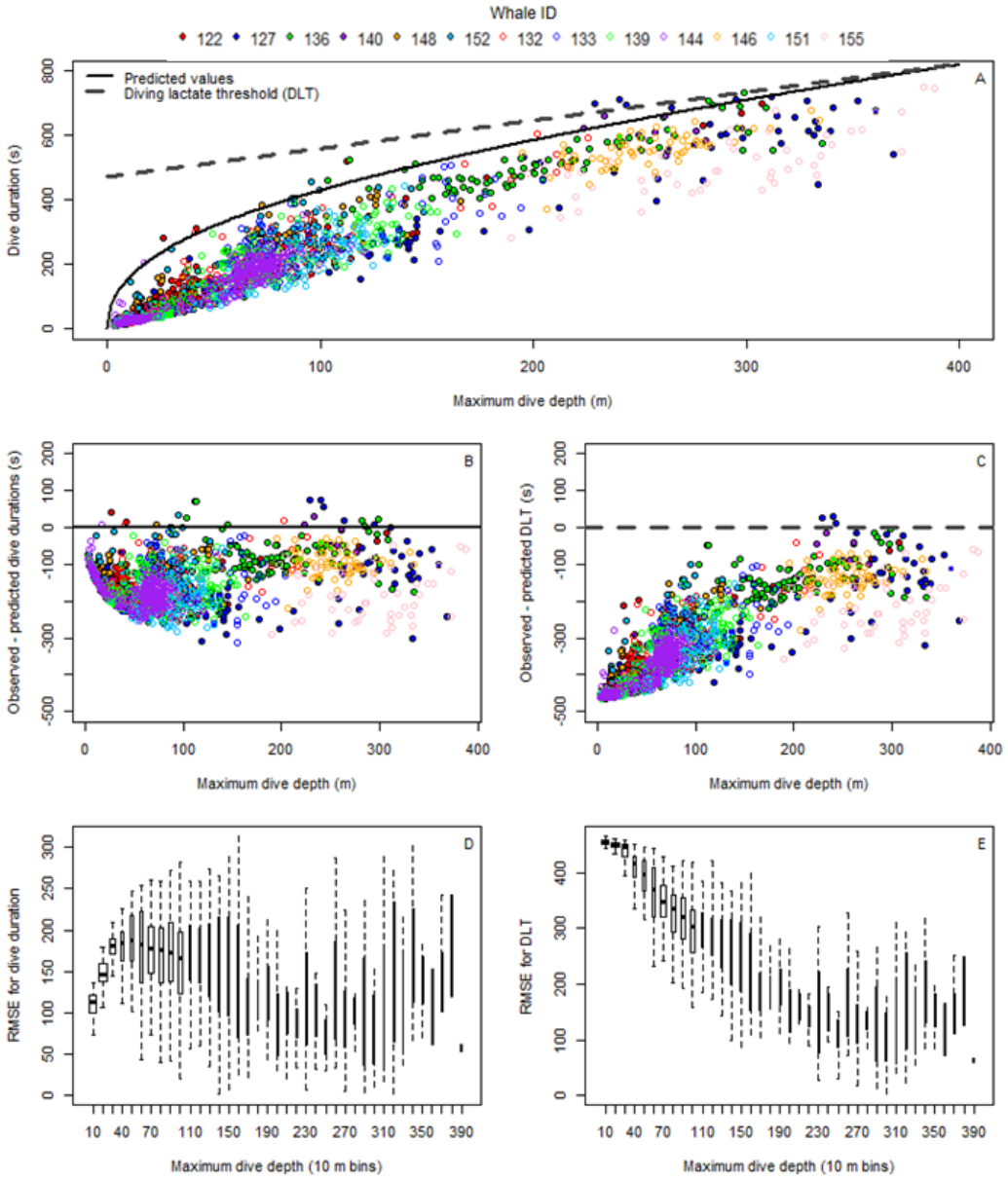

Figure 14: Observed and predicted values (A), raw residuals ($y_i - \hat{y}_i$) (B and C), and root mean squared errors (D and E) of dive durations and the diving lactate threshold, DLT, respectively, as a function of maximum dive depth. Note: values are color coded by whale ID (A, B, and C) for comparison. The boxes in D and E are drawn with widths proportional to the square-roots of the number of observations in each group and outlying data points are excluded (R Core Team 2013).

3.3.1.3 Observed Versus Predicted Post-Dive Surface Durations

The OFT model predicted that s^* would increase with increasing dive depths (Figure 15 A). While s did increase with maximum dive depths ($y = -10.29 + 1.15x$, $R^2 = 0.40$, $p < 0.001$), the model did not describe the data ($ME = -7.50$; $r = 0.63$, $p < 0.001$) and most foraging dives had s shorter than s^* ($N = 2356$, 99.62%; Figure 15). The slope of the linear regression of s versus s^* ($y = 310.13 + 1.30x$, $R^2 = 0.39$, $p < 0.001$) as well as the residuals (Figure 15 B) and RMSE values (Figure 15 C) suggests that prediction accuracy of s varied by depth: increasing maximum dive depth resulted in s that were increasingly shorter than s^* (Figure 15 B, C). In addition, the mean maximum dive depths of foraging dives with s shorter or longer than s^* were significantly different (mean ± SD = 65.44 ± 74.12 m and 228.37 ± 134.04 m, respectively; Wilcoxon Rank Sum Test: $W = 16942$, $p < 0.001$). It should be noted that 77.78 % of the s that were greater than s^* ($N = 9$) were from dives that were executed before 3 pm and after 7 am (local time) the next morning. In general, s increased with increasing maximum dive depths ($y = -10.29 + 1.16x$, $R^2 = 0.40$, $p < 0.001$) and increasing u ($y = -12.66 + 0.49x$, $R^2 = 0.34$, $p < 0.001$) and were moderately positively correlated to these parameters ($r = 0.63$, $p < 0.001$; $r = 0.58$, $p < 0.001$; respectively).

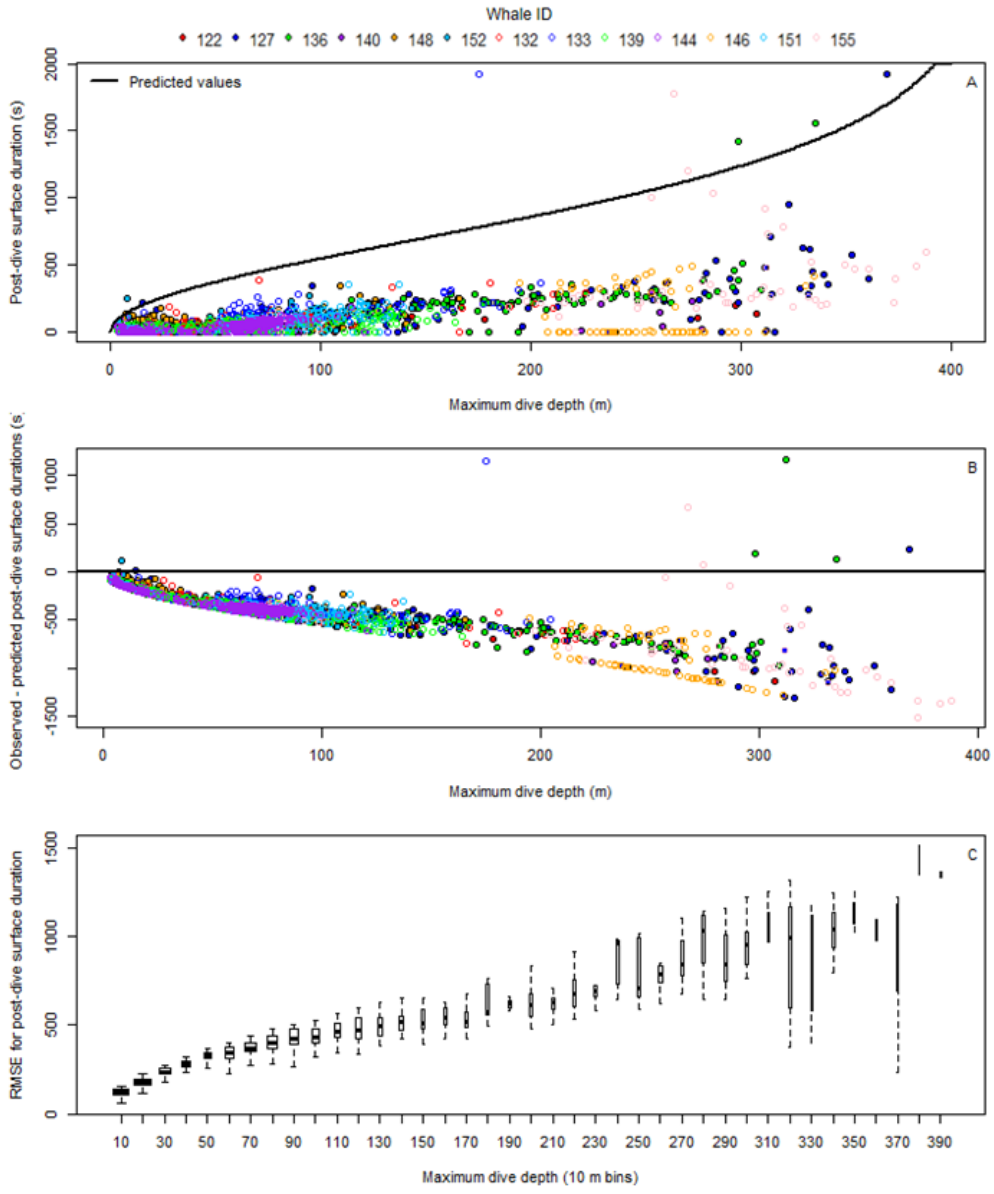

Figure 15: Observed and predicted values (A), raw residuals (yi – ŷi) (B), and root mean squared errors (C) of post-dive surface durations as a function of maximum dive depths. Note: values are color coded by whale ID (A and B) for comparison. The boxes in C are drawn with widths proportional to the square-roots of the number of observations in each group and outlying data points are excluded (R Core Team 2013).

3.3.1.4 Individual Variation

It is important to note that individuals did vary in their behaviors: individual whales had significantly different foraging durations (AOV: $df = 12, 2352$, $F = 149.41$, $p <$

0.001), lunge counts (AOV: $df = 12, 2352$, $F = 111.51$, $p < 0.001$), diving durations (AOV: $df = 12, 2352$, $F = 278.29$, $p < 0.001$), and post-dive surfacing durations (AOV: $df = 12, 2352$, $F = 90.392$, $p < 0.001$). These differences resulted in varied agreement between their observed and predicted behaviors (Table 6). Despite this, a principal component analysis revealed that whale ID was not a large source of the variation present in the data (Figure 16). The first component of the analysis explained 57.36 % of the variation in the data and Whale ID as well as time of day were not correlated to this component ($r = 0.01$ and $r = 0.01$, respectively). Instead, dive duration ($r = 0.49$), maximum dive depth ($r = 0.47$), forage duration ($r = 0.47$), lunge counts ($r = 0.45$), and post-dive surface durations ($r = 0.33$) were most correlated to this component. Whale ID and time of day, instead, were most correlated to the second component ($r = -0.71$ and $r = -0.70$, respectively), which accounted for 18.09 % of the variance in the data.

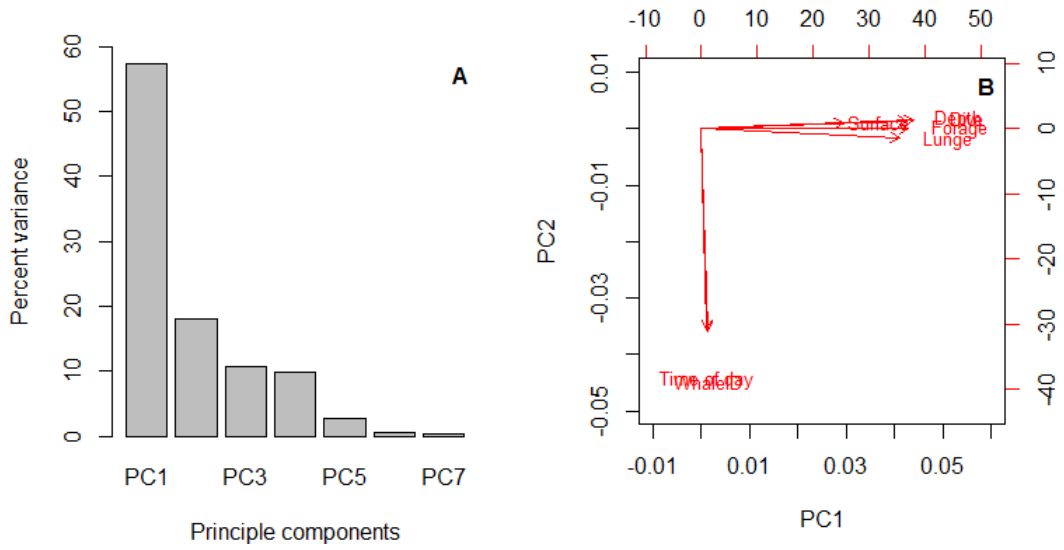

Figure 16: Results of a principal component analysis aimed to determine which paramters contributed the most to variability amongst the data: whale ID (Whale), maximum dive depths (Depth), Times of day (Time of day), dive durations (Dive), post-dive surface durations (Surface), forage durations (Forage), and number of lunges per dive (Lunges). A) The percent variance that each principle component contributed to the data. B) A biplots of PC1 and PC2, which reveal the parameters that were most strongly correlated with these components.

Table 6: Pearson's product moment correlation coefficients (*r*) and model efficiencies (ME) for each individual whale for observed foraging durations (*t*), lunge counts (*l*), dive durations(*u*), and post-dive surface durations (*s*) against corresponding optimal foraging durations (*t) , lunge counts (*l**), dive durations (*u**), dive-lactate threshold durations (DLT), and surface durations (*s**). Strongly positively correlated coefficients (r > 0.90; Cohen 1988) are indicated with a §. ME values close to one indicate a near-perfect match between observed and predicted values, while negative values cannot be recommended (Loague & Green 1991, Mayer & Butler 1993).**

Whale		*t**			*l**			*u**			DLT			*s**	
ID	*r*	*p*	*ME*	*r*	*p*	*ME*	*r*	*P*	ME	*r*	*p*	ME	*r*	*p*	ME
122b	0.49	< 0.001	-7.60	0.51	< 0.001	-5.10	0.91§	< 0.001	-2.72	0.94§	< 0.001	-26.84	0.73	< 0.001	-161.12
127a	-0.45	< 0.001	-0.45	-0.16	0.135	-0.39	0.94§	< 0.001	0.49	0.95§	< 0.001	-0.61	0.64	< 0.001	-5.50
136a	-0.17	0.017	-1.06	-0.13	0.237	-0.57	0.84	< 0.001	-0.07	0.85	< 0.001	-1.95	0.55	< 0.001	-3.10
140a	0.08	0.860	-0.15	-0.02	0.961	-0.40	-0.43	0.340	-2.19	-0.43	0.339	-5.13	0.08	0.865	-71.74
148a	0.75	< 0.001	-0.80	0.76	< 0.001	-0.31	0.93§	< 0.0 1	-0.81	0.94§	< 0.001	-11.02	0.55	< 0.001	-23.61
152a	0.71	< 0.001	-2.24	0.73	< 0.001	-0.85	0.91§	< 0.001	-1.10	0.94§	< 0.001	-19.07	0.48	< 0.001	-41.88
132a	0.34	<0.001	-0.84	0.32	0.001	-0.32	0.93§	< 0.001	-0.20	0.93§	< 0.001	-5.26	0.66	< 0.001	-19.23
133a	-0.16	0.103	-0.57	-0.16	0.103	-0.74	0.80	< 0.001	-1.72	0.78	< 0.001	-8.91	0.41	< 0.001	-3.38
139a	0.70	< 0.001	-0.75	0.69	< 0.001	-0.53	0.92§	< 0.001	-1.44	0.92§	< 0.001	-11.72	0.57	< 0.001	-83.17
144a	0.66	< 0.001	-2.95	0.68	< 0.001	-0.71	0.91§	< 0.001	-4.42	0.93§	< 0.001	-24.72	0.66	< 0.001	-99.50
146a	-0.34	0.005	-18.42	-0.29	0.018	-18.03	0.70	< 0.001	-3.19	0.70	< 0.001	-7.02	0.01	< 0.001	-26.46
151a	0.71	< 0.001	-0.75	0.71	< 0.001	-0.07	0.89	< 0.001	-2.03	0.91§	< 0.001	-11.28	0.69	< 0.001	-29.37
155a	-0.83	< 0.001	-2.26	-0.80	< 0.001	-2.45	0.92§	< 0.001	-0.64	0.92§	< 0.001	-1.77	0.39	0.002	-6.05

3.3.1.5 Adherence of Data to Model Assumptions

Oxygen utilization and acquisition rates were calculated to assess whether each whale had *K* oxygen stores available at the beginning of every foraging dive and that all of *K* was used during that foraging dive as assumed by the OFT model (Figure 17 A, B). Oxygen losses and gains per dive were only approximately equivalent for 1.06 % (N = 25) of foraging dives (i.e., oxygen used during a dive was within 5 L of oxygen gained after these dive). Instead, oxygen stores of foraging dives were generally not replenished at the surface following a dive (Figure 17): 90.96 % (N = 2151) of foraging dives had negative oxygen gains. In general, oxygen losses per dive were within a few hundred liters: 54.07 % (N = 1163) of these losses were within 200 L, while 96.84 % (N = 2083) of these losses were within 600 L. The time of day a foraging dive was executed poorly predicted whether oxygen would be balanced during a dive cycle (Figure 17 A; y = -290.32 + 1.79x, $R^2 < 0.001$, $p < 0.001$). The maximum depth of a dive, however, was a stronger predictor of oxygen balance (Figure 17 B; y = -48.72 – 3.04, $R^2 = 0.52$, $p < 0.001$): increasing maximum dive depths resulting in greater net oxygen losses. The loss of oxygen stores dive per dive resulted in an increased gross loss of oxygen as the whales continued to execute foraging dives throughout the tagging periods (Figure 17 C). The consequence of this behavior was that proportion of oxygen stores available to perform a dive cycle decreased throughout the tagging period (Figure 17 D). These finding suggests that the assumption of oxygen balance in the OFT model was not upheld and may contribute to the disagreement observed and predicted behaviors described above.

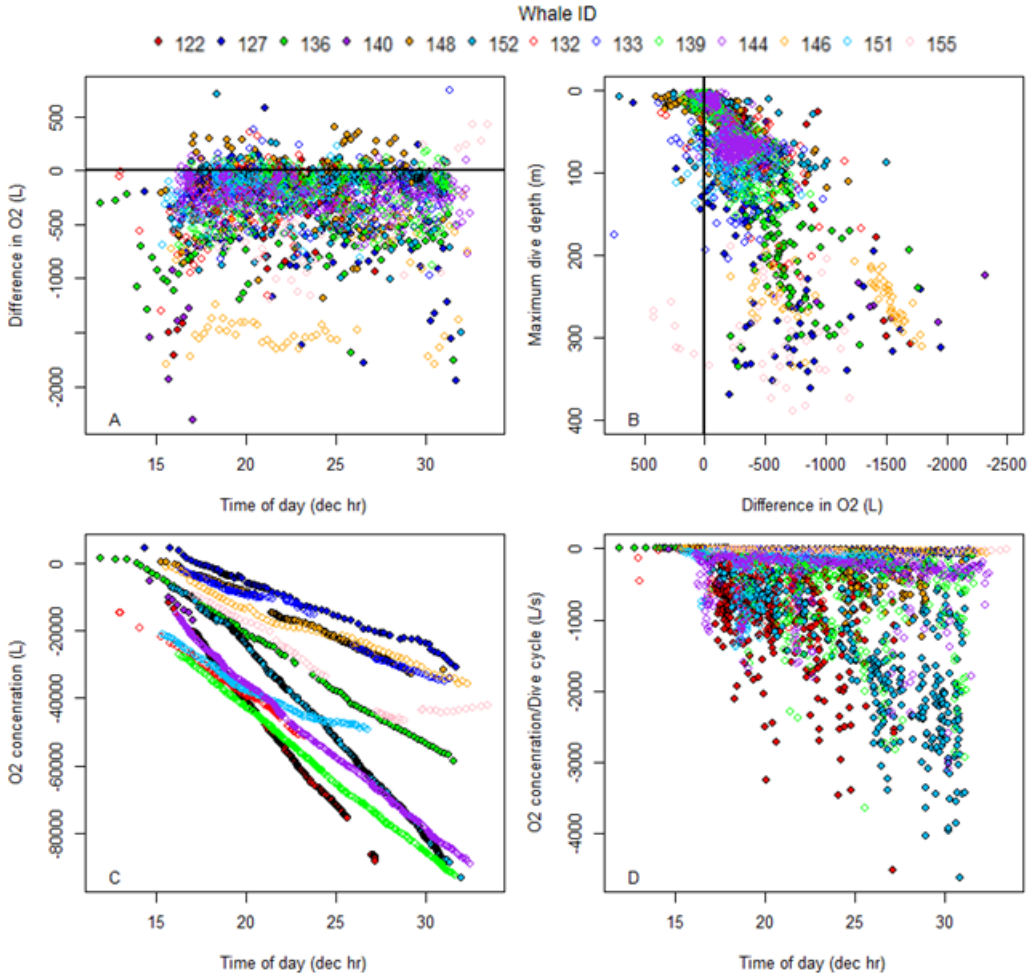

Figure 17: Oxygen balance, utilization and acquirement rates: A) oxygen balance per dive against time of day each dive was executed; B) oxygen balance per dive against maximum dive depth; C) the cumulative rate of oxygen loss over the tagging period; and D) the cumulative rate of oxygen loss over the tagging period represented as the amount of oxygen available for each dive cycle. Note: values are color coded by whale ID.

3.3.2 Proportional Foraging Behaviors

Because the assumptions of the OFT model were violated, I examined the proportions of time whales spent diving, descending, foraging, ascending, and surfacing as well as their lunging rates as a function of maximum dive depth out of the total dive

cycle ($u + s$) to assess the efficiency of foraging patterns (Figure 18). The proportion of time spent surfacing varied by maximum dive depth (AOV: $df = 38, 2326$, $F = 4.84$, $p < 0.001$) and generally increased with increasing maximum dive depth (Figure 18 A; mean ± SD = 0.22 ± 0.17). The proportion of time spent diving, conversely, decreased with increasing maximum dive depths (Figure 18 B; mean ± SD = 0.78 ± 0.17). The proportions of time spent diving and surfacing were more variable at shallow depths.

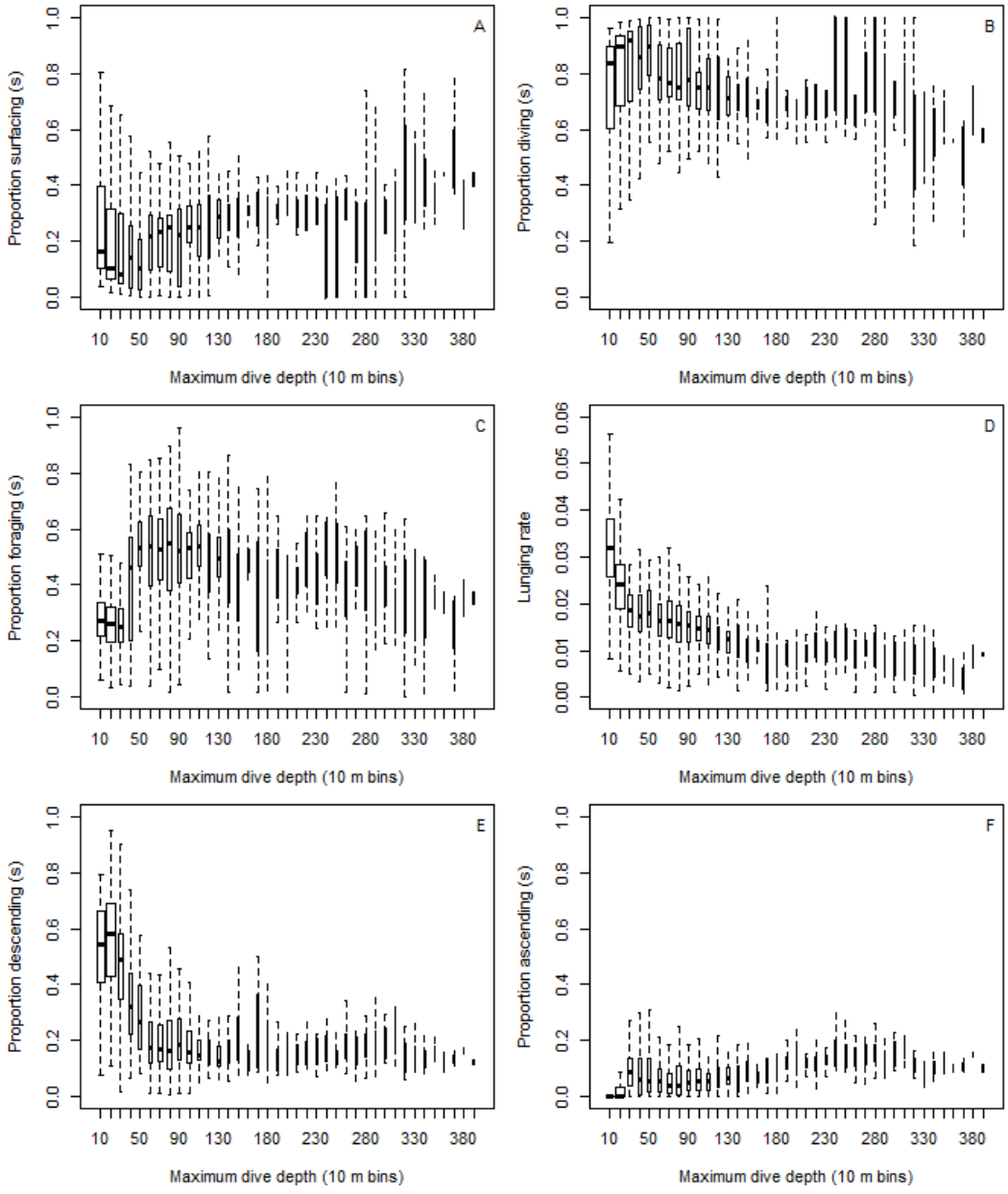

Figure 18: Proportion of time spent during each dive cycle versus maximum dive depth. A) the proportion of time spent diving, B) the proportion of tine spent surfacing, C) the proportion of time spent foraging foraging, D), the lunging rate (number of lunges per second of the dive cycle; note different y-axis scale), E) the proportion of time spent descending, and F) the proportion of time spent ascending. Outliers are not included in the figure and each box is drawn with widths proportional to the square root of the number of observations in each group (R Core Team 2013).

The proportion of dive time spent foraging was generally high across all maximum dive depths (mean ± SD = 0.38 ± 0.19) and was statistically similar for dives with maximum dive depths greater than 110 m (mean ± SD = 0.43 ± 0.17; Tukey multiple comparisons of means, $p > 0.05$; Figure 18 C). The shallowest dives had the lowest mean proportions of foraging times; dives with maximum depths shallower than 30 m had significantly similar mean foraging proportions (mean ± SD = 0.28 ± 0.12; Tukey multiple comparisons of means, $p > 0.05$). Dives with intermediate maximum depths (between 50 m and 90 m) had the highest proportions of foraging times (mean ± SD = 0.69 ± 0.07). Lunging rates varied by maximum dive depth (AOV: $df = 38, 2326$, $F = 61.71$, $p < 0.001$) and were highest for dives with shallow maximum depths (i.e., less than 20 m; Figure 18 D). Lunge rates were statistically similar for all dives having maximum depths greater than 80 m (Tukey multiple comparisons of means, $p > 0.05$).

Descent and ascent rates were variable according to maximum dive depth (Figure 18 E and F, respectively). The proportion of time spent descending on a dive was highly variable for dives with maximum dive depths shallower than 100 m (mean ± SD = 0.40 ± 0.22) but was lower and more consistent on dives with maximum depths greater than 100 m (mean ± SD = 0.18 ± 0.10; Figure 18 F). During dives with maximum depths greater than 60 m, whales spent statistically similar proportions of dive time descending to their target foraging depth (Tukey multiple comparisons of means, $p > 0.05$; mean ± SD = 0.19 ± 0.12). The proportion of time spent ascending on a dive was typically low across all maximum dive depths (Figure 18 G), but dives with maximum depths greater

than 30 m had significantly similar ascent durations (Tukey multiple comparisons of means, $p > 0.05$; mean ± SD = 0.10 ± 0.10).

3.4 Discussion

The humpback whales observed in this study exhibited foraging behaviors that were not predicted by the Houston and Carbone (1992) time allocation model. Despite this, these whales exhibited foraging behaviors that were in agreement with many of the theoretical predictions of OFT and may be regarded as 'clever' (*sensu* Owens-Smith & Novellie 1982). For instance, humpbacks generally foraged in shallow depths (i.e., < 100 m; Figure 11) where they had a high rate of feeding (i.e., lunging; Figure 18 D), and when forced to dive to greater depths they adjusted their behaviors so that they could maximize their foraging durations and increase their lunging rates (Figure 18; Charnov 1976, Mori 1998, Thompson & Fedak 2001, Doniol-Valcroze et al. 2011). Interestingly, these whales also appeared to accept short term (i.e., dive by dive) costs associated with depleted oxygen stores in favor of maximizing long term (i.e., daily) energetic gains. These findings suggest that these whales were exhibiting behaviors to maximize their energetic gains and minimize their energetic costs over time scales longer than those examined by many OFT models (e.g., Houston & Carbone 1992).

The humpback whales observed in this study were spatially and temporally correlated with super-aggregations of Antarctic krill (*Euphausia superba*), which were up to 10s of km wide in the horizontal plane and 410 m thick in the vertical plane and had estimated biomasses of up to 2.0 million tons (Nowacek et al. 2011, Espinasse et al. 2012).

Friedlaender et al. (2013) reported that humpbacks in this region exhibit extreme diel foraging behaviors, whereby they initiate feeding near dusk when krill begin their vertically migration to the surface (Zhou & Dorland 2004), feed throughout the night, and cease feeding soon after sunrise when the krill begin to migrate back to depth (note: Friedlaender et al. (2013) examined the same humpbacks examined in this study). They suggest that this behavior allowed these whales to limit the amount of time and energy spent diving when prey are deep and instead focus their foraging efforts in shallow depths, where they can maximize their feeding rates and potentially their foraging efficiency. The findings reported here support this hypothesis and further suggest that this diel behavior was related to these whales' preferences in maximizing feeding rates over balancing their oxygen stores dive per dive while feeding. While the extreme daily resting behaviors observed in these whales may have been related to processing ingested food from the previous night (Friedlaender et al. 2013), they were also likely related to the energetic demand associated with replenishing the oxygen stores they so severely depleted during that c.a. 16 hr foraging bout. These whales, therefore, were clever: they adjusted their foraging behaviors in accordance to the behaviors of their prey and focused their foraging efforts on periods when prey was most easily accessible and less costly to acquire (i.e., near the surface).

During their nightly foraging bouts, humpbacks observed in this study focused their efforts in the upper 100 m of the water column (Figure 11). Dive durations were shorter than predicted for these depths, but lunging rates were high, with the majority of dives having one (57.28 %) or two (10.46 %) recorded lunges. The high rate of lunging

near the surface is likely associated with looping behaviors describe by Ware et al. (2011; a collaborative project), whereby whales repeatedly loop back and forth while lunging, presumably exploiting a single, small krill patch. This looping behavior allowed these whales to feed almost continuously: by incorporating their breathing into the lunge cycle they almost eliminated the need to spend additional time at the surface replenishing depleted oxygen stores and instead could forage at a high and consistent rate (Ware et al. 2011).

When forced to dive to depth (i.e., > 100), the humpbacks observed in this study adjusted their behaviors so that they could maintain a high feeding rate (Figure 18). Such adjustments allowed these whales to exhibit longer foraging durations and have a higher lunge count than predicted by the OFT model: 84.70 % and 66.82 % of dives to maximum depths deeper than 100 m had longer t than t^* (Figure 12) and more l than l^*, respectively. The disagreement between observed and predicted values may be related to lunges being executed on both the ascending and descending portions of feeding dives (Ware et al. 2011), which are not accounted for in the OFT model (Houston & Carbone 1992). These behaviors, as well as changes in their ascent and descent rates, allowed these whales to minimize the costs associated with traveling to depth while simultaneously maximize the proportion of time spent foraging (Figure 18; Mori 1998, Thompson & Fedak 2001), thereby increasing overall energetic gains.

Doniol-Valcroze et al. (2011) found that blue whales had shorter recovery times following deep dives than predicted and suggested that this may be a consequence of the value they used for α not being a realistic measure of oxygen exchange in large

whales. Stephens et al. (2008) noted that the model predictions of Houston and Carbone (1992) are very sensitive to α, and suggested that future research should work towards obtaining more realistic measures of physiology in diving predators. If the values used in this study to predict humpback whale physiology were not accurate (Table 4), the predictions of the OFT model as well as the estimates of temporal oxygen balance may be inaccurate. Unfortunately, the physiology of humpback whales and other rorquals is not well understood and are estimated primarily from relationships based on crude estimates of body mass (Leaper & Lavigne 2001). Therefore, the potential for error is high, which further stresses the importance for further examining and estimating rorqual physiology. In addition, the true size of the whales examined in this study was unknown, which restricted the model predictions to be generalized to that of an average sized humpback. Body size can have a large influence on metabolic rates (Potvin et al. 2009, Goldbogen et al. 2010, Potvin et al. 2012) and oxygen storage capabilities (Tenney & Remmers 1963, Lasiewski & Calder 1971, Kooyman 1973, Halsey et al. 2006, Stephens et al. 2008), and therefore may have influenced the varied agreement between predicted and observed behaviors reported in this study for individual whales (Table 6; Mori 2002).

While individual variation was apparent in foraging behaviors (Table 6), a principle component analysis revealed that individualized behaviors did not explain much of the variance observed in the data: whale ID was not correlated to the first component, which explained 57.36 % of the variance. This finding suggests that examining these whales as a group to assess general foraging patterns is acceptable.

Despite this, future research should examine these individual differences in more depth to assess whether some whales are more 'clever' than others. For example, the repetitive looping behaviors at the surface described by Ware et al. (2011) may be a learned behavior that only a small number of individuals perform. Such knowledge would likely be advantageous for these whales and may have direct and advantageous fitness implications. For instance, these individuals may be able to deal with fluctuations in prey resources attributed to environmental conditions (e.g., decreases in overall krill abundance and krill recruitment associated with rapid climate changes; Loeb et al. 1997, Siegel et al. 1998, Quetin & Ross 2003, Vaughan et al. 2003, Atkinson et al. 2004) more effectively than individuals that exhibit less efficient foraging behaviors.

The humpback whales observed in this study exhibited clever foraging behaviors. They accepted short term costs (e.g., gross loss of oxygen stores) for long term gains (e.g., increased foraging durations and lunging rates), which allowed them to take advantage of their prey when they were most vulnerable (i.e., when krill were foraging near the surface at night). While the behaviors observed here did not conform to the time allocation OFT model (Houston & Carbone 1992), they were supported by many of the theoretical predictions of OFT, and they stress the importance of examining multiple temporal scales when evaluating optimization of foraging behaviors (e.g., Fortin et al. 2002, Austin et al. 2006). Future work should examine the efficiency of foraging behaviors in humpbacks and other rorquals at additional temporal scales (e.g., multiple days, a foraging season), and how energy maximization may vary with prey patch structure. Humpbacks in the WAP were able to take advantage of a temporally and

spatially stable dense krill aggregation (Nowacek et al. 2011, Espinasse et al. 2012) that allowed them to exploit their prey in a very efficient (and clever) manner. Rorquals in other regions (e.g.., Gulf of Maine, Gulf of Alaska) may not have the same luxury.

4. Physiology of Foraging Humpback Whales: Insights from an Optimality Approach

4.1 Introduction

Physiological studies of free-living, diving marine predators can be difficult to conduct due to the inherent difficulties associated with studying these animals (Hunt et al. 2013). Doubly labelled water techniques (e.g., Lifson & McClintock 1966, Nagy 1987, Speakman & Racey 1988, Boyd et al. 1995, Butler et al. 2004), heart rate recordings (e.g., Butler et al. 1992, Boyd et al. 1995, Woakes et al. 1995, Butler et al. 2004), and the training of animals to swim to metabolic stations (Boyd 1997, Yazdi et al. 1999, Boyd 2002) have been used to estimate physiological parameters such as metabolic rates of some marine mammals and diving birds. Metabolic rates and oxygen availability of baleen whales (mysticetes), however, cannot currently be estimated using these methods because their large size and wide-ranging behaviors limit their application. Instead the direct collection of whale faecal samples, respiratory samples, and biopsy samples (see Hunt et al. 2013 for a review) can be used to estimate some aspects of their physiology by examining, for example, their diet (e.g., stable isotopes, fatty acids). These methods, however, present several logistical and/or validation concerns and do not provide much information regarding the rate of energetic losses or gains.

Because of these constraints, physiological studies of baleen whales often use allometric relationships to estimate parameters such as an individual's total oxygen storage capabilities and their metabolic rate. Many of these relationships, however, were

developed using estimates of terrestrial, captured, or captured and released species' physiology (e.g., Kleiber 1975, Lockyer 1976, Halsey et al. 2006, Stephens et al. 2008, Wiedenmann et al. 2011) and few have been empirically tested. In fact, Leaper and Lavigne (2001) pointed out that many of the parameters used to model the energetics of cetaceans are often 'based on little more than guess work.' Despite this, these parameters have been used to model behaviors (e.g., foraging, energetics) of whales and to evaluate their response to current environmental conditions and/or to predict their response to future environmental changes. For example, optimal foraging theory (OFT) models, based on the premise that natural selection should favor foraging strategies that are efficient in minimizing costs (in time and energy) while simultaneously maximizing benefits (e.g., energy, nutrients) (Macarthur & Pianka 1966), have been used to assess the foraging efficiency of foraging dives executed by blue (*Balaenoptera musculus*) and fin whales *(Balaenoptera physalus*) (e.g., Croll et al. 2001, Acevedo-Gutierrez et al. 2002, Doniol-Valcroze et al. 2011). These models, however, require estimates of the whale's metabolic rates and of their oxygen storage capacities and replenishment rates. Because much is still unknown regarding these physiological parameters of whales, estimates of their foraging efficiency based on OFT models may be inaccurate to an unknown degree.

In this chapter, I used Maximum Likelihood Estimation (MLE) techniques within a Bayesian framework to estimate the metabolic rates, total oxygen storage capacities, and oxygen replenishment rates of humpback whales (*Megaptera novaeangliae*) during foraging dives executed along the Western Antarctic Peninsula (WAP). I developed and used a model built upon the assumption that recorded observations of humpback whale

diving behavior recorded with a high-resolution bio-logging tool were true and that the observed whales were allocating their time optimally on foraging dives according to optimal foraging theory (OFT; i.e., they were maximizing their foraging durations while minimizing their recovery and travel durations; Kramer 1988, Houston & Carbone 1992). I calculated posterior densities of the physiological parameters of interest by finding the values of these parameters that result in the recorded observations being most probable assuming these whales were in fact foraging optimally. This method offers an alternative approach to allometric equations and scaling relationships for estimating these parameters, which may provide insights into both the accuracy of these relationships and the true values of these parameters.

4.1.1 Current Understanding of Humpback Whale Metabolic Rates

Direct estimates of metabolic rates in humpback whales are not currently available, but computational modelling techniques have been developed to try to gain a better understanding of the energetic cost of feeding and traveling in Balaenopterids (e.g., blue whales, fin whales, humpback whales; hereafter referred to as rorquals) (e.g., Goldbogen et al. 2007, Potvin et al. 2009, Goldbogen et al. 2010, Potvin et al. 2010, Goldbogen et al. 2011, Potvin et al. 2012). Observations of dive durations for foraging rorquals are much shorter than expected for their large body side (Dolphin 1988, Croll et al. 2001, Acevedo-Gutierrez et al. 2002, Goldbogen et al. 2006, Goldbogen et al. 2007, Goldbogen et al. 2008, Doniol-Valcroze et al. 2011), suggesting that their feeding behaviors are energetically costly. Rorquals forage by accelerating with a burst of

energetic fluking towards and engulfing a mass of prey-laden water that may be larger than the whale itself (Goldbogen et al. 2010); a process termed lunge feeding. Potvin et al. (2010) used an unsteady hydrodynamic model to estimate the amount of energy spent during the pre-engulfment and engulfment phase of lunge feeding in fin whales. Doniol-Valcroze et al. (2011) assumed that the rate reported by Potvin et al. (2010) could be scaled for blue whales because fin whales are morphologically similar to blue whales and because use the energetic costs of lunge feeding likely scale allometrically with body length (Goldbogen et al. 2010). Assuming that this rate applied to the entire foraging time (i.e., that it applies to the time spent while lunging as well as the time spent between consecutive lunges), Doniol-Valcroze et al. (2011) reported a metabolic rate while foraging for blue whales equal to 1.78 times their metabolic rate during traveling.

More recently, Potvin et al. (2012) derived engulfment metabolism rates (EMR) for rorquals from simulations based on hydrodynamic models that coupled rorqual structure and function, fluid dynamics, and krill escape behaviors. They derived scaling equations to estimate EMRs with respect to rorqual body length; however, the equation reported for humpbacks is only applicable to the duration of the mouth-opening phase during a lunge (2.2 sec for a 14 m humpback; Potvin et al. 2012). Potvin et al. (2012) found that EMRs during the mouth opening stage significantly increase with rorqual body size but that this rate converges with the rorqual average active metabolic rate (RAMMR, a new assessment for active metabolism specific to rorquals; Potvin et al. 2012) at small body sizes: EMR is approximately equal to RAMMR for a 10 m whale (e.g., a small-medium sized humpback whale) but approximately 3.7 times RAAMR for

a 27 m whale (e.g., a very large blue whale). Based on these findings, Potvin et al. (2012) suggests that the metabolic expenditure during engulfment by smaller whales, such as humpbacks, is similar to their metabolic expenditure during non-feeding swimming. Alternatively, other estimates of metabolic expenditures during feeding in marine mammals have suggested that this rate is 4 times AMR (active metabolic rate; Boyd & Croxall 1996, Croll et al. 2001). This variability in estimates needs to be further examined to fully assess the potential energetic costs of feeding, specifically in humpback whales.

Energy used during traveling to and from target feeding depths also needs to be accounted for when trying to calculate the total energetic costs of feeding in humpback whales. Potvin et al. (2012) derived equations for RAAMRs for blue, fin, and minke (*Balaenoptera bonaerensis*) whales under an assumption of steady travel that took into account power expenditures calculated from thrust data and the average speed of transport calculated from long duration tracking data (Bose & Lien 1989, Potvin et al. 2012). They were unable, however, to calculate this rate for humpback whales because their fluke morphology is significantly different than fin whales (Woodward et al. 2006), the species they used in their model to calculate the amount of thrust generated by fluking (Bose & Lien 1989). Therefore, the best known estimate of a humpback whale AMR can be calculated with the following allometric equation that relates body mass to power:

$$AMR = 3 \times 2 \times (4M_c^{0.75}), \quad (10)$$

where AMR is estimated in Watts (Costa & Williams 1999, Croll et al. 2006, Potvin et al. 2012). This rate is based on previous studies of marine mammal metabolism (Costa &

Williams 1999, Williams 1999, 2006) and assumes a basal metabolic rate (BMR) that is twice that of terrestrial animals expressed via Kleiber's scaling formula (Kleiber & Rogers 1961, Kleiber 1975). Croll et al. (2006) noted, however, that AMR-based studies have yielded estimates of AMR that have differed by as much as 100 % depending of the AMR-BMR relationship and BMR model used. Again, this variability needs to be addressed.

Further complicating the ability to estimate humpback AMRs is the observation that rorquals, like many marine mammals, can extend their aerobic dive durations by gliding for periods of time during a dive (e.g., Williams et al. 2000, Croll et al. 2001, Davis et al. 2001, Nowacek et al. 2001, Nousek-McGregor et al. 2014). Typically, rorquals begin a dive with a period of active fluking followed by a period of gliding to their target depth. While ascending, they generally alternate between periods of fluking and gliding before gliding to the surface to breathe (e.g., Croll et al. 2001, Nowacek et al. 2001, Ware et al. 2006, Goldbogen et al. 2008, Goldbogen et al. 2010, Tyson et al. 2012). In Weddell seals (*Leptoncychotes weddellii*), gliding reduces oxygen consumption during a dive by an average of 27.80% (Williams et al. 2000). However, in Steller sea lions (*Eumetopias jubatus*) metabolic savings from gliding are generally proportional to the additional energetic costs of active swimming during the ascending phase of a dive (Fahlman et al. 2008). Humpback whales exhibit gliding behaviors during feeding dives (e.g., Goldbogen et al. 2008, Ware et al. 2011, Tyson et al. 2012) but it is unknown to what extent, if any, gliding reduces their energetic costs.

4.1.2 Current Understanding of Humpback Whale Oxygen Stores and Replenishment Rates

The amount of oxygen available for use during a dive is related to the amount of time available for acquiring energy through foraging; the more oxygen that is available, the longer an animal can stay submerged searching for and capturing prey. Marine mammals have evolved a variety of adaptations that allow them to maximize the amount of time they can spend diving, including storing a proportion of oxygen in their skeletal muscles and blood (Castellini et al. 1981) and collapsing their lungs at depth (Kooyman & Ponganis 1997). Because of these adaptations, the total oxygen storage capacity of marine mammals (hereafter referred to as *K*) is believed to scale approximately proportionally with mass (Tenney & Remmers 1963, Lasiewski & Calder 1971, Kooyman 1973, Halsey et al. 2006, Stephens et al. 2008):

$$K = 0.03 M_c^{1.05}. \quad (11)$$

Values calculated using this proportion are similar to predicted estimates of these values based on observed dive-pause ratios in birds and mammals (Halsey et al. 2006) including blue whales (Croll et al. 2001, Doniol-Valcroze et al. 2011). This suggests that equation 11 may be a reliable estimate of *K* for humpbacks, although to my knowledge no studies have examined this.

Between dives, whales must replenish their oxygen stores so that an adequate amount of oxygen is available for the subsequent dive. The time it takes to replenish oxygen at the surface is time that cannot be spent actively foraging. Therefore the rate of oxygen acquisition affects the amount of time whales have for foraging and ultimately

the amount of food they can consume. The rate of oxygen replenishment in divers is logistically hard to estimate directly, and only a few studies have attempted to measure it (e.g., Parkes et al. 2002, Halsey et al. 2003). This rate, termed the initial rate of oxygen replenishment α (expressed as a proportion of total available stores, K), depends on the speed of oxygen uptake. Current theory suggests two different scaling relationships to derive estimates of α, both of which are based on an animal's mass. The first is a surface area relationship whereas oxygen uptake is expected to be limited by the surface area available for gaseous exchange (implying a scaling exponent of approximately two thirds; Stephens et al. 2008):

$$\alpha = 0.75 M_c^{\beta_\alpha}. \quad (12)$$

Stephens et al. (2008) suggested that α will likely scale with an allometric exponent in the region of β_α = -0.33 because α is proportional to K. The second relationship follows the principle of symmorphosis (Weibel et al. 1998) whereby each component of the oxygen chain must evolve to supply oxygen at the rate required by the muscles (Taylor & Weibel 1981). Under this scenario oxygen uptake is believed to scale with the same exponent as metabolism (i.e., $\beta_\alpha = \beta_m - 1$):

$$\alpha = 0.75 M_c^{\beta_m - 1} \quad (13)$$

(Stephens et al. 2008, Potvin et al. 2012). Stephens et al. (2008) derived the values for the slopes in both of these relationships in an *ad hoc* manner to obtain realistic dive times for divers of intermediate mass (150 kg). Therefore these slope values may not provide a realistic measure of oxygen exchange performance by large whales (Doniol-Valcroze et al. 2011). Currently, there is disagreement regarding which relationship is most accurate

for estimating α but many agree that this value is a critically important parameter in models used to scale surface durations of diving animals (Stephens et al. 2008).

4.2 Methods

4.2.1 Humpback Whale Dive Behavior

Observations of humpback whale dive behavior were collected in 2009 and 2010 along the coastal waters of the Western Antarctic Peninsula (WAP) with high-resolution digital acoustic recording tags (Dtags; Johnson & Tyack 2003) (Table 4; Nowacek et al. 2011, Ware et al. 2011, Stimpert et al. 2012, Tyson et al. 2012, Friedlaender et al. 2013). Dtags were placed via 4 silicon suction cups on the dorsal surface of each animal, between the dorsal fin and the blowhole, using an 8 m carbon-fiber pole. Other than startle responses by a few individuals, whale behavior was not visibly affected by the tagging events. Dtags recorded each whale's depth, pitch, roll, and heading at 50 Hz for up to 24 hrs via an internal pressure sensor, a three-axis accelerometer, and a three-axis magnetometer, respectively. The tool also recorded any and all sounds produced in the environment at 96 kHz with an embedded hydrophone. After a pre-programmed time, an active release caused the suction cups to release the Dtags from the whales, causing them to float to the surface where they were retrieved by hand. Once the Dtags were collected they were immediately calibrated and the recorded data were downloaded via infrared transmission.

Table 7: Dtag deployment information. Whale ID, tag on date, tag start time, and tagging location, tag on time, and the number of foraging dives recorded for each humpback whale.

Whale ID	Tag on date	Tag start time (GMT − 5 h)	Tagging location	Total tag on time (hr)	Number of foraging dives
122b	2009-May-02	14:28:44	Wilhelmina Bay	18.4	419
127a	2009-May-07	08:42:03	Wilhelmina Bay	24.6	89
136a	2009-May-16	09:09:54	Anvord Bay	23.0	82
140a	2009-May-20	10:58:03	Anvord Bay	22.5	7
148a	2009-May-28	09:48:17	Wilhelmina Bay	25.2	225
152a	2009-June-01	10:39:24	Wilhelmina Bay	22.3	462
132a	2010-May-12	09:58:38	Wilhelmina Bay	23.1	97
133a	2010-May-13	12:03:50	Wilhelmina Bay	22.2	102
139a	2010-May-19	11:02:58	Wilhelmina Bay	20.6	292
144a	2010-May-24	14:05:18	Wilhelmina Bay	21.1	307
146a	2010-May-26	15:17:42	Flandres Bay	20.0	64
151a	2010-May-31	10:23:51	Wilhelmina Bay	24.6	160
155a	2010-June-04	09:42:03	Flandres Bay	22.2	59
				Total Foraging Dives:	2365

I used custom code built for Dtag analyses (Johnson & Tyack 2003) to determine the dive durations, surface durations, and maximum dive depths of each dive (defined as any submergence greater than 3 m) for each tagged whale in the software program MATLAB® (MathWorks 2013b). I used TrackPlot (Ware et al. 2006) to identify discrete feeding lunges executed by each whale from these records (see Ware et al. 2006, Tyson et al. 2012, Friedlaender et al. 2013 for details). I defined feeding dives as any dive for which a feeding lunge deeper than 3 m was detected (Friedlaender et al. 2013); non-feeding dives were not examined in the following analysis. I divided feeding dives into three parts for use in the simulated model: i) travel duration to and from the whales feeding depths τ; ii) foraging duration, t; and iii) post-dive surface duration, s. For the purposes of this chapter, I calculated t as the duration of time lasting from the moment

the first lunge was executed (i.e., mouth opening) on a dive to the moment the last lunge on that dive was completed (I included an estimated filter duration to this time for an average sized humpback whale: 13.00 sec; Goldbogen et al. 2012). Accordingly, I calculated τ as

$$\tau = u - t, \tag{14}$$

where u is the observed dive duration ($u = \tau + t$).

4.2.2 Optimal Foraging Model

The time allocation optimal foraging model treats the diver as a central place forager with the surface acting as the central place: the diver must repeatedly come to the surface to breathe (Kramer 1988, Houston & Carbone 1992). An assumption of the model is that a diver that spends time s on the surface following dive duration u and gains oxygen as

$$x(s) = K(1 - e^{-\alpha s}). \tag{15}$$

During the subsequent dive, the diver uses all of this stored oxygen, x(s), as

$$x(s) = m_\tau \tau + m_t t, \tag{16}$$

where m_τ is the metabolic rate while traveling (τ) and m_t is the metabolic rate while foraging (t). Thus, the diver balances oxygen stores over the dive cycle (Houston & Carbone 1992). It is also assumed that a diver will maximize the proportion of time it spends foraging during a dive cycle,

$$\pi = \frac{t}{t + s + \tau}, \tag{17}$$

which is equivalent to maximizing

$$\pi = \frac{t}{s + \tau} \tag{18}$$

(see Houston & Carbone 1992). By substituting

$$t = \frac{x(s) - m_{\text{T}}\tau}{m_t} \tag{19}$$

from equations 15 and 16 into equation 18, it is shown that a dive is maximized when

$$\pi(\text{s}) = \frac{\text{K}(1 - e^{-\alpha s}) - m_\tau \tau}{m_{\text{T}} \times (s + \tau)} \tag{20}$$

(Houston & Carbone 1992) and that the value of s that maximizes $\pi(s)$ will also maximize the proportion of time spent foraging. Because of the optimality condition that

$$\pi'(s^*) = 0, \tag{21}$$

the value of s that maximize $\pi(s)$, s^*, is found by solving

$$x'(s^*) = \frac{x(s^*) - m_\tau \tau}{(s^* + \tau)} \tag{22}$$

numerically for s^* ($x'(s^*) = m_{\text{T}}$). This solution, however, does not rely on m_t, one of the parameters I am interesting in estimating, but the solutions for the optimal foraging time, t^*:

$$t^* = \frac{x(s^*) - m_\tau \tau}{m_t}. \tag{23}$$

and for the optimal dive time, u^*, do:

$$u^* = \frac{x(s^*) - m_\tau \tau}{m_t} + \tau. \tag{24}$$

(Houston & Carbone 1992). I used u^* in my simulated model (described in more detail below) because it relies on both s^* and t^* and thus all of the physiological parameters I

am interested in estimating. I performed all computations using custom written code in the statistical software program R (R Core Team 2013; Appendix C).

4.2.3 The Simulated Model

I calculated the likelihood of the observed values of u based on the predicted values of u^* for each foraging dive, where u^* was calculated following equation 24 with observed values of τ and candidate values of K, α, m_τ, and m_t. I assumed that observed values of u were normally distributed, thus the likelihood function that described the probability of u assuming that the optimal model was correct is:

$$L = \prod_{i=1}^{n} N(u_i|\tau_i, K, \alpha, m_\tau, m_t; \sigma^2) = \prod_{i=1}^{n} N(u_i|u_i^*, \sigma^2), \tag{25}$$

where σ^2 is the model variance. I found the values of K, α, m_τ, and m_t that maximize this function by summing the log of this likelihood,

$$\ln L \propto -n \ln \sigma - \frac{1}{2\sigma^2} \sum_{i=1}^{n} (u_i - u_i^*)^2, \tag{26}$$

differentiating it for each parameter value, and setting them equal to zero (Clark 2007).

I used this MLE approach within a Bayesian statistical framework because Bayesian methods allow for prior information regarding model parameters to influence the estimation of the posterior values of interest. Following Bayes theorem (Bayes & Price 1763), I estimated posterior densities of K, α, m_τ, and m_t as

$$p\ (\tau, K, \alpha, m_\tau, m_t|u) = \frac{p(u|\tau, K, \alpha, m_\tau, m_t)p(\tau, K, \alpha, m_\tau, m_t)}{p(u)}. \tag{27}$$

Here, the probability of τ, K, α, m_τ, and m_t given observed durations of u is equal to the product of the likelihood, $p(u|c, K, \alpha, m_\tau, m_t)$, and the prior density of the proposed values, $p(\tau, K, \alpha, m_\tau, m_t)$, divided by the probability of the observed u, $p(u)$. I used candidate values of K, α, m_τ, and m_t estimated following equations provided in Table 8 to produce their prior densities. The equations I used provide, in my opinion, the most conservative estimates of these parameters based on the current understanding of their true value (as discussed previously).

Table 8: Descriptions, equations, and values of parameters used as priors in the simulated model. Notes: values of m_τ, and m_t were converted from Watts to L O_2 s^{-1} for use in the optimal model.

Parameter	Description (units)	Equation	Reference
L	Length (m)		
M	Body Mass (kg)	$16.473 \times L^{2.95}$	Lockyer (1976)
m_τ	Metabolic rate while traveling (L O_2 s^{-1})	$6 \times 4 \times M^{0.75}$	Potvin et al. (2012)
m_t	Metabolic rate while foraging (L O_2 s^{-1})	$1.78 \times m_\tau$	Potvin et al. (2009), Goldbogen et al. (2010), Donio-Valcroze et al. (2011)
K	Total oxygen storage capacity (L O_2)	$0.03 \times M^{1.05}$	Stephens et al. (2008)
α	Initial proportional rate of oxygen replenishment (s^{-1})	$0.075 \times M^{-0.33}$	Stephens et al. (2008)

I used a Markov Chain Monte Carlo (MCMC) simulation with a Gibbs sampler and a Metropolis sampling algorithm to obtain the posterior densities of K, α, m_τ, and m_t. A Gibbs sampler allows for the estimation of multivariate distributions for multiple parameters (i.e., K, α, m_τ, and m_t), to be simulated by alternatively sampling from the conditional distributions of each parameter (German & German 1984). The Metropolis sampling algorithm is a MCMC technique that allows for the construction of a random walk of each parameter having a stationary distribution described by the target distribution (Metropolis et al. 1953, Hastings 1970). Within the Metropolis sampling algorithm, I proposed values of each parameter at iterative steps (g) and compared them to random candidate values selected from a symmetric 'jump' density of each parameter conditioned on the current values of each parameter (Gelman et al. 1995):

$$J(K^*, \alpha^*, m_\tau^*, m_t^* | K^{(g)}, \alpha^{(g)}, m_\tau^{(g)}, m_t^{(g)}), \tag{28}$$

where parameter* is a random candidate value and parameter$^{(g)}$ is the current value. I used a truncated normal density with mean values given by the current parameter vectors and a covariance matrix $\mathbf{V}$ to calculate the jump density:

$$J\left(K^*, \alpha^*, m_\tau^*, m_t^* \middle| K^{(g)}, \alpha^{(g)}, m_\tau^{(g)}, m_t^{(g)}\right) \tag{29}$$

$$= \int_{(100,\ 0.0001,\ 0.01,\ 0.01)}^{(5000,\ 1,\ 50,\ 50)} N_P\left(K^*, \alpha^*, m_\tau^*, m_t^* \middle| K^{(g)}, \alpha^{(g)}, m_\tau^{(g)}, m_t^{(g)}, \boldsymbol{V}\right).$$

I based the values for the upper and lower bounds of this truncated normal density on prior knowledge of these parameters (e.g., Table 8) but set them to be wide so that the

observed whale dive data would have a larger influence on the model than the prior estimate values (i.e., I used vague priors in my simulation). I set the starting parameter values of each simulation to be equal to those calculated using equations listed in Table 8 for a random sized whale (a random length of 12 m was selected). I set **V** to be equal to the priors values of each parameter (Table 8) divided by 10000. **V** dictates the size and direction of the iterative steps in the Metropolis algorithm and this value resulted in high convergence of the MCMC chains.

I determined the density of the candidate values relative to that of the current values following

$$z = \frac{p(K^*, \alpha^*, m_\tau^*, m_t^*)}{p\left(K^{(g)}, \alpha^{(g)}, m_\tau^{(g)}, m_t^{(g)}\right)}. \quad (30)$$

If $z \geq 1$ (i.e., the probability that the candidate values exceeded the current values), I accepted the candidate values in the simulation. If $z < 1$ I accepted the candidate values as new values (i.e., $K^{(g)}$, $\alpha^{(g)}$, $m_\tau^{(g)}$, and $m_t^{(g)}$) with probability z if $z > y$, where y was a randomly drawn univariate between zero and one. Otherwise, I retained the current values (i.e., $K^{(g+1)}$, $\alpha^{(g+1)}$, $m_\tau^{(g+1)}$, and $m_t^{(g+1)} = K^{(g)}$, $\alpha^{(g)}$, $m_\tau^{(g)}$, and $m_t^{(g)}$) (Hastings 1970). Because I used a Gibbs sampler, each value was updated before proceeding to the next step in the simulation. Also, I accepted and rejected the parameters together as a block because they are conditionally dependent. Finally, I repeated the simulation using prior densities estimated from a variety of sized whales to examine the effect that prior values

had on the model: 10 m, 12 m, 13.45 m (average length of a humpback whale, Clapham & Mead 1999) , and 15 m.

Because there are no specific rules for stopping the simulation (e.g., Cappe & Robert 2000), I ran the simulations long enough to obtain a MCMC sequence that adequately represented the target distribution of each parameter estimate. I used the density function in the stats package in R (R Core Team 2013) to calculate their respective normal Kernel density distributions (I applied the default kernel bandwidth smoothing parameters). I computed the mean, median, standard deviation, and 2.5%, and 97.5% credible limits for each parameter's posterior estimate from the MCMC sequences derived for each parameter. In the discussion, I compared these posterior estimates from each simulation to the prior estimates and discuss the implications of my findings.

4.3 Results

4.3.1 Observed Whale Behavior

I recorded 2365 feeding dives executed by the thirteen whales listed in Table 7. Maximum dive depths ranged from 3.29 to 388.16 m (mean ± SD: 66.06 ± 75.06 m), while dive durations (u) ranged from 10.60 to 748.60 sec (mean ± SD: 163.64 ± 166.02 sec). Dives were successfully split into their respective durations of τ, t, and s (Figure 19): τ values ranged from 0 to 609.80 sec (mean ± SD: 67.48 ± 77.30 sec), t values ranged from 5.91 to

547.40 sec (mean ± SD: 96.16 ± 110.80 sec), and s values ranged from 0 to 2466.8 sec (mean ± SD: 65.78 ± 136.79 sec). Of τ and t, τ was found to have a greater influence on the predicted value of s ($s \sim \tau + t$: $y = -15.39 + 0.86\tau + 0.24t$, $R^2 = 0.38$, $p < 0.001$). In addition, all durations were significant and positively correlated with maximum dive depth and each other (Table 9).

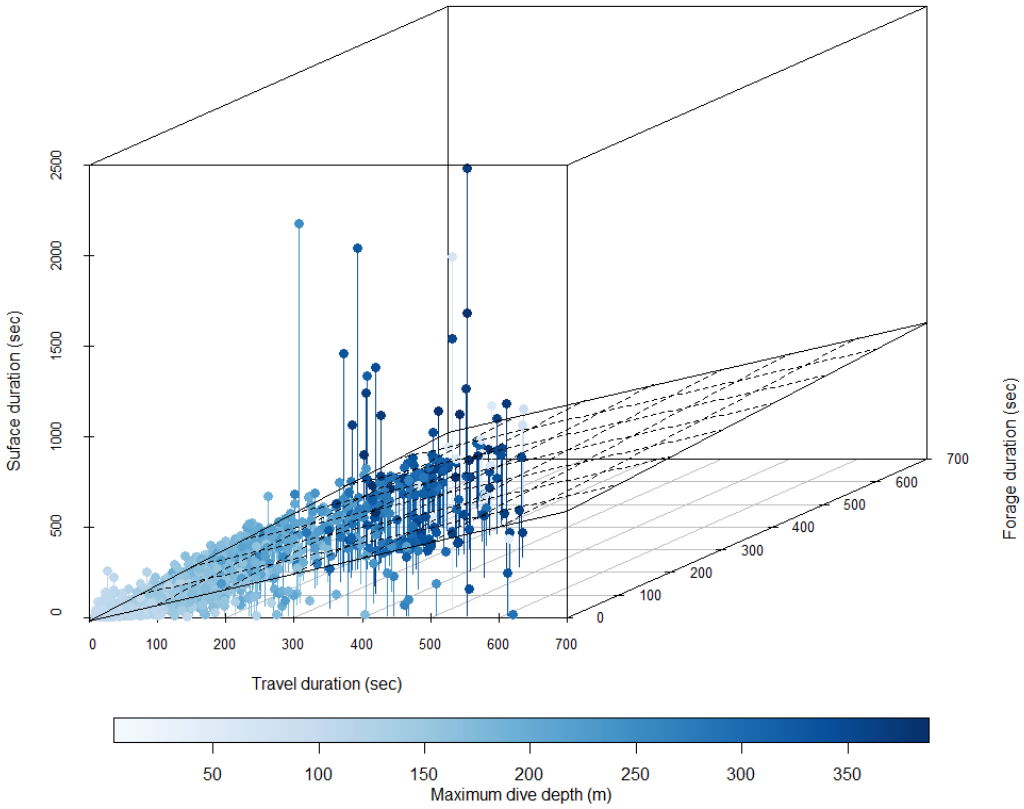

Figure 19: Durations of each discrete behavior within a dive cycle (surfacing, *s*; traveling, τ; and foraging, *t*) plotted with their respective maximum dive depth (m). The plane through the plot represents the linear regression $s \sim \tau + t$ ($y = -15.39 + 0.86\tau + 0.24t$, $R^2 = 0.38$, $p < 0.001$). The vertical lines represent the values of *s* against their respective values of τ and *t*.

Table 9: Pearsons r correlation coefficients for maximum dive depths, post-dive surface durations (s), travel durations (τ), forage durations (t), and dive durations (u). All correlations were significant (i.e., $p < 0.001$).

	Maximum dive depth	Post-dive surface duration (s)	Travel duration (τ)	Forage duration (t)	Dive duration (u)
Maximum dive depth	-----	-----	-----	-----	-----
Post-dive surface duration (s)	0.63	-----	-----	-----	-----
Travel duration (τ)	0.83	0.59	-----	-----	-----
Forage duration (t)	0.84	0.46	0.54	-----	-----
Dive duration (u)	0.95	0.58	0.83	0.92	-----

4.3.2 Results of Simulation

I used all values of s, u, τ, and t in each simulation to derive posterior estimates of K, α, m_τ, and m_t (i.e., I did not run the simulation separately for each individual whale) and the agreement between observed and simulated values was high (Model efficiency = 0.69; Pearson product-moment correlation coefficient = 0.87, $p < 0.001$). Convergence of chains varied by parameter and by simulation run. Therefore, I discarded the first 3000 iterations (of 100000; i.e., the burn in) of each chain to ensure that each MCMC sequence had reached convergence and that they were comparable before I calculated each parameter's posterior densities (Figure 20). The posterior estimates and associated summary statistics of each parameter and simulation are found in Table 10. Prior values for each simulation are included for comparison.

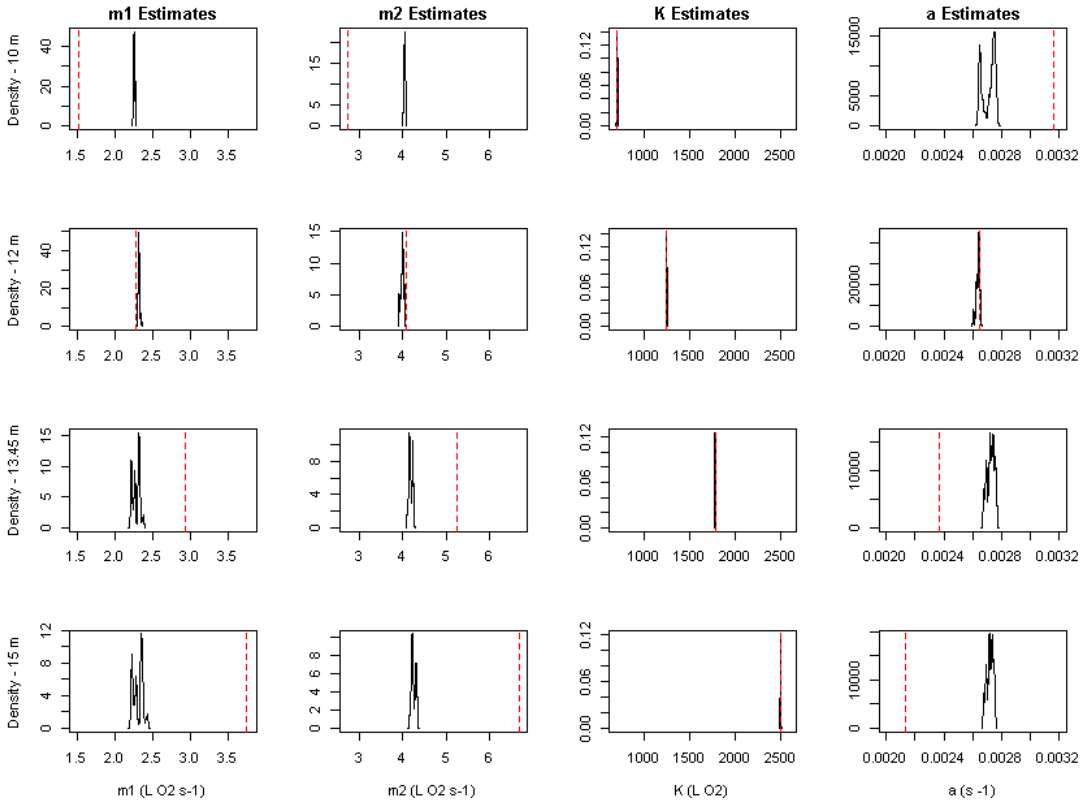

Figure 20: Kernel density estimates for humpback whale metabolic rates while traveling and (m_τ) and foraging (m_t), and for total oxygen capacity (K) and initial rate of oxygen replenishment (α). Each column represents a different physiological parameter while each row represents a simulation run using different prior values (i.e., prior values were calculated for whales of the following lenghts: 10 m (first row), 12 m (second row), 13.45 (third row), and 15 m (forth row)). The red vertical lines indicate the respective prior parameter values, which were calculated using equations found in Table 2.

Table 10: Posterior estimates of humpback whale metabolic rates while traveling and (m_T) and foraging (m_t), total oxygen capacity (K), and initial rate of oxygen replenishment (α); estimates are given as the posterior means, medians, standard deviations (SD) and 2.5% and 97.5% credible limits (CL).

	Prior values		Posterior estimates					
Parameter	Whale length (m)	Parameter value	Mean	Median	SD	2.5 % CL	97.5% CL	Units
m_T	10.00	1.53	2.26	2.26	0.01	2.24	2.28	L O_2 s^{-1}
	12.00	2.29	2.32	2.32	0.01	2.30	2.35	
	13.45	2.95	2.34	2.31	0.05	2.21	2.37	
	15.00	3.75	2.31	2.33	0.06	2.22	2.42	
m_t	10.00	2.72	4.04	4.04	0.01	4.01	4.07	L O_2 s^{-1}
	12.00	4.07	3.98	3.99	0.03	3.91	4.04	
	13.45	5.24	4.18	4.18	0.04	4.10	4.25	
	15.00	6.68	4.25	4.25	0.05	4.16	4.33	
K	10.00	711.59	711.70	711.50	4.29	704.39	722.16	L O_2
	12.00	1251.69	1251.71	1251.65	3.05	1245.66	1256.51	
	13.45	1782.17	1782.07	1782.08	3.24	1775.62	1787.41	
	15.00	2498.48	2498.50	2498.55	3.10	2493.59	2503.47	
α	10.00	3.16×10^{-3}	2.71×10^{-3}	2.73×10^{-3}	4.41×10^{-5}	2.64×10^{-3}	2.76×10^{-3}	s^{-1}
	12.00	2.65×10^{-3}	2.64×10^{-3}	2.64×10^{-3}	1.27×10^{-5}	2.60×10^{-3}	2.65×10^{-3}	
	13.45	2.37×10^{-3}	2.72×10^{-3}	2.73×10^{-3}	2.59×10^{-5}	2.67×10^{-3}	2.76×10^{-3}	
	15.00	2.13×10^{-3}	2.72×10^{-3}	2.72×10^{-3}	2.56×10^{-5}	2.67×10^{-3}	2.75×10^{-3}	

Mean posterior estimates of m_τ from each simulation were similar despite using prior values calculated for whales of different sizes (Figure 20; Table 10: all posterior estimates had a 2.5 – 97.5 % CL ranging between 2.22 and 2.42 L O_2 s^{-1}). The mean posterior estimates calculated from the simulations that used prior values derived for 10 m and12 m whales had the lowest SDs (0.01), but the latter mean posterior estimate was most similar to its prior value (mean = 2.32 L O_2 s^{-1}; prior value of m_τ for a 12 m whale = 2.29 L O_2 s^{-1}); the former mean posterior estimate was larger than its prior value by an estimated 0.71 L O_2 s^{-1}. The mean posterior estimates calculated from the simulations using prior values of m_τ derived for whales of 13.45 m and 15 m were smaller than their prior values by an estimated 0.61 and 1.41 L O_2 s^{-1}, respectively (Figure 20; Table 10), albeit having SDs of only 0.05 and 0.06. Interestingly, the 2.5 – 97.5% CLs of the posterior estimates calculated using prior values of m_τ for 10 m whales (2.24 – 2.28 L O_2 s^{-1}) and 12 m whales (2.30 – 2.35 L O_2 s^{-1}) were within the 2.5 – 97.5 % CLs of the posterior estimates calculated using prior values of m_τ derived for 13.45 m and 15 m whales (2.21 – 2.37 L O_2 s^{-1} and 2.22 – 2.47 L O_2 s^{-1}, respectively).

The mean posterior estimates of m_t were also similar to one another despite being calculated using increasing prior values of m_t in the simulated models (Figure 20; Table 10). Again, the mean posterior estimate of m_t calculated from the simulation that used

prior values of m_t derived for a 12 m whale was most similar to its prior value (mean = 3.98 L O_2 s^{-1}, SD = 0.03; prior value = 4.07 L O_2 s^{-1}). While the SDs of the posterior means calculated using prior values of m_t derived for 10 m, 13.45 m, and 15 m whales were low (0.01, 0.04, and 0.05), the estimates were 1.32 L O_2 s^{-1} larger and 1.06 L O_2 s^{-1} and 2.43 L O_2 s^{-1} smaller than their respective prior values (Table 8). Also, none of the 2.5 – 97.5% CLs calculated from the simulations included the respective prior values used for m_t, although they were similar to one another (Table 10). The 2.5 – 97.5% CL calculated from the simulation using a prior value of m_t derived for a 12 m whale was most similar to its prior value (prior value = 4.07 L O_2 s^{-1}; CL = 3.91 – 4.04 L O_2 s^{-1}).

Prior values used in the simulated model had a strong influence on the posterior estimates of K (Figure 20; Table 10). Each simulation resulted in a mean posterior estimate of K that was within 1 L O_2 of its prior value. In addition, the 2.5 – 97.5% CL of each simulation included their respective prior value but none of them overlapped with a CL from another simulation. Finally, SDs of each simulation were less than 4.30 L O_2 (Table 10).

Posterior densities of α converged upon mean values ranging from 2.64 x 10^{-3} to 2.72 x 10^{-3} s^{-1} (Figure 20, Table 10). Similarly to the mean posterior estimates of m_τ and m_t, the mean posterior estimate of α calculated from the simulation that used prior values

derived for a 12 m whale had the lowest SD (1.27×10^{-5} s^{-1}) and was most similar to its prior value (mean = 2.64×10^{-3} s^{-1}; prior value = 2.65×10^{-3} s^{-1}). The mean posterior estimates calculated using prior values of α for 10 m, 13.45 m, and 15 m whales all were extremely similar to one another with 2.5 – 97.5% CLs ranging within 2.64×10^{-3} s^{-1} and 2.76×10^{-3} s^{-1} (Table 10). The 2.5 – 97.5% CL of the posterior estimates of α calculated with a prior value of α derived for a 12 m whale ranged from 2.60×10^{-3} s^{-1} to 2.65×10^{-3} s^{-1}. SDs of all simulations were less than 4.5×10^{-5} s^{-1}.

4.4 Discussion

In this study, I implemented MCMC simulations with a Gibbs sampler and a Metropolis sampling algorithm to estimate posterior values of K, α, m_τ, and m_t for humpback whales based on the likelihood that observed dive behaviors were optimal according to OFT. I was able to use 2365 feeding dives from humpback whales in the simulations that included a wide range of s, t, and u durations (Figure 17), which were positively correlated with one another (Table 9). Repeated simulations using an assortment of prior values estimated for different sized humpbacks revealed high convergence of MCMCs, specifically in regards to m_τ, m_t, and α, that centered on prior values estimated for a 12 m humpback whale from allometric equations listed in Table 8.

The simulations also revealed a strong influence of prior values on posterior estimates of K.

Prior values of m_τ, m_ι, and α had little influence on the calculation of their posterior distribution suggesting that the observed dive data instead drove the model. Despite the use of a range of prior values for each of these parameters, the posterior estimates converged upon similar distributions. Interestingly, these distributions all converged on estimates that are similarly obtained using the allometric equations listed in Table 8 for a humpback whale 12 m in length. This could mean either that the whales observed in this study were, on average, approximately 12 m in length or that the whales have a different approximate mean length and the prior values obtained from the equations listed in Table 8 are inaccurate. A preliminary analysis aimed at estimating the lengths of 11 of the 13 whales observed in this study using photogrammetry techniques suggest that the mean size of whales tagged in this study was 12.9 m (average SD = ± 1.29, CV = 9.98%; Kutcher, unpublished data; Appendix D).

If I assume that the whales observed in this study were on average 12 m in length then the current allometric equation used to calculate m_τ ($AMR = 3 \times 2 \times 4M_c^{0.75}$; equation 10) may be accurate. The observed dive data of humpback whales suggests that their m_τ ranged from 2.21 to 2.42 L O_2 s^{-1}; the value of m_τ

calculated using equation 10 for a 12 m humpback is 2.32 L O_2 s^{-1}. However, if the whales observed in this study were either larger or smaller than 12 m, estimates of m_τ calculated with equation 10 may overestimate or underestimate this rate, respectively. For example, if the whales observed in this study were on average 12.9 m in length, their predicted m_τ value from equation 10 would be 2.69 L O_2 s^{-1}; a value slightly higher than that predicted by my simulations (Table 10). This suggests that values of m_τ derived from equation 10 may overestimate m_τ by an increasingly large amount with increasing body size. This may be related to the increased volumetric mass that is associated with increased body size (Goldbogen et al. 2010).

The calculation for m_τ used in my model does not take into account any energetic savings that may be the result of gliding. If the posterior estimates I obtained did account for energy saved by gliding, the finding that the posterior estimates were lower than those predicted by AMR may be attributed to energy being saved through this behavior. This is reasonable to assume because the prior values did not appear to have a strong influence on the model. The amount of energy saved from gliding in rorquals, however, has not been adequately measured; future research efforts will hopefully address this more fully.

The mean posterior estimates of m_t obtained from the simulations ranged from 3.98 to 4.25 L O_2 s^{-1}. If the whales observed in this study were 12 m in average length then the multiplicative factor of 1.78 x m_τ derived by Doniol-Valcroze et al. (2011) and based on simulations of blue and fin whales computed by Goldbogen et al. (2010) and Potvin et al. (2010) may be an accurate calculation for m_t. That calculation results in a value of m_t equal to 4.07 L O_2 s^{-1}, a value that is within the CLs of all but one of the simulations I ran (Table 10). However, if the observed whales were smaller or larger than 12 m, the calculation derived by Doniol-Valcroze et al. (2011) likely overestimates or underestimates the true value of m_t, respectively. Nonetheless, it appears that the true value of m_t lies somewhere in the range of 1.62 – 1.96 x m_τ (values were calculated from the smallest value of m_t obtained from the 2.5 % CLs divided by the largest value of m_τ obtained from the 97.5 % CLs, and the largest value of m_t obtained from the 97.5 % CLs divided by the smallest value of m_τ obtained from the 2.5 % CLs, respectively).

The manner in which I derived durations of τ and t may have affected the posterior estimates I obtained from my simulations. I chose to define foraging durations as the duration of time lasting from the moment the first lunge was executed (i.e., mouth opening) on a dive to the moment the last lunge on that dive was completed, which included a filter duration of 13.00 sec (Potvin et al. 2012). Other studies have defined this

duration as the amount of time spent between first reaching the mean depth of feeding activity on a dive and the time they last exit that depth (e.g., Doniol-Valcroze et al. 2011) or as the time spent at depths greater than 75 % of the maximum depth of dive (e.g., Acevedo-Gutierrez et al. 2002). Because I was able to explicitly identify feeding events during a dive, I chose to calculate foraging times based on these lunges and to apply m_t to this entire duration. If periods of travel between consecutive lunges were included in the calculation of foraging durations the results of the simulation may have been biased to an unknown degree. Previous examinations, however, suggest that this definition of travel time is appropriate (see Chapter 2).

The posterior estimates of α that I obtained in the simulations were remarkably similar despite the difference in prior values used, with mean values ranging from 2.13 x 10^{-3} to 3.16 x 10^{-3} s^{-1} (Table 10). Again, the simulations converged on posterior estimates that were most similar to the prior value I used to calculate α with for a 12 m whale. As with m_τ and m_t, if the observed whales were on average 12 m in length then the equation of α that assumes oxygen uptake is limited by the surface area available for gaseous exchange (equation 12) may be accurate. It is unclear whether running the simulations using prior values following the principle of symmorphosis, whereby each component of the oxygen chain must evolve to supply oxygen at the rate required by the muscles

(equation 13; Weibel et al. 1998) would have resulted in different posterior estimates. Here, I used the surface area relationship to estimate α, where oxygen uptake is expected to be limited by the surface area available for gaseous exchange, because it is more commonly used to derive estimates of α in baleen whales and thus perhaps more comparable to other studies (e.g., Doniol-Valcroze et al. 2011). I predict that simulations using α derived via the principle of symmorphosis would also converge on similar values because changing the prior values in the simulations did not appear to have a large influence on the model output (the observed data had a stronger influence than the prior values of α). Future research should address the effect that these two methods would have on this model's estimation of α because this parameter is highly critical in models aimed to scale surface durations of diving animals (Stephens et al. 2008).

Interestingly, the posterior estimates of K were strongly influenced by their prior value: mean posterior estimates of K were within 1 L 0_2 of their prior values for all simulations (Table 10). This extreme influence of prior values on the model suggests that K is strongly influenced by an animal's body size. This finding is intuitive because larger whales will have a greater ability to store oxygen than smaller whales based strictly on the size of their lunges and muscles and increased volumes of blood. These results also suggest that the equation used to calculate the prior values of *K* (equation 2; Tenney &

Remmers 1963, Lasiewski & Calder 1971, Kooyman 1973, Halsey et al. 2006, Stephens et al. 2008) is an accurate method to estimate this parameter. This finding agrees with other studies that have reported that values calculated using this proportion are similar to predicted estimates of these values based on observed dive-pause ratios in birds and mammals (e.g., Croll et al. 2001, Halsey et al. 2006, Doniol-Valcroze et al. 2011).

The true size of the each individual whale observed in this research and their respective number of foraging dives may have influenced the posterior estimates of the simulations. For example, if the whales that executed the most foraging dives (e.g., 122a, 152a) were 12 m in length their observations may have biased the simulations such that the posterior estimates applied mostly to their dives. According to preliminary predictions of these whales from photogrammetry data (Appendix D: Kutcher unpublished data), however, the lengths of observed whales that executed 300 or more feeding dives (i.e., 122b, 152a, and 144a) ranged from 9.32 m (144a) to 13.48 m (122b; no length estimate is available for 152a). Therefore, the results from my simulations may represent the average values of these parameters for humpback whales.

The results of this study offer insights into the appropriateness of the current techniques used to estimate the metabolic rates and oxygen storage capacities and replenishment rates. These findings are extremely useful for directing future research as

they suggest that parameters such as *K* are adequately estimated using the respective current allometric equations, while the estimation of metabolic rates of rorquals while foraging and while traveling need to be addressed further. Future research efforts will use this model to simulate these physiological parameters in additional diving species, such as southern elephant seals (*Mirounga leonina*) and/or Weddell seals where metabolic rates may be available for groundtruthing the model, and will explore how mixed-metabolism models would influence the posterior estimates.

5. Current Knowledge, Data Gaps, and Future Research Directions

In this dissertation, I use high-resolution bio-logging tools to examine the fine-scale foraging behaviors of humpback whales (*Megaptera novaeangliae*) in the coastal waters of the Western Antarctic Peninsula (WAP). I identified discrete feeding lunges of humpback whales recorded via high-resolution digital acoustic recording tags during the austral fall of 2009 and 2010 from within several embayments along the Peninsula. I used these data to describe several fundamental elements of humpback whale foraging ecology, including the foraging efficiency of adult humpback whales as well as the foraging behaviors and synchrony of a mother and calf. I also used these data to increase the understanding of aspects of humpback whale physiology so that future modelling efforts may be more accurate. I hope that this work significantly advances the current understanding of humpback whale foraging behaviors along the WAP so that appropriate measures can be taken to aid in their recovery and in the sustainability of the Antarctic marine ecosystem.

5.1 Current Knowledge

In order to be evolutionarily successful, animals must dedicate a portion of their available time to foraging (animals can't survive to reproduce if they don't fulfill their energy requirements). Natural selection, therefore, should favor foraging strategies that are efficient in minimizing costs (in time and energy and exposure to predation) while simultaneously maximizing benefits (e.g., energy, nutrients) (Macarthur & Pianka 1966). In this research, I found that humpback whales in the near-shore waters of the WAP exhibit efficient foraging strategies with minimal energetic costs (Chapter 3). They feed at a continuous and high rate, favoring energy gains over oxygen balance, from approximately dusk to dawn (Figure 21; see Friedlander et al. 2013) and spend approximately 40.00 % of this time actively lunging for prey (~ 8 hrs; Chapter 3). These behaviors allow them to exploit their prey when they are most vulnerable and less costly to acquire (i.e., at night when krill are foraging near the surface).

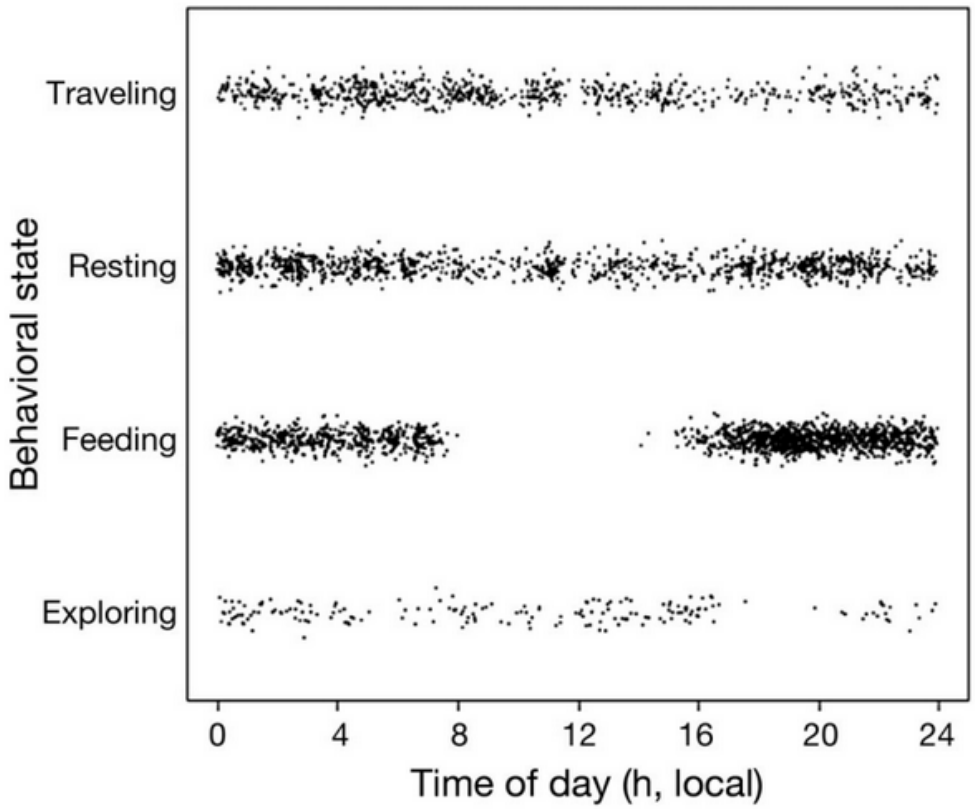

Figure 21: Frequency and temporal distribution of all dives categorized by behvioral state for whales tagged in Wilhelmina Bay in 2009 and 1010 in local time (GMT – 5 h). Individidual dives are staggered along the vertical axis for each behavioral state to show the density of points. (From Friedlaender et al. 2013).

The high rate of foraging observed in this research allows these whales to store a large volume of energy in the form of blubber, which can be used to replenish energy reserves diminished from the recent migration and increasing energy reserves for successful future migrations (Lockyer 1981). This is particularly beneficial for nursing

mothers who must also replenish energy reserves lost due to the added cost of lactation and the caring of their calf, and the calf who must acquire energy for growth (Chapter 2). My findings suggest that the whales examined in this study were foraging efficiently and in a clever manner and that the current structure of the Antarctic marine ecosystem is favorable to the fitness and recovery of the humpback whales in the Southern Ocean.

5.2 Data Gaps and Future Research Directions

While this dissertation provides added information to the baseline foraging behaviors of humpbacks, much about their behaviors is still unknown. Some of the biggest questions still apparent are those regarding the energetics and physiology of baleen whales. While the model presented in Chapter 4 provides important information regarding the accuracy of current methods used to estimate aspects of rorqual physiology (e.g., metabolic rates and oxygen replenishment rates), it represents just a step towards obtaining the true values of these parameters. Future research directions will be focused on ground-truthing this model with data such as the dive records of seals that have concurrent measurements of metabolic rates so that the true accuracy of its predictions can be better assessed. This is critically important because these parameters can be used to predict foraging behaviors in response to fluctuations in prey

resources (e.g., Wiedenmann et al. 2011) , a prediction that is of high value in the face of a changing Antarctic marine ecosystem.

Since the 1950s, the WAP has experienced rapid climate change. Most strikingly, winter atmospheric temperatures have increased by 6°C (Vaughan et al. 2003) and the duration and spatial extent of winter sea-ice have decreased (Smith & Stammerjohn 2001, Vaughan et al. 2003, Parkinson 2004, Stammerjohn et al. 2008a, Stammerjohn et al. 2008b). Further decreases in the duration and spatial extent of winter sea-ice may result in longer foraging seasons for migrating species, such as humpback whales, and a reduction in the standing stock of Antarctic krill. In addition, an expanding commercial krill fishery in the region and a whale population recovering from exploitation may further constrain this system (Nicol & Foster 2003).

Wiedenmann et al. (2011) suggest that whales in the Antarctic marine ecosystem may be able to reduce the impacts of declines in krill abundance if they can change their foraging behaviors in response to changes in the local environment. Humpback whales and other baleen whales have demonstrated plastic behaviors in response to prey types and distributions (Juarasz & Juarasz 1979, Hain et al. 1982, Hays et al. 1985, Friedlaender et al. 2009, Ware et al. 2011, Wiley et al. 2011, Ware et al. 2013), however, the plasticity of whales in the Southern Ocean has not been examined. Such plasticity would be

beneficial for whales if, for instance, the competition for krill is significantly increased and should be examined.

Ware et al. (2011) described both deep and shallow lunge types exhibited by humpback whales along the WAP, but a preliminary analysis of the tag data suggests that several behaviors never before described in baleen whales are executed by the humpback whales examined in this research (e.g., surface loops, and spiraling ascending and descending lunges). Currently, it is unknown whether these behaviors are individually specific or if they are used broadly by the population. Specialized feeding patterns (defined as the consistent use of a pattern of foraging, feeding technique, or prey species, or some combination of these, by an individual or group of animals within a population where other foraging strategies are also employed; Partridge & Green 1985) have been described for a variety of cetacean species including minke whales (Hoelzel et al. 1989) and humpbacks feeding at the surface (Weinrich et al. 1992, Wiley et al. 2011) and presumably allow individuals to exploit prey patches with increased efficiency or to access highly mobile prey that would be otherwise unavailable (Wiley et al. 2011). Future research should examine the different behaviors exhibited by rorquals in the Southern Ocean and attempt to determine their associated energetic costs and gains to assess the potential for plasticity in rorqual feeding behaviors in this region.

Finally, while this research advances the current knowledge of fine-scale foraging behaviors of humpback whales, specifically along the WAP, much is still unknown regarding their ecological relationships with other species in these waters, including other baleen whales. Friedlaender et al. (2009b, 2011) suggest that humpbacks and other krill predators may be able to partition their resources to reduce their competition. It is unknown, however, what factors may reduce their ability to maintain their ecological niches and how, if forced to compete, that will affect the structure and function of the Antarctic marine ecosystem. Therefore, future research along the WAP should focus on placing studies of individual species in the context of their potential competitors and the extreme Antarctic environment.

Appendix A

Description of acronyms used throughout the dissertation (in order of appearance).

Acronym	Description
WAP	Western Antarctic Peninsula
VGB	Ventral Groove Blubber
ASRV	Antarctic Science Research Vessel
RVIB	Research Vessel Ice Breaker
USAP	United States Antarctic Program
NSF	National Science Foundation
MCDW	Modified Current Deep Water
Dtag	Digital Acoustic Recording Device
VHF	Very High Frequency
GPS	Geographic Positioning System
ILI	Inter-Lunge Interval
OFT	Optimal Foraging Theory
DLT	Dive Lactate Threshold
RMSE	Root Mean Square Error
ME	Modelling Efficiency
AOV	Analysis of Variance
MLE	Maximum Likelihood Estimate
EMR	Engulfment Metabolism Rate
RAAMR	Rorqual Active Metabolic Rate
AMR	Active Metabolic Rate
BMR	Basal Metabolic Rate
MCMC	Markov Chain Monte Carlo

Appendix B

Description of mathematical symbols used throughout the dissertation (in order of appearance).

Symbol	Description
r	Pearson R Correlation Coefficient
t	Student's T-test
CV	Coefficient of variation
SD	Standard deviation
df	Degrees of Freedom
p	Significance Level
F	F-Statistic
R^2	Multiple R-Squared
τ	Travel Duration
t	Forage Duration
s	Surface Duration
u	Dive Duration
K	Total Oxygen Storage Capacity
α	Initial Proportional Rate of Oxygen Replenishment
m_τ	Metabolic Rate During Traveling
m_t	Metabolic Rate During Foraging
π	Dive Cycle
s^*	Optimal Surface Duration
V	Whale speed
t^*	Optimal Forage Duration
u^*	Optimal Dive Duration
l^*	Optimal Lunge Count
L	Observed Lunge Count
L	Whale Length
M	Whale Mass
p	Depth
N	Number of Foraging Dives
W	Wilcoxon Rank-Sum Distribution
$\beta\alpha$	Scaling Exponent for α

L	Likelihood
σ^2	Model Variance
i	Iteration
MCMC	Markov Chain Monte Carlo
K^*	Candidate Value
$K^{(g)}$	Current Value
V	Covariance Matrix
g	Index of the Process in the Model Simulation
z	The Probability of the Candidate Values
CL	Credible Limits

Appendix C

Custom written R code (R Core Team 2013) used in Chapter 4 to estimate posterior values of humpback whale total oxygen capacity (K), initial rate of oxygen replenishment (α), and metabolic rates while traveling (m_T; m1 in the code) and foraging (m_I; m2 in the code).

```
################################################################################
#Subset dive durations from observed data
 tau   <- data$travel_time
 t     <- data$forage_time
 s     <- data$surface_time
 u     <- tau + t

#Function to calculate physiological parameters for a whale of length X:
 Physparam <- function(length){
  mass  <- 0.016473*(length)^2.95   #W is body weight in tones and L is body length in
                                    #m (Lockyer 1976)
  mass  <- mass*1000                #convert mass from tones to kilograms
  K     <- 0.03*mass^(1.05)         #Total oxygen storage capacity (L) (Stephens et al.
                                    2008)
  a     <- 0.075*mass^(-0.33)       #Initial rate of oxygen replenishment (s-1) if
                                    #symmorphsis holds (Stephens et al. 2008)
  m1    <- 3 * 2 * (4*mass^0.75)    #Metabolic rate while traveling in Watts (Potvin et al.
                                    #2012)
  m1    <- m1*0.0143                #Convert Watts to kcal/min
  m1    <- m1/5                     #Convert kcal/min to VO2 in L/min
  m1    <- m1* 0.0167               #Convert L/min to L/sec
  m2    <- m1*1.78                  #Metabolic rate while foraging (Doniol-Valcroze et
                                    #al. 2011)
 return(as.numeric(rbind(K,a,m1,m2)))
 }
```

```
#Calculate physiological parameters for average whale to be used as prior values
  priors    <- physparam(13.45)
  K         <- priors[1]
  a         <- priors[2]
  m1        <- priors[3]
  m2        <- priors[4]

#Function to estimate the amount of oxygen gained by a diver that spends time s on the
#surface
 o2 <- function (s) {K*(1-exp(-1*a*s))}

#Function to predict optimal durations for observed values of tau
 opt_predictions <- function(tau){
  optST  <- vector()                              #create empty vector for surface time
  ratio   <- function(s) { (o2(s)-m1*tau)/(m2*(s+tau)) }          #ratio of t to s + tau
  optST  <- optimize(f=ratio, interval=c(0,2000), maximum=T)$maximum
                                                                  #determine s*
  optFT  <- (o2(optST)- m1*tau)/m2                                #determine t*
  optDT <- optFT+tau                                              #determine u*
 }

#Function to get means of physiological parameters based on optimal equation
 getMu  <- function(pars){
   m1    <- pars[1]
   m2    <- pars[2]
   K     <- pars[3]
   a     <- pars[4]
   apply(tau,1,opt_predictions)     #find the optimal prediction of u* for all values of tau
  }

#Define the physiological parameters:
 pars <- c(m1,m2,K,a)

#Function to calculate the sum of the negative log Likelihood
 diveLik <- function(pars){ -sum(dnorm(u,getMu(pars),sqrt(sg),log=T))}
```

```
#Set standard deviation of the normal distribution:
 sg <- 1

#Function to update standard deviation in the gibbs sampler
 updateS  <- function(){
    u1      <-  s1 + n/2
    u2      <- s2 + .5*sum( (getMu(pars) -  u)^2 )
    1/rgamma(1,u1,u2)
 }

#where:
 n       <- length(u) #the number of observed dives
 s1      <- 1
 s2      <- 1

#Pick the starting values of the Metropolis Sampler
 xg      <- physparam(12)   #chose a random (but realistic) length for a humpback whale
 Kg      <- xg[1]
 ag      <- xg[2]
 m1g     <- xg[3]
 m2g     <- xg[4]

#Function to update model parameters (i.e., run the Metropolis algorithm)
 updatePars <- function(){
   sprop         <- c(m1,m2,K,a)/10000                    #Covariance matrix
   pars          <- c(m1g,m2g,Kg,ag)                      #current values of physiological
                                                          #parameters
   parNew        <- tnorm(4,c(0.001,0.001,100,0.001),c(50,50,5000,1),pars,sprop)
                    #create new candidate values for parameters based on a truncated
                    #normal distribution assuming mean values are the current parameters
                    #and the error is equal to the covariance matrix
   pnow          <- diveLik(pars) + sum(dnorm(pars,c(m1,m2,K,a),sqrt(10),log=T))
                    #likelihood of u based on current values + likelihood of current values
   pnew          <- diveLik(parNew) + sum(dnorm(parNew,c(m1,m2,K,a),sqrt(10),log=T))
                    #likelihood of u based on candidate values + likelihood of candidate
                    #values
```

```
    #Metropolis Step to determine which of these parameter values result in
    #observed values of u being more probable if u* is true:
      a         <- exp(pnew - pnow)
      z         <- runif(1,0,1)     #sample as a block
      if (z < a) {pars <- parNew}
      pars
 }

#Select number of iterations for the MCMC
 ng  <- 1000000

#Create empty matrix with column names to hold values
 pgibbs               <- matrix(NA,ng,5)
 colnames(pgibbs) <- c('m1','m2','K','a','s')

#Run the Gibbs Sampler
 for(g in 1:ng){
    pars          <- updatePars() #update parameter values using the metropolis algorithm
    m1g           <- pars[1]          #set the updated parameter values
    m2g           <- pars[2]
    Kg            <- pars[3]
    ag            <- pars[4]
    sg            <- updateS()      #set the updated error value
    pgibbs[g,]    <- c(pars,sg)     #store these values
 }
```

Appendix D

The lengths of tagged whales used in this research estimated using photogrammetry methods using the Dtag on the whales as an estimate of scale (Table 15). High quality photographs (i.e., in focus, low contrast) taken approximately perpendicular to the whales and with clear views of the Dtag were examined in the software program UTHSCSA ImageTool. Proportional relationships known to be significant indicators of total whale length (e.g., the blowhole to posterior emargination of the dorsal fin length, tip of rostrum to blowhole length, width of the fluke; Matthews 1937) were measured and used to estimate the total body length. To reduce observational error, the spatial scale of these tracings were calibrated using the known dimensions of the Dtag (Johnson & Tyack 2003) and multiple photographs of each whale and each proportion (when available) were used.

Table 11: Body length estimates for tagged Antarctic humpback whales from the Western Antarctic Peninsula region. Lengths were measured using photogrammetric techniques on digital photographs taken in the fall of 2009 and 2010. Data are compiled from Kutcher (unpublished data). Total body lengths are represented as means ± SD

Whale ID	Number of measuring photos	CV of total body length (%)	Total body length (m)
122b	1	-	13.48
127a	7	21.35	12.14±2.59
136a	13	5.52	15.90±0.88
140a	14	1.68	15.85±0.27
148a	2	8.80	11.41±1.00
152a	--	--	--
132a	16	18.66	13.48±2.51
133a	1	-	15.44
139a	7	20.79	13.94±2.90
144a	1	--	9.32
146a	--	--	--
151a	3	0.69	10.07±0.07
155a	3	1.88	8.26±0.16

References

Acevedo-Gutierrez A, Croll DA, Tershy BR (2002) High feeding costs limit dive time in the largest whales. Journal of Experimental Biology 205:1747-1753

Ainley DG, Ballard G, Dugger KM (2006) Competition among penguins and cetaceans reveals trophic cascades in the Western Ross Sea, Antarctica. Ecology 87:2080-2093

Altmann J (1974) Observational study of behavior - sampling methods. Behaviour 49:227-267

Aoki K, Watanabe YY, Crocker DE, Robinson PW and others (2011) Northern elephant seals adjust gliding and stroking patterns with changes in buoyancy: Validation of at-sea metrics of body density. Journal of Experimental Biology 214:2973-2987

Arnould JPY, Luque SP, Guinet C, Costa DP, Kingston J, Shaffer SA (2003) The comparative energetics and growth strategies of sympatric antarctic and subantarctic fur seal pups at Iles Crozet. Journal of Experimental Biology 206:4497-4506

Atkinson A, Siegel V, Pakhomov E, Rothery P (2004) Long-term decline in krill stock and increase in salps within the southern ocean. Nature 432:100-103

Austin D, Bowen WD, McMillan JI, Iverson SJ (2006) Linking movement, diving, and habitat to foraging success in a large marine predator. Ecology 87:3095-3108

Baker CS, Herman LM, Perry A, Lawton WS and others (1986) Migratory movement and population structure of humpback whales (Megaptera novaeangliae) in the central and eastern north pacific. Marine Ecology Progress Series 31:105-119

Baraff L, Weinrich MT (1993) Separation of humpback whale mothers and calves on a feeding ground in early autumn. Marine Mammal Science 9:431-434

Bayes T, Price R (1763) An essay towards solving a problem in the doctrine of chance. By the late rev. Mr. Bayes, communicated by mr. Price, in a letter to John Canton, a. M. F. R. S. Philosophical Transactions of the Royal Society of London 53:370-418

Bel'Kovich VM (1991) Herd structure, hunting, and play: Bottlenose dolphins (*Tursiops truncatus*). In: Pryor K, Norris K (eds) Dolphin societies: Discoveries and puzzles. University of California Press, Berkeley, p 17-78

Bender CE, Herzing DL, Bjorklund DF (2009) Evidence of teaching in atlantic spotted dolphins (*Stenella frontalis*) by mother dolphins foraging in the presence of their calves. Animal Cognition 12:43-53

Berman CM (1980) Mother-infant relationships among free-ranging rhesus monkeys on cayo santigo: A comparison with captive pairs. Animal Behaviour 28:860-873

Bose N, Lien J (1989) Measurements of the bodies of flukes of several cetacean species. Proceedings of the Royal Society of London B 242:163-173

Boyd IL (1997) The behavioural and physiological ecology of diving. Trends in Ecololgy and Evolution 12:213-217

Boyd IL (2002) Estimating food consumption of marine predators: Antarctic fur seals and macaroni penguins. Journal of Applied Ecology 39:103-119

Boyd IL, Croxall JP (1996) Dive durations in pinnipeds and seabirds. Canadian Journal of Zoology 74:1696-1705

Boyd IL, Woakers AJ, Butler PJ, Davis RW, Williams TM (1995) Validation of heart rate and doubly labelled water as measures of metabolic rate during swimming in California sea lions. Functional Ecology 9:151-160

Brodie PF (1993) Noise generated by the jaw actions of feeding fin whales. Canadian Journal of Zoology 71:2546-2550

Butler PJ (2006) Aerobic dive limit. What is it and is it always used appropriately? Comparative Biochemistry and Physiology a-Molecular & Integrative Physiology 145:1-6

Butler PJ, Green JA, Boyd IL, Speakman JR (2004) Measuring metabolic rate in the field; the pros and cons of the doubly labelled water and heart rate methods. Functional Ecology 18:168-183

Butler PJ, Jones DR (1997) Physiology of diving of birds and mammals. Physiological Reviews 77:837-899

Butler PJ, Woakers AJ, Boyd IL, Kanatous S (1992) Relationship between heart rate and oxygen consumption during steady-state swimming in california sea lions. Journal of Experimental Biology 170:35-42

Canning C, Crain D, Eaton TS, Nuessly K and others (2011) Population-level lateralized feeding behavior in north atlantic humpback whales, *Megaptera novaeangliae*. Animal Behaviour 82:901-909

Cappe O, Robert CP (2000) Markov chain monte carlo: 10 years and still running! Journal of the American Statistical Association 95:1282-1286

Carbone C, Houston AI (1996) The optimal allocation of time over the dive cycle: An approach based on aerobic and anaerobic respiration. Animal Behaviour 51:1247-1255

Cartwright R, Sullivan M (2009) Behavioral ontogeny in humpback whale (Megaptera novaeangliae) calves during their residence in hawaiian waters. Marine Mammal Science 25:659-680

Castellini MA, Somero GN, Kooyman GL (1981) Glycolytic enzyme activities in tissues of marine and terrestrial mammals. Physiological and Biochemical Zoology 143:191-198

Charnov EL (1976) Optimal foraging, marginal value theorem. Theoretical Population Biology 9:129-136

Chittleborough RG (1958) The breeding cycle of the female humpback whale, *Megaptera nodosa* (bonnaterre). Australian Journal of Marine and Freshwater Research 9:1-8

Chittleborough RG (1965) Dynamics of of two populations of the humpback whale, *Megaptera novaeangliae* (borowski). Australian Journal of Marine and Freshwater Research 16:33-128

Clapham CJ, Mead JG (1999) Megaptera novaengliae. Mammalian Species 604:1-9

Clapham PJ (1996) The social and reproductive biology of humpback whales: An ecological perspective. Mammal Review 26:27-49

Clapham PJ, Mayo CA (1987) Reproduction and recruitment of individually identified humpback whales, Megaptera-novaeangliae, observed in Massachusetts Bay, 1979-1985. Canadian Journal of Zoology 65:2853-2863

Clark JS (2007) Models for ecologica data: An introduction, Princeton University Press

Cohen J (1988) Statistical power analysis for the behavioral sciences, Lawrence Erlbaum Associates, Inc., Hillsdale, NJ, USA

Corkeron PJ, Ensor P, Matsuoka K (1999) Observations of blue whales feeding in Antarctic waters. Polar Biology 22:213-215

Costa DP, Williams TD (1999) Marine mammal energetics. In: Reynolds JE, Rommel SA (eds) Biology of marine mammals. Smithosnian Institution Press, Washington, D. C., p 176-217

Croll DA, Acevedo-Gutierrez A, Tershy BR, Urban-Ramirez J (2001) The diving behavior of blue and fin whales: Is dive duration shorter than expected based on oxygen stores? Compatative Biochemical Physics A 129:797-809

Croll DA, Kudela RM, Tershy BR (2006) Ecosystem impact of the decline of large whales in the north pacific. In: Estes JA (ed) Whales, whaling and ocean ecosystems. University of California Press, Berkley, CA, p 202-214

Croll DA, Marinovic B, Benson S, Chavez FP, Black N, Ternullo R, Tershy BR (2005) From wind to whales: Trophic links in a coastal upwelling system. Marine Ecology Progress Series 289:117-130

Davis RW, Fuiman LA, Williams TD, Le Boeuf BJ (2001) Three-dimensional movements and swimming activity of a northern elephant seal. Comparative Biochemistry and Physiology a-Molecular & Integrative Physiology 129:759-770

Dinniman MS, Klinck JM, Smith WO (2011) A model study of circumpolar deep water on the west antarctic peninsula and ross sea continental shelves. Deep-Sea Research Part II: Topical Studeis in Oceanography 58:1508-1523

Dolphin WF (1987a) Dive behavior and estimated energy expenditure of foraging humpback whales in southeast alaska. Canadian Journal of Zoology 65:354-362

Dolphin WF (1987b) Prey densities and foraging of humpback whales, megaptera novaeangliae. Experientia 43:468-471

Dolphin WF (1987c) Ventilation and dive patterns of humpback whales, Megaptera novaeangliae, on their Alaskan feeding grounds. Canadian Journal of Zoology 65:83-90

Dolphin WF (1988) Foraging dive patterns of humpback whales, Megaptera novaeangliae, in southeast Alaska - a cost-benefit analysis. Canadian Journal of Zoology 66:2432-2441

Doniol-Valcroze T, Lesage V, Giard J, Michaud R (2011) Optimal foraging theory predicts diving and feeding strategies of the largest marine predator. Behavioral Ecology 22:880-888

Espinasse B, Zhou M, Zhu Y, Hazen ELand others (2012) Austral fall-winter transition of mesozooplankton assemblages and krill aggregations in an embayment west of the Antarctic peninsula. Marine Ecology Progress Series 452:63-80

Espmark Y (1971) Mother-young relationship and ontogeny of behaviour in roe deer (*Caprelous capreolus* l.). Journal of Comparative Ethology 29:42-81

Estes RD (1976) The significant of breeding synchrony in wildebeest. East African Wildlife Journal 14:135-152

Fahlman A, Svard C, Rosen DAS, Jones DR, Trites AW (2008) Metabolic costs of foraging and the management of 0_2 and co_2 stores in steller sea lions. Journal of Expimental Biology 211:3573-3580

Fellner W, Bauer GB, Harley HE (2006) Cognitive implications of synchrony in dolphins: A review. Aquatic Mammals 32:511-516

Fisher DO, Blomberg SP, Owens IPF (2002) Convergent maternal care strategies in ungulates and macropods. Evolution 56:167-176

Florez-Gonzalez L (1991) Humpback whales *Megaptera novaeangliae* in the gorgona island,columbia pacific breeding waters: Population and pod characteristics. Memoirs of the Queensland Museum 20:291-295

Fortin D, Fryxell JM, Piolote R (2002) The temporal scale of foraging decisions in bison. Ecology 83:970-982

Friedlaender AS, Halpin PN, Qian SS, Lawson GL, Wiebe PH, Thiele D, Read AJ (2006) Whale distribution in relation to prey abundance and oceanographic processes in shelf waters of the Western Antarctic peninsula. Marine Ecology Progress Series 317:297-310

Friedlaender AS, Hazen EL, Nowacek DP, Halpin PN and others (2009) Diel changes in humpback whale Megaptera novaeangliae feeding behavior in response to sand lance ammodytes spp. Behavior and distribution. Marine Ecology Progress Series 395:91-100

Friedlaender AS, Tyson RB, Stimpert AK, Read AJ, Nowacek DP (2013) Extreme diel variation in the feeding behavior of humpback whales along the Western Antarctic Peninsula during autumn. Marine Ecology Progress Series 494:281-289

Gelman A, Roberts GO, Gilks WR (1995) Efficient metropolis jumping rules. Bayesian Statistics 5:599-607

German S, German D (1984) Stochastic relaxation, gibbs distributions, and the bayesian restoration of images. IEEE Transactions on Pattern Analysis and Machine Intelligence 6:721-724

Goldbogen JA, Calambokidis J, Croll DA, Harvey JT and others (2008) Foraging behavior of humpback whales: Kinematic and respiratory patterns suggest a high cost for a lunge. Journal of Experimental Biology 211:3712-3719

Goldbogen JA, Calambokidis J, Friedlaender AS, Francis J and others (2013) Underwater acrobatics by the world's largest predator: 360 degrees rolling manoeuvres by lunge-feeding blue whales. Biological Letters 9:20120986

Goldbogen JA, Calambokidis J, Oleson E, Potvin J, Pyenson ND, Schorr G, Shadwick RE (2011) Mechanics, hydrodynamics and energetics of blue whale lunge feeding: Efficiency dependence on krill density. Journal of Experimental Biology 214:131-146

Goldbogen JA, Calambokidis J, Shadwick RE, Oleson EM, McDonald MA, Hildebrand JA (2006) Kinematics of foraging dives and lunge-feeding in fin whales. Journal of Experimental Biology 209:1231-1244

Goldbogen JA, Potvin J, Shadwick RE (2010) Skull and buccal cavity allometry increase mass-specific engulfment capacity in fin whales. Proceedings of Biological Science 277:861-868

Goldbogen JA, Pyenson ND, Shadwick RE (2007) Big gulps require high drag for fin whale lunge feeding. Marine Ecology Progress Series 349:289-301

Gubbins C, McCowan B, Lynn SK, Hooper S, Reiss D (1999) Mother-infant spatial relations in captive bottlenose dolphins, Tursiops truncatus. Marine Mammal Science 15:751-765

Guisan A, Zimmerman NE (2000) Predictive habitat distribution models in ecology. Ecological Modelling 135:147-186

Hain JHW, Carter GR, Kraus SD, Mayo CA, Winn HE (1982) Feeding behavior of the humpback whale, Megaptera novaeangliae, in the western north atlantic. Fish B-Noaa 80:259-268

Halsey LG, Butler PJ, Blackburn TM (2006) A phylogenetic analysis of the allometry of diving. American Naturalist 167:276-287

Halsey LG, Woakes AJ, Butler PJ (2003) Testing optimal foraging models for air-breathing divers. Animal Behaviour 65:641-653

Hastings WK (1970) Monte carlo sampling methods using markov chains and their applications. Biometrika 57:97-109

Hays HE, Winn HE, Petricig R (1985) Anomalous feeding behavior of a humpback whale. Journal of Mammals 66:819-821

Hazen EL, Friedlaender AS, Thompson MA, Ware CR, Weinrich MT, Halpin PN, Wiley DN (2009) Fine-scale prey aggregations and foraging ecology of humpback whales Megaptera novaeangliae. Marine Ecology Progress Series 395:75-89

Heaslip SG, Bowen D, Iverson SJ (2014) Testing predictions of optimal diving theory using animal-borne video from harbour seals (*Phoca vitulina concolor*). Canadian Journal of Zoology 92:309-318

Hoelzel RA, Dorsey EM, Stern SJ (1989) The foraging specializations of individual minke whales. Animal Behaviour 38:786-794

Houston A (2011) Assessing models of optimal diving. Trends in Ecology and Evolution 26:292-297

Houston AI, Carbone C (1992) The optimal allocation of time during the diving cycle. Behavioral Ecology 3:255-265

Houston AI, Mcnamara JM (1985) A general theory of central place foraging for single-prey loaders. Theoretical Population Biology 28:233-262

Hunt KE, Moore MJ, Rolland RM, Kellar NM and others (2013) Overcoming the challenges of studying coservation physiology in large whales: A review of available methods. Conservation Physiology 1:1-24

Ichii T, Kato H (1991) Food and daily food-consumption of southern minke whales in the antarctic. Polar Biology 11:479-487

Johnson MP, Tyack PL (2003) A digital acoustic recording tag for measuring the response of wild marine mammals to sound. IEEE Journal of Oceanic Engineering 28:3-12

Johnston DW, Friedlaender AS, Read AJ, Nowacek DP (2012) Initial density estimates of humpback whales *Megaptera novaeangliae* in the inshore waters of the Western Antarctic peninsula during the late autumn. Endangered Species Research 18:63-71

Juarasz C, Juarasz V (1979) Feeding modes of the humpback whale in southeast alaska. Scientific Report of Whales Resesearch Institute fo Tokyo 31:69-83

Kawamura A (1994) A review of baleen whale feeding in the southern ocean. Report of the International Whaling Commision 44:261-271

Kleiber M (1975) The fire of life: An introduction to animal energetics. Huntington, New York: Krieger

Kleiber M, Rogers TA (1961) Energy metabolism. Annual Review of Physiology 23:5-36

Kooyman GL (1973) Respiratory adaptations in marine mammals. American Zoologist 13:457-468

Kooyman GL (1985) Physiology without restraint in diving mammals. Marine Mammal Science 1:166-178

Kooyman GL, Ponganis (1997) The challenges of diving to depth. American Scientist 85

Kooyman GL, Ponganis PJ (1998) The physiological basis of diving to depth: Birds and mammals. Annual Review of Physiology 60:19-32

Kramer DL (1988) The behavioral ecology of air breathing by aquatic animals. Canadian Journal of Zoology 66:89-94

Lasiewski RC, Calder WA (1971) Preliminary allometric analysis of respiratory variables in resting birds. Respiration Physiology 11:152-166

Leaper R, Lavigne D (2001) Scaling prey consumption to body mass in cetaceans. Paper SC/J02/FW2 presented to the IWC Scientific Committee

Lent PC (1974) Mother-infant relationships in ungulates. In: The behaviour of ungulates and its relation to management, p 14-55

Lifson N, McClintock R (1966) Theory of use of the turnver rates of body water for measuring energy and material balance. Journal of Theoretical Biology 12:46-74

Loague K, Green JA (1991) Statistical and graphical methods for evaluating solute transport models: Overview and application. Journal of Contaminant Hydrology 7:51-73

Lockyer C (1976) Body weights of some species of large whales. Journal du Conseil 36:259-273

Lockyer C (1981) Growth and energy budgets of large baleen whales from the southern hemisphere In: Mammals in the Seas Vol III, General Papers and Large Cetaceans FAO Fish Ser 5, , p 379-487

Lockyer C (2007) All creatures great and smaller: A study in cetacean life history energetics. Journal of the Marine Biological Assocociation of the UK 87:1035-1045

Loeb V, Siegel V, Holm-Hanson. O, Hewitt R, Fraser W, Trivelpieve W, Trivelpiece S (1997) Effects of sea-ice extent and krill or salp dominance on the Antarctic food web. Nature 387:897-900

Macarthur RH, Pianka ER (1966) On optimal use of a patchy environment. American Naturalist 100:603-609

Mackintosh NA (1965) The stocks of whales. Fish News (Books) Ltd, Lond:232

MathWorks (2013b) Matlab and statistics toolbooks release, Natick, Massachusetts, United States

Matthews LH (1937) The humpback whale, Megaptera nodoso. Discovery Reports 17:7-92

Mayer DG, Butler DG (1993) Statistical validation. Ecological Modelling 68:21-32

Metropolis N, Rosenbluth AW, Rosenbluth MN, Teller AH, Teller E (1953) Equations of state calculations by fast computing machines. Journal of Chemical Physics 21:1087-1092

Miller PJO, Johnson MP, Tyack PL, Terray EA (2004) Swimming gaits, passive drag and buoyancy of diving sperm whales physeter macrocephalus. Journal of Experimental Biology 207:1953-1967

Mori Y (1998) Optimal choice of foraging depth in divers. Journal of Zoology 245:279-283

Mori Y (2002) Optimal diving behaviour for foraging in relation to body size. Journal of Evolutionary Biology 15:269-276

Nagy KA (1987) Field metabolic rate and food requirement scaling in mammals and birds. Ecological Monographs 57:111-128

Nicol S, Foster J (2003) Recent trends in the fishery for Antarctic krill. Aquatic Living Resources 16:42-45

Noren SR, Biedenbach G, Redfern JV, Edwards EF (2008) Hitching a ride: The formation locomotion strategy of dolphin calves. Functional Ecology 22:278-283

Noren SR, Edwards EF (2011) Infant position in mother-calf dolphin pairs: Formation locomotion with hydrodynamic benefits. Marine Ecology Progress Series 424:229-236

Norris KS, Schilt CR (1988) Cooperative societies in three-dimensional space: On the origin of aggregations, flocks and schools, with special reference to dolphins and fish. Ethology and Sociobiology 9:149-179

Nousek-McGregor AE, Miller CA, Moore MJ, Nowacek DP (2014) Effects of body condition on buoyancy in endangered North Atlantic right whales. Division of Comparative Physiology and Biochemistry, Society for Integrative and Comparative Biology 87:160-171

Nowacek DP, Friedlaender AS, Halpin PN, Hazen EL and others (2011) Super-aggregations of krill and humpback whales in Wilhelmina Bay, Antarctic Peninsula. PLoS One 6(4): e19173. doi:10.1371/journal.pone.0019173 6

Nowacek DP, Johnson MP, Tyack PL (2004) North atlantic right whales (Eubalaena glacialis) ignore ships but respond to alerting stimuli. Proceedings of the Royal Society London B Biological Sciences 271:227-231

Nowacek DP, Johnson MP, Tyack PL, Shorter KA, McLellan WA, Pabst DA (2001) Buoyant balaenids: The ups and downs of buoyancy in right whales. Proceedings of the Royal Society of London B 268:1811-1816

Orians GH, Pearson NE, Horn DJ, Mitchell DR, Stairs GR (1979) On the theory of central place foraging In: Analysis of ecological systems. Ohio State University Press, Columbus, Ohio, p 155

Owens-Smith N, Novellie P (1982) What should a clever ungulate eat? American Natualist 119:151-188

Parkes R, Halsey LG, Woakes AJ, Holder RL, Butler PJ (2002) Oxygen uptake during post dive recoevery ina diving bird iaythya fuligulai: Implications for optimal foraging models. Journal of Experimental Biology 205:3945-3954

Parkinson C (2004) Southern ocean sea ice and its wider linkages: Insights revealed from models and observations. Antarctic Science 16:387-400

Partridge L, Green P (1985) Intraspecific feeding specialization and population dynamics. In: Silby RM, Smith RH (eds) Behavioral ecology: Ecological conseqences of adaptive behaviour. Blackwell Scientific Publishers, Oxford, p 207-226

Potvin J, Goldbogen JA, Shadwick RE (2009) Passive versus active engulfment: Verdict from trajectory simulations of lunge-feeding fin whales balaenoptera physalus. Journal of the Royal Society, Interface / the Royal Society 6:1005-1025

Potvin J, Goldbogen JA, Shadwick RE (2010) Scaling of lunge feeding in rorqual whales: An integrated model of engulfment duration. Journal of Theoretical Biology 267:437-453

Potvin J, Goldbogen JA, Shadwick RE (2012) Metabolic expenditures of lunge feeding rorquals across scale: Implications for the evolution of filter feeding and the limits to maximum body size. PLoS One 7:e44854

Prezelin BB, Hofmann EE, Mengelt C, Klinck JM (2000) The linkage between upper circumpolar deep water (UCDW) and phytoplankton assemblages on the west Antarctic peninsula continental shelf. Journal of Marine Research 58:165-202

Quetin LB, Ross RM (2003) Episodic recruitment in Antarctic krill Euphausia superba in the palmer lter study region. Marine Ecology Progress Series 259:185-200

R Core Team (2013) R: A language and environment for statistical computing R Foundation for Statistical Computing, Vienna, Austria

Sargeant BL, Mann J (2009) Developmental evidence for foraging traditions in wild bottlenose dolphins. Animal Behaviour 78:715-721

Schmidt V, Weber TC, Wiley DN, Johnson MP (2010) Underwater tracking of humpback whales (Megaptera novaeangliae) with high-frequency pingers and acoustic recording tags. IEEE Journal of Oceanic Engineering 35:821-836

Schoener TW (1987) Theory of feeding strategies. Cc/Agr Biol Environ:16-16

Schreer JF, Kovacs KM (1997) Allometry of diving capacity in air-breathing vertebrates. Canadian Journal of Zoology 75:339-358

Sibley RM, Calow P (1986) Physiological ecology of animals, Blackwell, Oxford

Siegel V, Loeb V, Groger J (1998) Krill (*euphausia superba*) density, proportional and absolute recruitment and biomass in the elephant island region (antarctic peninsula) during the period 1977 to 1997. Polar Biology 19:393-398

Simon M, Johnson M, Madsen PT (2012) Keeping momentum with a mouthful of water: Behavior and kinematics of humpback whale lunge feeding. Journal of Experimental Biology 215:3786-3798

Smith EP, Rose KA (1995) Model goodness-of-fit analysis using regression and related techniques. Ecological Modelling 77:49-64

Smith RC, Stammerjohn SE (2001) Variations of surface air temperature and sea-ice extent in the western Antarctic peninsula region. Annals of Glaciology 33:493-500(498)

Speakman, Racey (1988) Consequences of non steady-state co_2 production for accuracy of the doubly labelled water technique: The importance of recapture interval. Comparative Biochemistry and Physiology A-Molecular & Integrative Physiology 90A:337-340

Spitz SS, Herman LM, Pack AA, Deakos MH (2002) The relation of body size of male humpback whales to their social roles on the Hawaiian winter grounds. Canadian Journal of Zoology 80:1938-1947

Stammerjohn SE, Martinson DG, Smith RC, Iannuzzi RA (2008a) Sea ice in the western Antarctic peninsula region: Spatio-temporal variability from ecological and climate change perspectives. Deep Sea Research Part II: Topical Studies in Oceanography 55:2041-2058

Stammerjohn SE, Martinson DG, Smith RC, Yuan X, Rind D (2008b) Trends in Antarctic annual sea ice retreat and advance and their relation to el nino-southern oscillation and southern annular mode variability. Journal of Geophysical Research-Oceans 113

Stephens PA, Carbone C, Boyd IL, McNamara JM, Harding KC, Houston AI (2008) The scaling of diving time budgets: Insights from an optimality approach. American Naturalist 171:305-314

Stimpert AK, Peavey LE, Friedlaender AS, Nowacek DP (2012) Humpback whale song and foraging behavior on an Antarctic feeding ground. PLoS One 7:e51214

Stimpert AK, Wiley DN, Au WWL, Johnson MP, Arsenault R (2007) 'Megapclicks': Acoustic click trains and buzzes produced during night-time foraging of humpback whales (megaptera novaeangliae). Biology Letters 3:467-470

Szabo A, Duffus D (2008) Mother-offspring association in the humpback whale, Megaptera novaeangliae: Following behaviour in an aquatic mammal. Animal Behaviour 75:1085-1092

Taber S, Thomas P (1982) Calf development and mother-calf spatial relationships in southern right whales. Animal Behaviour 30:1072-1083

Taylor CR, Weibel ER (1981) Design of the mammalian respiratory system. I Problem and strategy: Respiration Physiology 44:1-10

Tenney SM, Remmers JE (1963) Comparative quantitative morphology of the mammalian lunge: Diffusing area. Nature 197:54-56

Thiele D, Chester ET, Moore SE, Sirovic A, Hildebrand JA, Friedlaender AS (2004) Seasonal variability in whale encounters in the western antarctic peninsula. Deep-Sea Research Pt II 51:2311-2325

Thomas PO, Taber SM (1984) Mother-infant interactions and behavioral development in southern right whales, eubalaena australis. Behaviour 88:42-60

Thompson D, Fedak MA (2001) How long should a dive last? A simple model of foraging decisions by breath-hold divers in a patchy environment. Animal Behaviour 61:287-296

Tyson RB, Friedlaender AS, Stimpert AK, Ware C, Nowacek DP (2012) Synchronous mother and calf foraging behaviour in humpback whales M*egaptera novaeangliae*: Insights from multi-sensor suction cup tags. Marine Ecology Progress Series 457:209-220

Van Lennep EW, Van Utretcht WL (1953) Preliminary report on the study of the mammary glands of whales. Norsk Hvalangsttidende 42:249-258

Vaughan DG, Marshall GJ, Connolley WM, Parkinson Cand others (2003) Recent rapid regional climate warming on the Antarctic peninsula. Climatic Change 60:243-274

Ware C, Arsenault R, Plumlee M (2006) Visualizing the underwater behavior of humpback whales. IEEE Computer Graphics 26:14-18

Ware C, Friedlaender AS, Nowacek DP (2011) Shallow and deep lunge feeding of humpback whales in fjords of the west Antarctic peninsula. Marine Mammal Science 27:587-605

Ware C, Wiley DN, Friedlaender AS, Weinrich M and others (2013) Bottom side-roll feeding by humpback whales (M*egaptera novaeangliae*) in the southern gulf of maine, U.S.A. Marine Mammal Science

Weibel ER, C. TR, Bolis L (1998) Principles of animal design. Cambridge University Press, Cambridge

Weinrich MT, Schilling MR, Belt CR (1992) Evidence for acquisition of a novel feeding-behavior - lobtail feeding in humpback whales, Megaptera-novaeangliae. Animal Behaviour 44:1059-1072

Whiten A (2001) Imitation and cultural transmission in apes and cetaceans. Behavior Brain Science 24:359-360

Whiten A, Ham R (1992) On the nature and evolution of imitation in the animal kingdom - reappraisal of a century of research. Advance in the Study of Behavior 21:239-283

Wiedenmann J, Cresswell KA, Goldbogen J, Potvin J, Marngel M (2011) Exploring the effects of reductions in krill biomass in the southern ocean on blue whales using a state-dependent foraging model. Ecological Modelling 222:3366-3379

Wiehs D (2004) The hydrodynamics of dolphin drafting. Journal of Biology 3:8

Wiley D, Ware C, Bocconcelli A, Cholewiak D, Friedlaender A, Thompson M, Weinrich M (2011) Underwater components of humpback whale bubble-net feeding behaviour. Behaviour 148:575-602

Williams TD, Davis CE, Fulman LA, Francis J and others (2000) Sink or swim: Strategies for cost-efficient diving by marine mammals. Science 288:133-136

Williams TM (1999) The evolution of cost efficient swimming in marine mammals: Limits to energetic optimization. Philosophical Transactions of the Royal Society B Biolgical Sciences 354:193-201

Williams TM (2001) Intermittent swimming by mammals: A strategy for increasing energetic efficiency during diving. American Zoologist 41:166-176

Williams TM (2006) Physiological and ecological consequences of extreme body size in whales. In: Estes JA, DeMaster DP, Doak DF, Williams TM, Brownell RL (eds) Whales, whaling and ocean ecosystems. Univesity of California Press, Berkeley, CA, p 191-201

Witteveen BF, Foy RJ, Wynne KM, Tremblay Y (2008) Investigation of foraging habits and prey selection by humpback whales (M*egaptera novaeangliae*) using acoustic tags and concurrent fish surveys. Marine Mammal Science 24:516-534

Woakes AJ, Butler PJ, Bevan RM (1995) Implantable data logging system for heart rate and body temperature: Its application to the estimation of field metabolic rates in Antarctic predators. Medical and Biological Engineering and Computing 33:145-151

Woodward BL, Winn JP, Fish FE (2006) Morphological specializations of baleen whales associated with hydrodynamic performance and ecological niche. Journal of Morphology 267:1284-1294

Würsig B, Dorsey EM, Fraker MA, Payne RS, Richardson WJ, Wells RS (1984) Behavior of bowhead whales, Balaena mysticetus, summering in the beaufort sea - surfacing, respiration, and dive characteristics. Canadian Journal of Zoology 62:1910-1921

Yazdi P, Killian A, Culik BM (1999) Energy expenditure of swimming bottlenose dolphins (*Tursiops truncatus*). Marine Biology 134:601-607

Zhou M, Dorland RD (2004) Aggregation and vertical migration behavior of *Euphausia superba*. Deep Sea Research Part II: Topical Studies in Oceanography 51:2119-2137

Zhou M, Niiler PP, Hu JH (2002) Surface currents in the Bransfield and Gerlache Straits, Antarctica. Deep-Sea Research Part II 49:267-280

Zimmer WMX, Johnson MP, Madsen PT, Tyack PL (2005) Echolocation clicks of free-ranging cuvier's beaked whales (Ziphius cavirostris). Journal of the Acoust Society of America 117:3919-3927

Zoidis AM, Smultea MA, Frankel AS, Hopkins JLand others (2008) Vocalizations produced by humpback whale (Megaptera novaeangliae) calves recorded in hawaii. Journal of the Acoust Society of America 123:1737-1746

Biography

Reny Blue Tyson
Born: December 12, 1983
Troy, New York

Education

PhD Marine Science and Conservation, Duke University 2014
MSc Biological Oceanography, Florida State University, 2008
BSc Psychology, Florida State University (Honors), 2006

Publications

Urian, K. W., Waples, D. M., Tyson, R. B., Williams Hodge, L. E., and Read, A. J. (2014). Abundance of bottlenose dolphins (*Tursiops truncatus*) in estuarine and coastal waters of North Carolina, USA. Journal of the North Carolina Academy of Science. 129(4): 165-171.

Friedlaender, A. S., Tyson, R. B., Stimpert, A. K., Read, A. J., Nowacek, D. P. (2013). Extreme diel variation in the feeding behavior of humpback whales along the Western Antarctic Peninsula during autumn. Marine Ecology Progress Series. 464: 284-289.

Gales, N., Bowers, M., Durban, J. W., Friedlaender, A. S., Nowacek, D. P., Pitman, R. L., Read, A. J., and Tyson, R. B. (2013). Advances in non-lethal research on Antarctic minke whales: biotelemertry, photo-identification and biopsy sampling. Report to the International Whaling Commission.

Tyson, R. B., Friedlaender, A. S., Stimpert, A. K., Ware, C., and Nowacek, D. P. (2012). Synchronous mother and calf foraging behaviour in humpback whales Megaptera novaeangilae: insights from multi-sensor suction cup tags. Marine Ecology Progress Series. 457: 209-220.

Tyson, R. B., Nowacek, S. M., and Nowacek, D. P. (2011). Community structure and abundance of bottlenose dolphins Tursiops truncatus in coastal waters of the northeast Gulf of Mexico. Marine Ecology Progress Series. 438: 253-265.

Friedlaender, A. S., Nowacek, D. P., Johnston, D. W., Read, A. J., Tyson, R. B., Peavey, L., and Revelli, E. M. S. (2010). Multiple sightings of large groups of Arnoux's beaked whales (*Berardius arnouxii*) in the Gerlache Strait, Antarctica. Marine Mammal Science. 26(1): 246-250.

Tyson, R. B., Nowacek, D. P., and Miller, P. J. O. (2007). Nonlinear phenomena in the vocalizations of North Atlantic right whales (*Eubalaena glacialis*) and killer whales (*Orcinus orca*). Journal of the Acoustical Society of America. 122(3): 1365-1373.

Awards and Scholarships
Endeavour Research Fellowship, 2014
Scientific Committee of Antarctic Research, 2013
Duke Marine Laboratory Writing Fellowship, 2013
Preparing Future Faculty Fellow, 2013
Ford Foundation Fellowship (Honorable Mention), 2013
Duke Dissertation Research Travel Award, Duke University, 2013
Graduate Women in Science Fellowship (Honorable Mention), 2012
Scientists with Stories Development Grant, 2012
U.S. Congress Antarctic Service Medal, 2011
Beneath the Sea's Jordan Viders Spirt of the Sea Scholarship, 2011
Early Career/Young Scientist Travel Award for the Tagging Through the Stages Workshop at the Fourth Science Symposium on Bio-logging, 2011
Oak Foundation Travel Grant, 2011
Woods Hole Oceanographic Institute, Duke University Fellowship, 2009
Eonfusion Scholarship, 2009
Bess Ward Honors Grant, 2004

Professional affiliations
Society of Marine Mammalogy
Animal Behavior Society
Association of Polar Early Career Scientists
Society for Conservation of Biology